COMPATIBILISATION OF POWDERED NITRILE RUBBER TOUGHENED POLYSTYRENE

Thesis submitted to the

COCHIN UNIVERSITY OF SCIENCE AND TECHNOLOGY

in partial fulfilment of the requirements
for the award of the degree of

DOCTOR OF PHILOSOPHY

under the

FACULTY OF TECHNOLOGY

by

SREENIVASAN P.V.

DEPARTMENT OF POLYMER SCIENCE AND RUBBER TECHNOLOGY
COCHIN UNIVERSITY OF SCIENCE AND TECHNOLOGY
KOCHI - 682 022, INDIA.

October 2007

DEPARTMENT OF POLYMER SCIENCE AND RUBBER TECHNOLOGY
COCHIN UNIVERSITY OF SCIENCE AND TECHNOLOGY
KOCHI-682 022, INDIA.

Dr. Philip Kurian
Professor

Phone: 0484-2575723 (Off)
0484-2575590 (Res)
E-mail: pkurian@cusat.ac.in

CERTIFICATE

This is to certify that the thesis entitled "***Compatibilisation of Powdered Nitrile Rubber Toughened Polystyrene***" is based on the authentic research carried out by Mr. Sreenivasan P.V. under my guidance and supervision, in the Department of Polymer Science and Rubber Technology, Cochin University of Science and Technology, Kochi-682 022, and no part of the work reported in the thesis has been presented for the award of any degree from any other institution.

Dr. Philip Kurian

Kochi-22
15 October 2007

DECLARATION

I hereby declare that the work presented in this thesis entitled "**Compatibilisation of Powdered Nitrile Rubber Toughened Polystyrene**" is based on the original research work carried out by me under the guidance and supervision of Dr. Philip Kurian, Professor, Department of Polymer Science and Rubber Technology, Cochin University of Science and Technology, Kochi-682 022 and no part of the work reported in this thesis has been presented for the award of any degree from any other institution.

Kochi-22
15 October 2007

Sreenivasan P.V.

Acknowledgements

The successful completion of the present research endeavour was made possible by the generous, enthusiastic and inspiring guidance of my supervising teacher Dr. Philip Kurian, Professor, Department of Polymer Science and Rubber Technology, Cochin University of Science and Technology, Kochi-22. I owe an immense debt of gratitude to him for the judicious encouragement, the scholarly and illuminating criticism and stimulating suggestions provided to me throughout the tenure of my research work.

I am thankful to Dr. Thomas Kurian, Head of the Department, Polymer Science and Rubber Technology, and former Heads of the Department, Dr. K.E. George and Dr. Rani Joseph for providing me the necessary facilities.

I am thankful to the faculty members of the Department of Polymer Science and Rubber Technology, Dr. Eby Thomas Thachil, Dr. Sunil K Narayanankutty, laboratory staffs, Mr. Ravi, Mr. Gopalakrishnan, Mr. Manoharan and the librarian, Mrs. Girija for their good wishes and support.

I would like to express my heartfelt thanks to all my co-researchers, especially Dr. Lovely Mathew, Mr. P. Raju, Mr. M.K. Joshi, Mr. Jude Martin Mendez, Ms. Maya, Ms. K.V. Aswathy, Mr. Parameswaran, Dr. Anoop, Mr. Bipinbal, Ms. Saritha Chandran, Ms. Dhanya, Ms. Prema, Ms. Ansu Jacob, Mr. Sinto Jacob, Ms. Suma, Ms. Mary Alexander and Ms. Bhuvaneswary for the fruitful interactions and supports given to me.

I gratefully acknowledge the support received from the Manager, Principal and former Principal Dr. Raju K John, Union Christian College, Aluva. With immense pleasure I take this opportunity to thank Ms. Roshni Mathew Maliakal, Dr. Benny Cherian and Dr. K.P. Unnikrishnan of the Dept. of Chemistry, Union Christian College, Aluva for their valuable support and encouragement. The endless inspiration and support I received from my family members are highly appreciated.

I wish to thank the University Grants Commission, New Delhi for the award of Teacher Fellowship for the completion of the research work.

Above all, I thank God Almighty for his blessings for successful completion of the research work.

Sreenivasan P.V.

Preface

The mechanical properties of polymer blends are strongly influenced by the strength of the interfaces between the different phases. Polymeric materials gain their strength and toughness from molecular entanglement or crosslinking between the chains. The main hindrance to crack propagation is the energy dissipated in the inelastic deformation around the nick. This deformation is triggered by the high stresses borne by the chains right at the crack tip. In uncrosslinked polymers chains at the crack-tip are not entangled on both sides of the interface and often experience facile pullout, initiating little inelastic deformation and contributing nothing to toughness. Interfaces between polymer phases are normally narrow in incompatible blends compared to average distance between entanglements along a chain, so there is little cross-interface entanglement. Hence, the strengths or toughness of interfaces are normally low.

The most common way to strengthen a polymer-polymer interface is to incorporate or synthesise a block or graft copolymer at the interface, so that one of the two types of block or graft chains mixes with each of the two substrate polymers. As long as the block or graft chains are long enough to entangle with the substrate polymers, the copolymer will increase the mechanical coupling and normally strengthen the interface. The other main reason for introducing block or graft copolymers into polymer blends is to refine the phase size by decreasing interfacial tension and suppressing phase coalescence. Effective phase size control does not require the block or graft copolymer chains to be long enough to entangle with those of the substrate polymers, so selection of the right compatibiliser at the optimum levels increases the interfacial area and interfacial adhesion..

The present study aims at the preparation of an ABS (acrylonitrile-butadiene-styrene) type toughened thermoplastic by melt blending

polystyrene (PS) and powdered nitrile rubber (NBR). The product is an interesting class of toughened thermoplastic, which would combine the superior mechanical and processing characteristics of PS and the excellent oil-resistant properties of NBR. In this thesis an attempt has been made to investigate systematically the effect of compatibilisation and dynamic vulcanisation on the morphology and properties of powdered nitrile rubber toughened polystyrene.

The results of the investigation on the compatibilisation of powdered nitrile rubber toughened polystyrene in this thesis are divided into seven chapters.

Chapter 1 presents the fundamentals of blending, need for compatibilisation and morphology development. A review of the current research in this field is also presented.

Chapter 2 discusses various materials used for the study. The experimental techniques used for blending, sample preparation and measurement of various properties are also discussed.

Chapter 3 focuses on the preparation of toughened thermoplastic polymer by melt blending polystyrene with uncrosslinked and partially crosslinked powdered nitrile rubber powder (NBR and XNBR) and to evaluate mechanical properties, morphology, dynamic mechanical properties, melt rheology and thermogravimetric analysis of the resulting blends.

Chapter 4 discusses the effects of dynamic crosslinking on the morphology, mechanical properties, dynamic mechanical properties, melt rheology and thermal properties of powdered nitrile rubber toughened polystyrene.

Chapter 5 discusses the compatibilisation of powdered nitrile rubber toughened polystyrene with maleic anhydride modified polystyrene (MAPS) and phenolic modified polystyrene (PhPS). The effect of compatibilisation on morphology, mechanical properties, dynamic mechanical properties, rheological

characteristics and thermal properties of nitrile rubber toughened polystyrene is also explained in this chapter.

Chapter 6 deals with the effect of styrene-acrylonitrile copolymer (SAN) as a compatibiliser for powdered nitrile rubber toughened polystyrene was investigated. The effect of compatibilisation on the mechanical properties, morphology, dynamic mechanical properties, rheological characteristics and thermal properties of nitrile rubber toughened polystyrene is also given.

Chapter 7 is the concluding chapter with emphasis on the major findings of the present work.

CONTENTS

Chapter 1

Introduction

Plastics play an important role in our daily lives. They are one of the most useful materials ever created. Plastics can be flexible or rigid and they can be shaped into an endless variety of objects, ranging from car bumpers to squeezable bottles and soft fabrics. Plastic products, especially those used by industries, often have a useful life of many years. According to their structure and behaviour, plastics can be classified as thermoplastics and thermosetting plastics or thermosets.

Thermoplastics soften or melt on heating and can be converted into any shape before they cool down to a solid. Melting and solidification of these polymers are reversible and they can be reshaped by the application of heat and pressure, each cycle causing some deterioration in properties. Their polymer chains consist of linear or branched chain molecules having strong intramolecular bonds but weak intermolecular bonds. They are semi-crystalline or amorphous in structure and the chains can move freely each time the plastics are melted or softened. They generally require less time to solidify compared to thermosets which undergo a cross-linking reaction before solidification. Important commercial examples include polyethylene, polyvinyl chloride, polystyrene, polypropylene, polyamides, polycarbonate, polyacetals and polyesters.

Thermosetting plastics have cross-linked or network structures with covalent bonds between molecules. Once solidified by the cross-linking process, they cannot be remelted or reshaped. Since thermosets cannot be remelted, engineers use them in applications that require high resistance to heat. Common examples include phenolics, aminoplastics, silicones, epoxy resins and unsaturated polyester resins.

1.1 Polystyrene

Styrene readily polymerises to polystyrene (PS) by a relatively conventional free radical chain mechanism. Either heat or initiators will begin the polymerisation. Initiators thermally decompose, thereby forming active free radicals that are effective in starting the polymerisation process. Typical initiators used in the suspension process include benzoyl peroxide and di-tert-butyl per-benzoate. Potassium persulphate is a typical initiator used in emulsion polymerisation. In the presence of inert materials, styrene monomer will react itself to form a homopolymer.

Polystyrene is an odourless, tasteless, rigid thermoplastic. PS has the following repeating unit in its molecular structure.

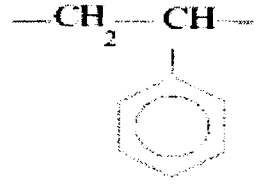

The homopolymer of styrene are also referred to as general purpose or crystal polystyrene. Because of the brittleness of crystal polystyrene, styrene is frequently polymerised in the presence of dissolved polybutadiene rubber to improve the strength of the polymer. Such modified polystyrene is called high

impact polystyrene (HIPS). The styrene content of HIPS varies from 88 to 97 percent.

Polystyrene is fourth largest thermoplastic by production volume. It is used for applications in the following major markets: packaging, consumer/institutional goods, electrical/electronic goods etc. Injection moulded grades of polystyrene are extensively used in the manufacture of cosmetic containers and photo film packages. Other polystyrene items include refrigerator door liners, audio and video cassettes, toys, picture frames, kitchen utensils, radio and television cabinets and computer housings.

1.2 Origin and development of rubber toughened plastics

The technology of rubber toughening, which involves blending small amounts of rubber with rigid polymers in order to increase their fracture resistance, has been used commercially in the late 1940s, when manufacturers began to produce `high-impact' grades of polystyrene, poly(styrene-co-acrylonitrile) (SAN) and poly(vinyl chloride) (PVC); the resulting products, high impact polystyrene (HIPS), acrylonitrile-butadiene-styrene (ABS)and rubber toughened polyvinyl chloride (RT-PVC) - are now well established as `commodity' polymers.

Multiphase polymers, in which a soft, rubber-like, toughening phase is combined with a rigid glassy or crystalline component, offer significant advantages over homogeneous glassy polymers. However, these advantages are obtained only when the properties of the two phases, their morphology, and the quality of the interface between them are carefully chosen or designed to meet certain criteria: The rigid phase should be relatively stiff, but ductile, with the ability to reach high tensile strains, and a shear yield stress that is not too high. Preferably, the shear modulus of the rubber phase should be as low as possible, the rubber should be present as discrete particles, and the level of adhesion between the rubber and rigid phase should be very high. The concentration φ and average diameter d of the

particles are very important, as is the distribution of particle sizes. Impact resistance increases with Φ but falls sharply when d is reduced below a critical diameter, which in the case of toughened PA 6 at 23°C is about 0.2 μm [1]. Toughness also decreases when the particle size is too large. It has been suggested by Wu [2] that the key parameter is not the particle size but the inter particle spacing, which is a function of both d and φ. In order to absorb energy at the tip of a notch or a propagating crack, the multiphase polymer must first strain-soften (yield), and then strain-harden, so that a limit is imposed on the local strains in the most highly stressed regions of the material. When the polymer exhibits this type of behaviour, regions further from the crack tip then begin to deform plastically, the yield zone spreads, and the fracture toughness is high. Stress fields at crack tips are largely dilatational in nature, especially in thick sections, and therefore tend to promote crack propagation rather than yielding. The most effective solution to this problem is to develop materials that form dispersed micro voids in the most highly stressed region ahead of the crack tip, thereby allowing the material to strain-soften and draw. This type of dilatational plastic response has been observed in many tough multiphase polymers, and probably applies to all members of this class. The soft phase provides sites for the initiation of voids, while the adjacent rigid phase not only yields but also strain hardens, through extension of its entangled network of long chains. The mechanism of strain hardening, which is more accurately, described by the term 'orientation hardening' is most clearly observed in cross-linked rubbers. Haward and Thackray [3] have drawn attention to the similarity between the ductile drawing behaviour of thermoplastics and the stress-strain behaviour of crosslinked rubbers, which have common origins.

1.3 Toughening mechanisms

The principal mechanisms of inelastic deformation in rubber toughened plastics are multiple crazing and shear yielding in the rigid matrix phase and cavitation in the dispersed soft rubber phase

1.3.1 Multiple crazing

The principal toughening mechanism in brittle polymers is matrix crazing. Under an applied stress, crazes are initiated at points of maximum principal strain, typically near the equator of rubber particles and propagate outwards normal to the maximum applied stress [4, 5]. Craze growth is terminated when another rubber particle is encountered, preventing the growth of very large crazes. The result is a large number of small crazes in contrast to a small number of large crazes formed in the same polymer in the absence of rubber particles. The dense crazing that occurs throughout a comparatively large volume of the multiphase material accounts for the high energy absorption observed in tensile and impact tests and the extensive stress whitening which accompanies deformation and failure.

A craze actually contains fibrils of polymer drawn across, normal to the craze surfaces, in an interconnecting void network [6, 7]. The void network is established at the craze tip. The craze tip advances by a finger like growth produced by the meniscus instability mechanism [8]. The fibrils are formed at the polymer webs between void fingers and contain highly oriented polymer with the chain axis parallel to the fibril axis [9]. As the craze tip advances, the craze thickens by drawing in more polymers from the craze surfaces. In the presence of relatively strong craze fibrils, that makes the craze load bearing and consequently differing from crack. It has been demonstrated experimentally in polymer matrices which fail by crazing that the optimum rubber particle size in the range 1–5 μm [10]. Donald and Kramer [11] studied the craze initiation mechanism in HIPS and suggested that the ease of initiation is related to particle size and that crazes are

rarely nucleated from particle sizes less than about 1 μm. They proposed two criteria necessary for craze initiation from a rubber particle:

- the initial elastic stress concentration at the rubber particle must exceed the stress concentration at a static craze tip;
- the distance over which this critical stress acts must extend at least three fibril spacing from the particle into the glassy matrix.

HIPS is usually prepared by polymerization of styrene monomer containing about 5–10 % of dissolved rubber. As the polystyrene forms, phase separation of rubber occurs as dispersion in the polystyrene solution. However, the dispersed rubber particles are swollen with styrene monomer, which continues to polymerise and forms a dispersion of polystyrene within the dispersed rubber particles [12]. This system has three-phase morphology. It was discovered that the larger particles only contained occluded polystyrene in the particle while the smaller ones tended to be rubber alone. This non-uniformity of particles appears to reduce the chances of premature craze breakdown. When crazes form around the rubber particles either by initiating or by intersecting them, significant lateral contraction and accompanied elongation of the particle in the applied stress direction occurs. As the contraction proceeded, debonding at the particle- craze interface resulted and a void was thus formed. Under increasing load the void grew, resulting in premature craze breakdown and subsequent crack initiation and propagation. In the non-uniform particles, occluded polystyrene accommodates the displacements due to crazing by local fibrillation of the rubber surrounding each subinclusion, without the formation of large voids.

Figures 1.1 and 1.2 are two electron microscope images of HIPS. One is taken from a tensile bar that was taken past its yield point, unloaded, stained with OsO_4 and then microtomed; the other was stretched in-situ in the TEM. Both show

evidence of fibrillation, which occurs not only in the PS matrix but also in the rubber phase.

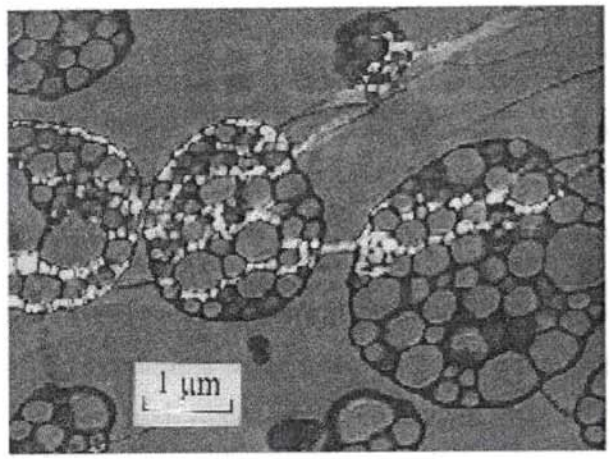

Fig. 1.1: Section of deformed HIPS, showing fibrillation in the rubber phase and crazing in the matrix. Specimen strained and prestained with osmium tetroxide.

[C.B. Bucknall, Journal of Microscopy, 201, 221(2001)].

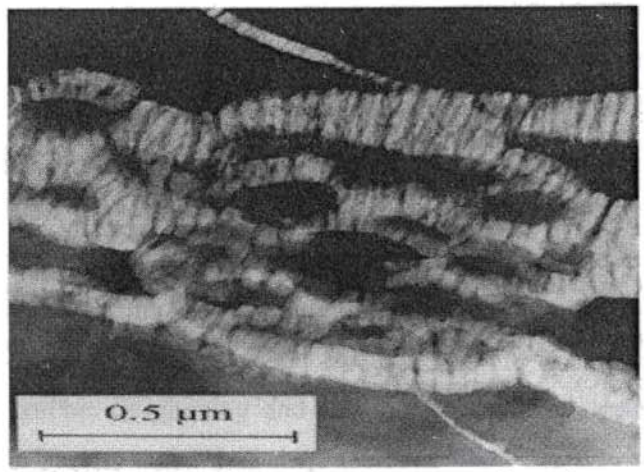

Fig.1.2: Section of HIPS strained in situ on the stage of an electron microscope, showing fibrillation of the rubber phase and crazing in the PS matrix.

[C.B. Bucknall, Journal of Microscopy, 201, 221(2001)].

From figure 1.1 it is evident that the rubber is present not as simple homogeneous spheres, but as complex particles with roughly spherical sub-inclusions of polystyrene embedded in the continuous polybutadiene (PB) phase.

The sub-inclusions are separated by thin membranes of rubber, which fibrillate in response to high tensile stresses, thereby providing an effective mechanism of strain softening. Grafting reactions ensure a good bond between PS and PB, so that the fibrillated rubber phase, when fully extended, is able to sustain high stresses and thus act as a strain hardening element in the deformation.

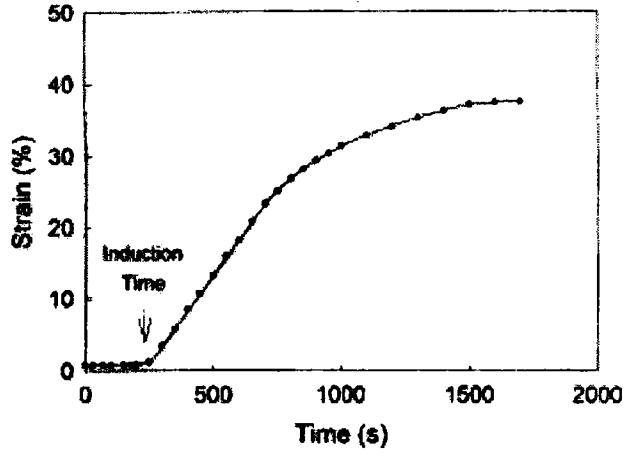

Fig.1.3: Creep curve for HIPS, showing strain softening, drawing and strain hardening. **[B. O'Connor, C.B. Bucknall, & J.L. Hahnfeld, Plast. Rubber Compos. Process Appl. 26, 360 (1997)]**

The strain-softening and strain-hardening effects due to fibrillation of the rubber particles and subsequent stretching of the fibrils are well illustrated in figure 1.3, which shows the creep behaviour of a HIPS specimen in tension. At short

loading times, cavitation begins in a few of the larger rubber particles, and crazes grow from these initiation points. As the crazes extend and thicken, cavitation is initiated in other rubber particles, and the creep rate accelerates (strain-softening), reaching a steady state at a strain of about 5%. The fibrils in some rubber membranes become fully stretched, thus limiting craze thickening in the adjacent matrix, but the strain rate is maintained through fresh cavitation in other rubber membranes. Eventually, a stage is reached at which most of the rubber has fibrillated, and no new crazes are initiated. The creep rate then falls, tending towards zero (strain hardening).The ability of well-designed, composite rubber particles both to initiate multiple crazing and to prevent the toughened polymer from reaching excessively high strains is a key feature of standard HIPS.

1.3.2 Shear yielding

Shear yielding is the usual mechanism of plastic deformation in ductile solids. In polymers deformation tends to be concentrated into localized bands. Newman and Strella [13] proposed that shear yielding in the matrix was responsible for rubber toughening of plastics. Mechanical property and optical property studies on ABS materials showed that in tensile tests, necking, drawing and orientation hardening occurred together with localised plastic deformation of the matrix around the rubber particles, indicative of shear yielding. The function of the rubber particles was to produce enough triaxial tension in the matrix so as to increase the local free volume and consequently to initiate shear yielding and drawing of the matrix. This proposal did not account for stress whitening characteristic of rubber toughening and the fact that triaxial tension promotes crazing and brittle fracture rather than shear yielding.

It is now generally accepted that the shear yielding mechanism constitutes cavitation of rubber particles followed by extensive shear yielding throughout the

matrix [14-17]. The cavitation of the rubber particles explains the observed stress whitening, as light scattering occurs which is enhanced by the holes enlarging. The voids created by cavitated rubber particles act further as stress concentrators [18]. Although cavitation of the rubber particles does not involve energy absorption, the enhanced shear yielding of the matrix is the major energy absorbing mechanism. However, cavitation of the rubber particles is a prerequisite for enhanced toughness where shear yielding is the principal mechanism.

Because of their high plastic strains, shear bands are strongly birefringent, and therefore easy to see in a polarizing light microscope. In PS and other relatively brittle polymers, there is little evidence of shear bands when the material is deformed in tension. To observe them, it is necessary to subject the polymer to compression. With appropriate lighting, it is possible to see shear bands in a transparent glassy polymer with the naked eye. Straining alters the refractive index tensor within the shear band, so that light is reflected from the interface between the optically anisotropic band and the adjacent, isotropic, bulk polymer.

It is more difficult to observe shear bands using electron microscopy, especially in non-crystalline polymers. In some cases, the magnitude of plastic deformation is so high that it becomes evident in the high levels of distortion in the second-phase particles. The most effective method for observing shear bands at lower overall strains is to use chemical etching. Plastic deformation raises the free energy of the polymer, and makes it more susceptible to chemical attack. For example, shear bands in PS are preferentially etched by concentrated chromic-phosphoric acid, which also attacks PB and other rubbery polymers. This method has been used to observe shear bands and rubber particles in ABS, and in blends of HIPS with poly 2, 6-dimethyl-1, 4-phenylene oxide [19]. The etched specimens can be studied using either reflection OM or SEM, or alternatively used to make replicas for examination by TEM.

1.3.3 Crazing and shear yielding

Crazing and shear yielding may occur simultaneously in many other rubber toughened plastics. The dominant mechanism is the one by which the unmodified matrix would typically fail. The contribution of each mechanism to the toughening of the system depends on a number of factors such as the rubber particle size and dispersion, concentration of the rubber particles, rate and temperature of the test.

1.3.4 Cavitation in rubber particles

Observations of void formation within rubber particles have been reported since the early 1970s [20]. In some cases, there are simple spherical voids in homogeneous particles. In others, cavitation takes more complex forms, as in the fibrillated rubber membranes shown in figures 1.1and 1.2. For many years these cavitation processes were largely ignored as being of no importance, or even artefacts, but there is now an increasing recognition that they play a critical role in the toughening mechanism.

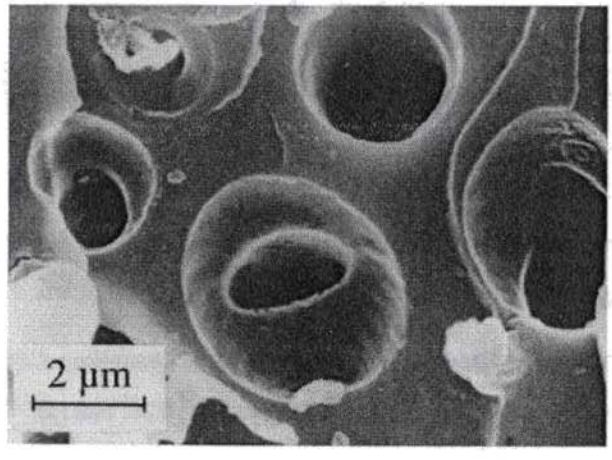

Fig. 1.4: Scanning electron micrograph of toughened epoxy resin, showing cavitation of homogeneous rubber particles on the fracture surface and retraction of the surrounding rubber shell. **[A.J. Kinloch, Proc. Instn. Mech.Engrs, 211, 307 (1997)]**

The evidence for rubber particle cavitation comes from SEM studies of the fracture surfaces of rubber toughened epoxy resins. In most cases, there is a relatively deep hemispherical depression near the centre of each half particle, surrounded by a shallow depression where the surrounding shell of rubber has retracted after fracture, as illustrated in figure 1.4.

It is obvious that the growth of the central void is accompanied by expansion of the surrounding rubber shell and yielding in the adjacent matrix, so that the radius of the particle increases until the crack bisects it. It is important to note that this mechanism applies only to lightly crosslinked resins, which retain some ductility and can therefore benefit from the addition of rubber particles [21].

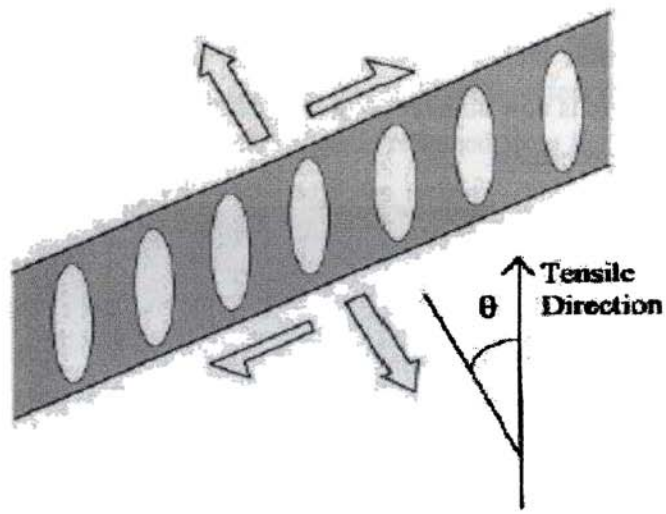

Fig. 1.5: Schematic diagram of a dilatational shear band. **[C.B. Bucknall, Journal of Microscopy, 201, 221(2001)].**

The association between cavitated particles and shear bands is an important one. They constitute a dilatation band as illustrated in figure 1.5. Bands of this type, which are also observed in metals, can deform by both shear in the plane of the band, and extension normal to it, thereby generating a dilatation.

The angle θ and the ratio of shear strain to volume strain depend upon: (a) the components of the local stress tensor; (b) the void content of the band; and (c) the pressure-dependence of the yield criterion for the bulk material. For an isotropic, void free material that obeys the von Mises or Tresca yield criterion, shear yielding occurs on planes of maximum shear stress, and the angle θ is therefore 45°. However, in polymers, because yielding is strongly dependent upon the mean stress σ_m, θ is typically about 38°. The introduction of voids increases the effect of σ_m on yielding, causing both a reduction in yield stress, and a decrease in θ.

Calculations by Lazzeri & Bucknall [22] on the behaviour of a cavitated polymer under uniaxial tension show that θ falls rapidly at void contents $\psi > 0.4$, reaching. $\theta = 0$ at $\psi = 0.53$. It is clear from the foregoing discussion that dilatation bands containing high volume fractions of cavitated rubber particles have much in common with crazes, and indeed a craze can be regarded as a particular type of dilatation band. However, it is useful to preserve the distinction between cavitated shear bands, in which the loss of cohesion is confined to a minor particulate phase, and crazes, which are formed by cavitation of a continuous matrix phase

The energy-balance theory developed by Lazzeri &Bucknall [23] shows that rubber particles cavitate when the dilatational strain energy stored in the surrounding material is large enough to initiate a void in the rubber. The dilatational strains might be at a higher level in the matrix than in the rubber particle, but cavitation will usually occur preferentially in the soft phase, where the resistance to void expansion is very much lower. Recent work by Bucknall [24] has

shown that the critical stage in cavitation involves surmounting an energy barrier at very small void sizes, and that thermal contraction stresses play an important part in generating the strain energy necessary to cross this minute energy barrier.

1.4 Miscibility and dispersion of the rubber phase

The rubber phase intended for rubber toughening must be dispersed as small particles in the plastic matrix. The particle size and size distribution of the dispersed particles will depend on the miscibility of the two phases and on the way in which they are mixed. If the miscibility is good, the particles of the rubber will be too small to promote toughening and may even be distributed on a molecular scale. If the two phases are immiscible, the rubber may be dispersed as macroscopic particles and too large to give toughening.

1.5 Problems with immiscible blends

Most immiscible blends have inferior mechanical properties relative to their components, and their phase morphology strongly depends on their processing history. The primary cause of such behaviour is the unfavourable interaction between molecular segments of the components, which is responsible for their immiscibility. An unfavourable interaction leads to (a) a large interfacial tension in the melt, which makes it difficult to disperse the components finely enough during mixing and drives phase rearrangements during low stress conditions, and (b) poor interfacial adhesion in the solid state, which causes mechanical failure. Compatibilisation of the two phases can be effected by the addition of appropriate block or graft copolymers that act as interfacial agents [25-34]. For effective compatibilisation, the molecular weight and architecture of the block copolymer need to be carefully optimised: Low molecular weight block copolymers tend to diffuse to the interface rapidly, but do not provide stability of morphology [35] while higher molecular weight block copolymers are

ineffective, because they do not readily diffuse to the interface and they have a low critical micelle concentration [36].

1.6 Miscibility of polymers: compatibilisation

Components that resist gross phase segregation and/or give desirable properties are frequently said to have a degree of compatibility. There are two types of compatibility, thermodynamic and technological [37-39]. Homogeneous miscibility in polymer blends requires a negative free energy of mixing:

$$\Delta G_{mix} = \Delta H_{mix} - T\Delta S_{mix}$$

However, if two high molecular weight polymers are blended, the gain in entropy, ΔS_{mix} is negligible, and the free energy of mixing can only be negative if the heat of mixing, ΔH_{mix} is negative. In other words, the mixing must be exothermic, which requires specific interactions between the blend components. These interactions may range from strongly ionic to weak and nonbonding interactions, such as hydrogen bonding, ion-dipole, dipole-dipole and donor acceptor interactions. Usually, only van der Waals interactions occur, which explains why polymer miscibility is the exception rather than the rule. The miscibility behaviour of two polymers is strongly dependent on temperature. Each polymer pair is characterized by an interaction parameter, which usually exhibits such a temperature dependence that possible miscibility at lower temperatures is lost at higher temperatures, e.g. during processing.

1.7 Role of compatibilisers in blending process

Compatibilisers are macromolecules species exhibiting interfacial activities in heterogeneous polymer blends. Usually the chains of a compatibiliser have a block structure with one block miscible with one polymer component. These block structures can be premade and added to the immiscible polymer blend, but they can also be generated in-situ during the blending process. The latter procedure is called

reactive compatibilisation and mutual reactivity of both blend components is required. Figure 1.6 presents a schematic picture of the supposed conformation of some compatibiliser molecules at the interface of a heterogeneous polymer blend.

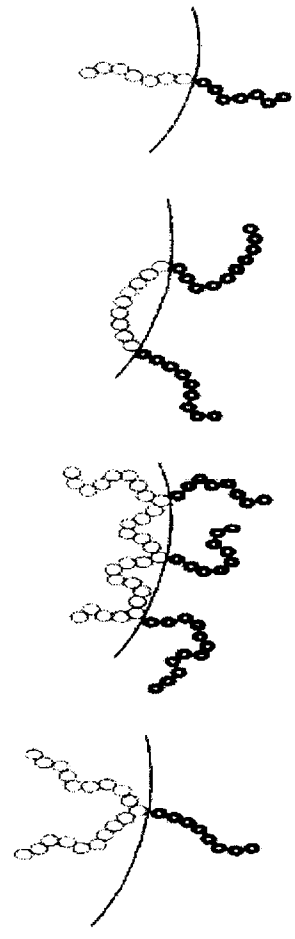

Fig. 1.6: Schematic picture of conformations for diblock, triblock, multi graft and single graft copolymers at the interface of a heterogeneous polymer blend.
[C. Koning *et al.* Prog. Polym. Sci., 23, 707 (1998)]

In the figure diblock, triblock, multi grafted and single grafted copolymers are shown. A heterogeneous blend of polymers A and B can be compatibilised by a diblock copolymer poly (C-b-D), provided that block C is miscible with polymer A (block C can also be polymer A) and that block D is miscible with polymer B (block D can also be polymer B), since phases A and B are merely solvents for blocks C and D, respectively. The mutual miscibility of phase A with block C and phase B with block D implies specific interactions between A and C, B and D, a poly (C-b-D) is usually the more effective compatibiliser for blend A/B.

The role of compatibilisers in the blending processes is firstly to retard the formation of Rayleigh disturbances on the generated threads of polymer, as a result of decreased interfacial tension. The presence of compatibiliser molecules at the surface prevents coalescence during subsequent processing. Compatibilisers are thus able to stabilise a fine morphology. Each block of a poly compatibiliser penetrates into the parent phase deeply enough to entangle with the consecutive chains and the interfacial adhesion is enhanced. Good interfacial adhesion is essential for stress transfer from one phase to the other. Refinement and stabilisation of the phase morphology and the enhancement of the interfacial adhesion usually upgrade an inferior and useless immiscible polymer blend to an interesting material.

1.8 Strategies for compatibilisation of polymer blends

There are several methods to compatibilise immiscible polymer blends. A detailed discussion with special reference to non reactive and reactive compatibilisation is given below.

1.8.1 Addition of graft and block copolymers

The emulsification of polymer blends has been proposed as the most efficient tool for obtaining fine phase morphology and good mechanical properties. The best way to validate that concept is to tailor block and grafted copolymers and

to investigate the beneficial effects that they can have on immiscible polymer blends. That approach allows the main molecular characteristic features of block and graft copolymers to be changed in a systematic way, for example, molecular architecture, composition and molecular weight, so that basic relationships can be drawn between the structural characteristics of these additives and the general properties of the polyblends.

Early efforts were concentrated on blends of diblock copolymer with homopolymers possessing repeat units identical or chemically similar to each segment of the copolymer. This type compatibilised blend will be designated as A/B/A-B system where the A-B diblock is an entropic acting copolymer. The emulsification of PE and PS blends by copolymer consisting of hydrogenated plybutadiene (HPB) and PS has been extensively studied by Fayt *et al* [40]. Recently this approach has been extended to A-C diblock copolymer, for filling the incompatibility gap between some A/B pairs, provided C is miscible with B. sPMMA containing diblocks are among the most universal compatibilisers for the A/B/A-C type systems. sPMMA is indeed quite miscible a number of important polymers (PVC, PVDF, SAN etc.) and it can be copolymerised in a two step living polymerisation with styrenes and dienes [41]. Another valuable family of diblock copolymers is based on PCL [42] which is miscible with phenoxy, SAN, PVC, nitrocellulose, PECH, Chlorinated polyether [43], Saran [44], chlorinated polystyrene [45], CPE [46], PC [47] and polyesters such as PET and PBT [48].

The use of graft copolymers is another possible route for the control of phase morphology and mechanical properties of immiscible polymer blends. In addition to polymer-polymer or polymer-monomer reactions a large variety of macro monomers has been prepared as precursors of graft copolymers [49, 50] with some control on the copolymer structure, since the length and number of grafts are dictated by the macro monomer molecular weight, the comonomer feed

and the comonomer reactivity ratios. Recently, ω-dihydroxy PS has been synthesized as a macro monomer for the synthesis of poly (PBT-g-styrene). The SEM analysis of fracture surfaces of blends containing PBT/PS 70/30 by weight shows spherical PS domains with diameters ranging from 1 to 4 μm. In addition, during the fracture process, many domains are pulled away from their previous positions and the surfaces of holes left by removed PS spheres appear to be very smooth. These observations suggest a poor compatibility between PBT and PS. As PBT-g-PS is added (10%) to the incompatible blend, the domain sizes of PS are reduced and the interface between the two phases becomes more diffuse. These features demonstrate the compatibilising effect of PBT-g-PS in the PBT/PS blend. Also, increased modulus, elongation at break and impact strength were observed in PBT/PS blend containing up to 10% compatibiliser [51].

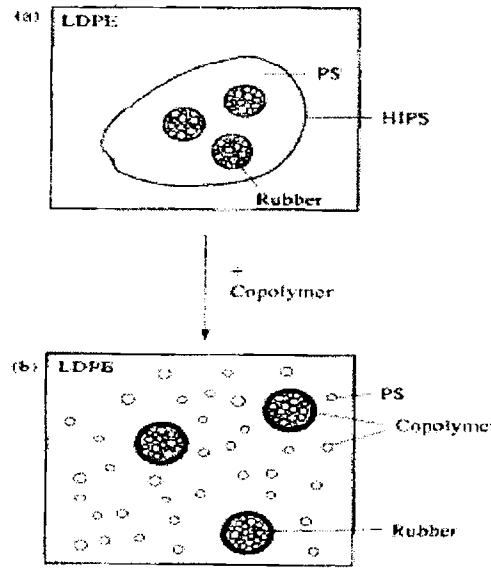

Fig. 1.7: Effect of the HPB-b-PS diblock copolymer on the dispersion of HIPS in a PE matrix. **[C. Koning *et al.* Prog. Polym. Sci., 23, 707 (1998)]**

Fayt and Teyssie [52] have studied the emulsification of LDPE and commercial HIPS blends by a hydrogenated tapered block copolymer of butadiene and styrene (MW= 80,000). In this diblock, there is smooth transition from pure PB block (MW= 32,000) to pure PS block (MW= 26,000) through an intermediate section of MW= 22,000 [53]. As expected the phase morphology of neat LDPE/HIPS blends is coarse and heterogeneous at all compositions and the interfacial adhesion is very poor. Upon the addition of the block copolymer (5%) there is a marked decrease in the particle size and a significant enhancement of the interfacial adhesion. Figure 1.7 illustrates the state of dispersion of HIPS in LDPE. Upon the addition of the hydrogenated poly (butadiene-b-styrene), PS becomes finely dispersed in LDPE whereas the PB particles still coated by an adherent layer of PS. This assumption is convincingly supported by the stability of the rubber particles against coalescence when LDPE content is decreased. Furthermore there is an improvement of the ultimate mechanical properties of the LDPE/HIPS blends when the diblock copolymer is added.

Braun *et al* [54] have investigated the compatibilising efficiency of a block-graft copolymer, which is prepared by radical grafting on a block copolymer, in immiscible PVC/PS blends. The copolymer PS-b-(PB-g-PCHMA), was prepared by radical grafting of cyclohexyl methacrylate on to the PB block of a PS-b-PB copolymer. As a result a long PS block is connected to PCHMA blocks through short PB segments. This copolymer refines the morphology of an immiscible PS/PVC (50/50) blend by forming an interfacial layer.

1.8.2 Reactive compatibilisation

An attractive alternate method for compatibilisation is to form the block or graft copolymer in situ during blend preparation via interfacial reaction of added functionalised polymeric components [55-57] as illustrated in figure 1.8. The functional groups may be the reactive chain ends that occur naturally in

condensation polymerisation provided that end- capping techniques are not used. For addition polymers, functional groups can be placed along the chain by copolymerisation or by grafting or at the chain end by special techniques [55, 56]. The functional groups must be carefully selected to ensure that adequate reaction can occur within the limited time-frame of melt processing, for which the only opportunity for encounter is within the interfacial region between the two polymer phases. Formation of the copolymer species at the interface reduces the interfacial tension; leads to steric stabilisation, which retards dispersed phase coalescence and strengthens the interface, in the solid state, between phases. A primary benefit is the significant reduction in the dimensions of the phase domains, which is critical for achieving good physical properties of the blend. In addition the morphology of the blend is more stable and predictable, which broadens the processing or fabrication conditions that can be used.

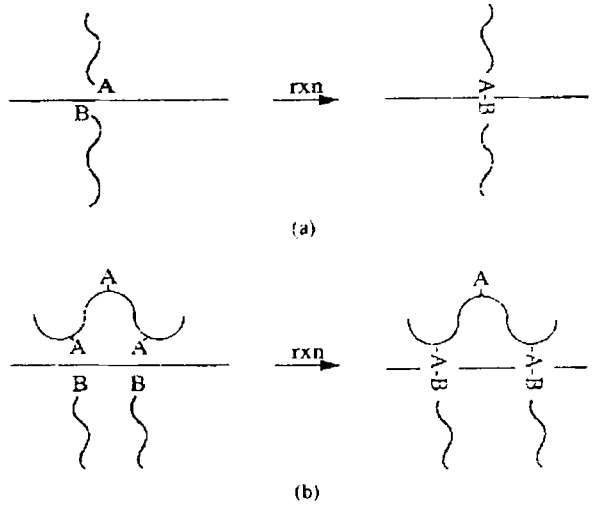

Fig. 1.8: Reaction of polymer-bound functional groups A and B to form (a) a block copolymer and (b) a graft copolymer at the interface between two immiscible polymer blends. **[D.R. Paul, C.B. Bucknall, eds. Polymer Blends, Vol.1, Ch.17, Wiley-Interscience, New York, (2000)]**

Theoretical predictions [58] show that presence of appropriate block or graft copolymers leads to reduction in the interfacial tension between phases in immiscible blends. The block or graft copolymers generated in-situ during the process of melting through reaction between chemical functionalities available on the polymer chains [59-100] affect the blend morphology and properties. It is important to note that the generation of morphology in multiphase polymeric systems through chemical reactions is a dynamic process. As breaking down the dispersed phase through interfacial reactions creates more surface area, the probability becomes higher for functional groups to find each other to react to form more copolymer, which results in an even finer dispersed particle size. However there are both chemical and physical limitations on the extent to which this process can proceed. The limitations of reaction kinetics can be severe, since the residence time in commercial compounding devices, typically extruders is on the order of one minute and the reaction can occur only at the interface between phases. Eventually, the surface density of copolymers at the interface could build up to a level that physically precludes further unreacted chains from coming together. Recent analysis of reactive interfaces [101,102] suggests that the interface becomes too crowded with copolymer before significant reduction in interfacial tension occurs. This suggestion implies that the dominant mechanism of reducing particle size is the suppression of droplet-droplet coalescence through steric hindrance at the interface.

Functional groups useful for reactive compatibilisation can be incorporated into polymers in a variety of ways. For example, anhydride units can be introduced by grafting [103-107] or copolymerisation [108] of maleic anhydride, end capping [109] and other schemes [110,111]. Among these schemes, reactive grafting has been the method of choice for attaching maleic anhydride groups into several polymers including polyolefines [103-107] polyphenylene ether (PPE) [112,113] and ABS [114]. For polyolefines, grafting is achieved by mixing the polymer with

maleic anhydride (MA) and an initiator in an extruder at elevated temperatures [107]. Various mechanisms have been proposed by Gaylord [104-106] for the grafting of MA to both unsaturated and saturated polyolefins. Heinen *et al* [107] concluded that MA is attached to polyolefins through a variety of mechanisms. When the polyolefin contains only methylene carbon atoms, MA is attached in the form of single succinic anhydride rings as well as oligomers. When there are tertiary hydrogen atoms, as in polypropylene, MA grafts onto the polymer backbone primarily in the form of single succinic anhydride groups, and chain scission often occurs, so that the anhydride unit is attached to the end of a short chain.

Reactive polymers undergo the usual chemical reactions seen in low molecular weight materials. However, there are a number of factors that limit the extent of reaction. For example, the steric hindrance to the reaction sites by polymer backbone reduces the reaction rate [115]. The reaction rate can also be reduced by the restricted diffusional mobility of the functional groups in the melt stage. The low concentration of the functional groups and the short reaction time are two other limiting factors that further limit the extent of reaction efficiency. Therefore in order to achieve successful compatibilisation of polymer blends, the polymers must have sufficiently reactive functional groups; the reaction should be fast, selective and preferably irreversible; and mixing conditions should be such as to minimize mass transfer limitations to reaction.

1.8.3 Addition of reactive polymers

The addition of a reactive polymer, miscible with one blend component and reactive towards functional groups attached to the second blend component results in the "in-situ" formation of block or graft copolymers. This technique has certain advantages over the addition of premade block or graft copolymers. Usually reactive polymers can be generated by free radical copolymerization or by melt

grafting of reactive groups on to chemically inert polymer chains. Furthermore, reactive polymers only generate block or graft copolymers at the site

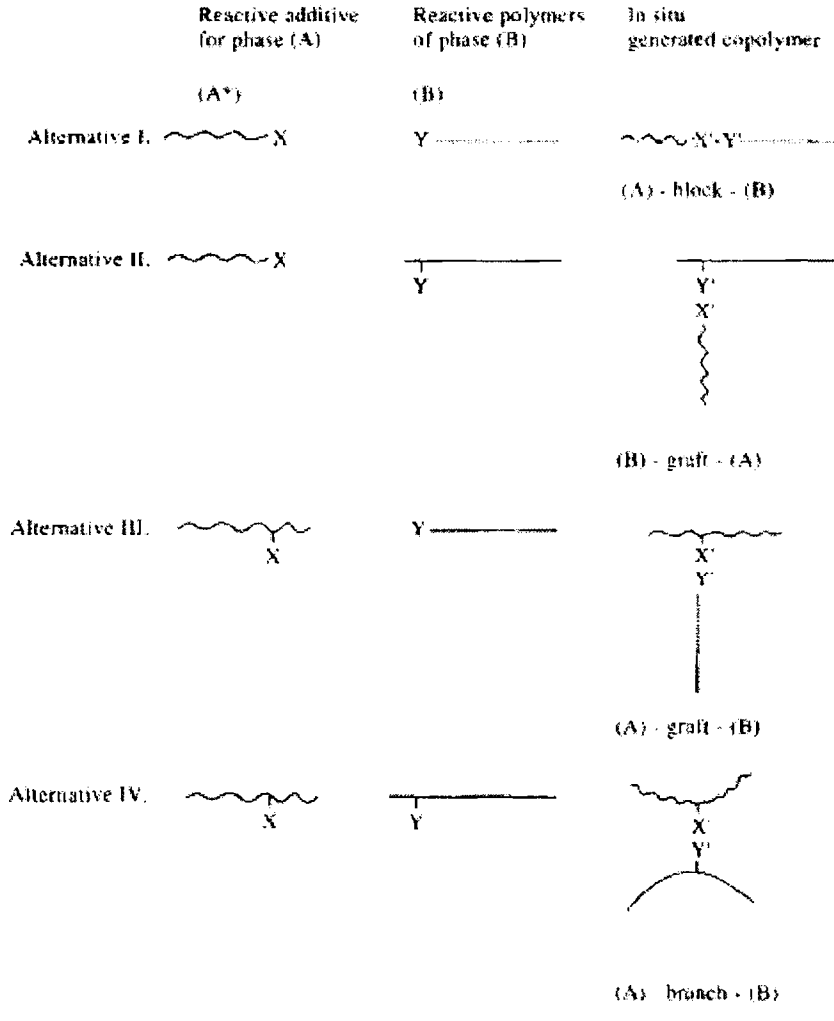

Fig. 1.9: Block and graft copolymer precursors and type of copolymer formed during reactive processing. **[C. Koning *et al.* Prog. Polym. Sci., 23, 707 (1998)]**

where they are needed, i.e. at the interface of an immiscible polymer blend. Although graft and (especially) block copolymers may form micelles after being added to or formed in a blend, the chance that the critical micelle concentration exceeded is actually higher in the case of pre-made structures. This is a drawback with respect to the efficiency of the compatibiliser. Finally, the melt viscosity of a linear reactive polymer is lower than that of a pre-made block or graft copolymer, at least if the blocks of the premade copolymer and the reactive blocks are of similar molecular weights. Lower molecular weight polymers will diffuse at a higher rate towards the interface. This is of utmost importance in view of the short processing times used in reactive blending which may be on the order of a minute or less. In order to successfully apply reactive polymers as block or graft copolymer precursors, the functional groups must have suitable reactivity in order to react across the melt phase boundary during the short blending time. In addition, the generated covalent bond must be sufficiently stable to survive subsequent processing conditions. Figure 1.9 illustrates the different block and graft copolymer precursors that can be added to a blend of immiscible polymer A and polymer B, as well as the type of copolymer formed. The unmodified polymer A is assumed to be unreactive towards polymer B. The reactive, polymeric additive (left column in scheme) may be either an X-functionalized polymer A or an X-functionalized polymer C, provided that polymer C is miscible with polymer A. Polymer B is supposed to have either end-reactive or pendant-reactive groups For example, amine and carboxylic acid groups if B is a polyamide, or succinic anhydride if B is a styrene-maleic anhydride copolymer.

1.9 Dynamic vulcanisation

Dynamic vulcanisation is a route to new thermoplastic elastomers which have properties as good or even in some cases, better than those of block copolymers. These new materials are prepared from blends of existing polymers, thereby eliminating new processes and materials. In short, dynamic vulcanisation is

a cost effective technique to achieve better properties. Improvements in properties include reduced permanent set, improved ultimate mechanical properties, improved fatigue resistance, greater resistance to attack by fluids at elevated temperature, improved high temperature utility, greater stability of phase morphology in the melt, greater melt strength and more reliable thermoplastic fabricability.

Dynamic vulcanisation is the process of vulcanising the elastomer during its melt mixing with a non-vulcanising thermoplastic polymer. The introduction of crosslinks in to one of the phases increases the viscosity of that phase leading to a change in the morphology of the blend [116,117]. The uncrosslinked phase is unaltered by the vulcanisation in the other phase, permitting easy processing of the blend. The modified blend can be additionally compounded, if required, and formed to shape. Because dynamic vulcanisation takes place inside the mixer, the mix cycle should be as short as possible, for economic reasons. It must be noted that thermoplastic elastomers (TPEs) are the fastest growing part of the elastomer market (12% per year).The world use of thermoplastic vulcanisates (TPVs)in 1995 was about 60 ktons [118].

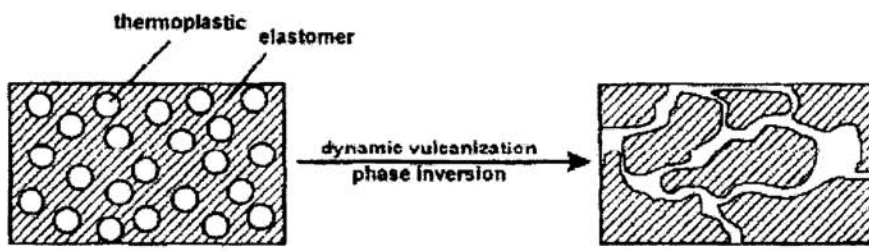

Fig. 1.10: Morphology of a thermoplastic/rubber blend before and after dynamic vulcanisation. **[C. Koning *et al.* Prog. Polym. Sci., 23, 707 (1998)]**

The morphological changes accompanying dynamic vulcanisation are shown in figure 1.10. Since an excess of rubber is used and the viscosities of the

thermoplastic and the rubber at the processing temperature do not deviate too much, the physical blend is a dispersion of the thermoplastic in a rubber matrix. Upon the addition of the crosslinking agent, the viscosity of the rubber phase increases and at a sufficient degree of curing phase inversion occurs [119]. The high degree of crosslinking of the rubber phase inhibits the process of strand break into smaller particles, the reduction of interfacial area by formation of smooth spheres and also the coalescence of the dispersed particles. As a result, the dispersion of a thermoplastic/rubber dynamic vulcanisate is very irregular (figure 1.10). The thin thermoplastic layers between the crosslinked rubber particles are somehow elastic and act as a kind of glue between the crosslinked rubber domains [120].

Thermoplastic vulcanisate compositions have been prepared from a great number of plastics and elastomers. However, only a limited number of elastomer-plastic combinations give technologically useful blends, even after dynamic vulcanisation. The best elastomer/plastic thermoplastic vulcanisates are those in which the surface energies of the plastic and elastomer are matched, when the entanglement molecular length of the elastomer is low and when the plastic is 15-30% crystalline [121].

The dynamic vulcanisation process was used by Gessler [122] in the preparation of semi-rigid elastomer-plastic compositions containing minor proportions of vulcanised elastomer. Fischer [123] used this process to prepare compositions containing varying amounts of partially vulcanised elastomer. Several recent articles deal with thermoplastic vulcanisates resulting from the dynamic vulcanisation of various rubber/plastic blends [124-129].

Sulphur/accelerator combinations, the most abundant crosslinking systems for static vulcanisation of elastomers, have been demonstrated to be applicable to dynamic vulcanisation of PP/EPDM blends [130]. An increase in the amount of

sulphur from 0 to 2.0 phr in combination with a standard zinc oxide/ stearicacid/ tetramethyl thiuram disulphide/ mercaptobenzathiazole vulcanisation recipe has resulted in a dramatic improvement of the elasticity of a 40/60 blend of PP/EPDM. The tensile strength increases from 4.9 to 24.3 MPa, the elongation at break increases from 190 to 530% and the tension set decreases from 66 to 16% (figure 1.11).

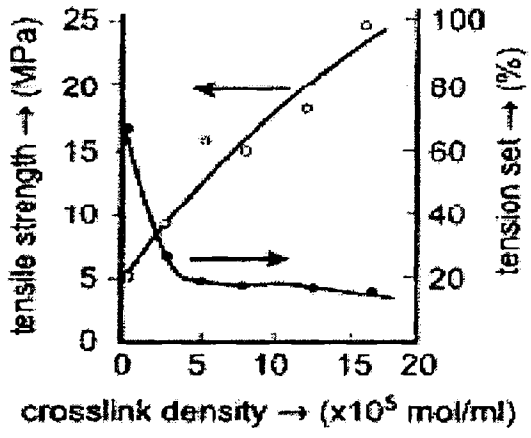

Fig. 1.11: Effect of crosslink density of the EPDM phase on tensile strength and tension setfor PP/EPDM 40/60 blends dynamically vulcanized with a sulphur cure system. **[C. Koning *et al.* Prog. Polym. Sci., 23, 707 (1998)]**

However, sulphur crosslinking systems are not used in commercial PP/EPDM TPVs, since PP has a relatively high melting point and the crosslinks lack thermal stability. Moreover, the production and processing of these TPVs suffer from severe stench problems. In the case of PP based TPVs, PP degradation by 1/3-scission may be initiated by the peroxide/co-agent cure system and this results in inferior properties. A specific crosslinking system, for example, PF resins prepared at high pH (resoles), is used in the commercial PP/EPDM dynamic

vulcanisation. The main reasons for using these crosslinking agents are their activities at temperatures above 200°C and the formation of thermally stable carbon-carbon crosslinks. Usually catalysts are added, such as stannous chloride dihydrate or a halogen donor, PVC or CPE, in combination with zinc oxide. The acidity of these catalysts allows the ether linkages and/or the alcohol end groups of the resole to be activated. The chemical structure of the crosslinked rubber has recently been elucidated by using low molecular weight models, and was shown to consist mainly of mono- and bisphenol units linked to the elastomer by methylene or cyclic chroman bridges. Dynamic vulcanisation of a PP/EPDM blend by increasing the amounts of resole results in improvements of tensile strength and, to a lesser extent, of elongation at break [131].

1.10 Addition of ionomers

Ionomers are polymeric species carrying a relatively low number of pendant ionic groups per molecule. Usually, the ionic group result from neutralisation of sulphonic acid or carboxylic acid groups. Either monovalent (Na^+, K^+) or divalent (Zn^{2+}) metal cations are used as counter ions. Sulphonic acid or carboxylic acid groups are introduced into the polymer chains by copolymerisation or chemical modification of existing polymers. Whatever be the cations, the ionic groups tend to associate into multiplets which at sufficiently high concentrations can associate into clusters. Multiplets and clusters act as physical crosslinks between polymer chains. At elevated temperatures, these ionic crosslinks become reversible. Now, if two different ionomers, based on two different and immiscible polymers, are intensively mixed in the melt, the ionic domains may reorganise. The newly formed clusters may contain ionic species of both immiscible polymers. As a result branched copolymers, in which the link between both polymer chains is an ionic bond, are generated at the interface, and a stable compatibilised multiphase blend is generated. Thus a blend of PE and PA66 can be compatibilised using ethylene - methacrylic based ionomer [132].

1.11 Addition of a third polymer partially miscible with all blend phases

According to this, a polymer C partially miscible with the two constitutive polymers A and B of a two phase binary blend, can act as a common solvent and accordingly can promote complete or partial miscibility of the originally immiscible polymers. The choice of polymers A, B and C is such that the binary interaction parameter is negative for the A/C and B/C pairs and positive for the A/B pair.

A number of elastomer-based modifiers have been blended with PVC for improving its impact resistance. PVC is however immiscible with most non-polar elastomers, so these blends have to be compatibilised. Yu-Der Lee *et al* [133] have investigated tricomponent blends of PVC/CPE/EPDM where EPDM is the very low temperature impact modifier and CPE is the compatibiliser.

1.12 Effect of reactive blending on phase morphology

The control of phase morphology is the key issue when desirable mechanical properties have to be imparted to polyblends. The shape, size and spatial distribution of the phases result from a complex interplay among viscosity and elasticity of the phases, interfacial properties, blend composition and processing parameters. The morphology development at short mixing times can be summarised as follows [134].

- the dispersed phase form, sheets or ribbon in the matrix
- holes appear in these sheets or ribbons as a result of interfacial instability
- size and number of holes increase which leads to lace structure
- lace breaks down into irregularly shaped pieces of diameter close to the ultimate particle size and

- break-up of drops and cylinders lead to the final spherical droplets.

At intermediate mixing times, thus in the melt state, mixing affects only the size of the largest particles which are transformed into smaller ones, so leading rapidly to an almost invariant morphology governed by the dynamic equilibrium between domain break-up and coalescence [135-139].

The pioneering work of Taylor on drop break up in Newtonian systems in a simple shear field has been the basis of investigations on more complex systems and flow fields [140,141]. The analysis of Taylor considers how the balance of applied shear forces and counteracting interfacial forces affects drop dimensions and stability. The results have been expressed in terms of the so-called capillary number (c_a) versus the viscosity ratio, p

$$p = \frac{\eta_d}{\eta_m}$$

$$c_a = \frac{\gamma_w \eta_m D}{2\sigma}$$

where D is the diameter of the droplet, γ_w the shear rate, η_m the matrix viscosity, η_d the dispersed phase viscosity, and σ the interfacial tension. According to Taylor's analysis, deformation of the droplet is enhanced by large shear rates, a high matrix viscosity, large droplet size and small interfacial tension. The deformation is retarded by large interfacial tension, high dispersed phase viscosity and small droplet size. Taylor noted that if a lower or equal viscosity droplet is placed in a high viscosity matrix, it is readily drawn out into a large filamentous ligament, which eventually breaks up. This was not the case for very high viscosity drops placed in a low viscosity matrix; these tend to retain their spherical shape. Several studies on Newtonian system in both shear and extensional flow were in agreement with Taylor's prediction [142,143]. However, it has been reported that drop break up was possible over a wide range of viscosity ratios in extensional

flow for Newtonian systems [144,145]. In the case of polymer blends, since the individual components exhibit large normal stresses in flow, the extension of Taylor's analysis to such systems has some limitations. The final morphology of polymer blends is the result of the balance of domain break-up and coalescence at the end of the mixing process. However, most of the studies on polymer blends in literature regarding domain size, expressed in terms of capillary number and viscosity ratio (based on Taylor's analysis), do not account for the coalescence process. In one of the most frequently cited studies on polyamide/rubber blends, Wu extrapolated an empirical equation fitting the capillary master curve [146]. According to this equation

$$\gamma_w \eta_m D/\sigma = 4(p)^{\pm 0.84} \text{ positive when } p> 1; \text{ negative when } p<1$$

Wu's correlation suggests a minimum particle size when the viscosities of the two phases are closely matched. The validity of this equation has been tested by researchers [147,148] who have indicated some disagreement with respect to the dependence of the particle size on viscosity ratio and the correlation proposed by Wu. On the other hand Serpe *et al* [149] found a good agreement of their experimental observations with Wu's results. An experimental minimum in the dispersed phase size with increasing shear rate was reported in the literature and this has been explained based on the high elasticity of the droplet and the resulting resistance to deformation at increased shear rates [150].

1.13 Phase morphology development in reactive blending

In the case of reactive melt blending, the effects of the chemical reaction at the interface on the phase morphology development are multi-fold. The chemical reaction at the interface leads to:

- a reduction in the average size of the dispersed phase due to the suppression of coalescence and the decrease of interfacial tension.

- an increase in the break-up of the largest particles in the size distribution of the dispersed phase.
- a substantial narrowing of the size distribution of the dispersed phase
- a decrease of the mobility of the interface which slows down the coalescence rate.

A number of systematic investigations have been reported in the literature on the phase morphology generation in reactively compatibilised polymer blends [151-156]. The study on the morphology development during reactive melt blending of PA 6 6 (PA 6) with EPM-MA and PS-Ox with EPM-MA is one of the early investigations [135]. These blends were prepared in a Haake batch mixer. The morphology of the non reactive and reactive blends was sampled at different melt-mixing times ranging from 1.5 to 15 minutes. It is shown that in both blend systems the morphology is characterised by a few very large particles along with a large number of small particles, which have nearly the same size as those observed after long mixing times. The major influence of prolonged mixing time is the reduction in size of the largest particles in the distribution. As expected, the average size of the dispersed phase particles in the reactive blends is smaller than in the nonreactive blends; the distribution of the particle size is also found to be narrower in the case of reactive blends.

The particle size distribution of the reactive and non-reactive blends after a mixing time of 15 minutes is compared. The major effects of the chemical reaction at the interface are a reduction in the average size of the dispersed phase particles and a narrowing of the size distribution. The change in the average diameter of the dispersed rubber particles as a function of the mixing time for non-reactive PA6/EPM and reactive PA6/EPM-MA blends are presented in figure 1.12. As can be seen, the interfacial chemical reaction has a dramatic influence on the

dispersed phase size even at very short mixing times. Additionally, the particle size distribution narrows at larger mixing time.

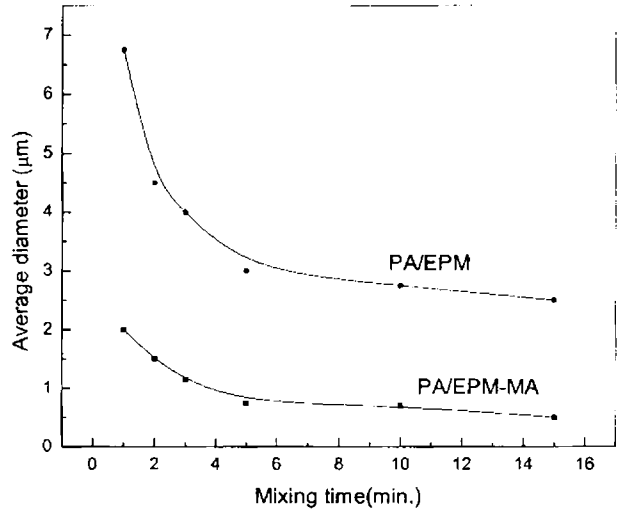

Fig. 1.12: Variation in the average diameter of the dispersed rubber particles for PA6/EPM and PA6/EPM-MA blends as a function of mixing time
[W.E. Baker, C.E. Scott, G.H. Hu, Hanser, Munich, 2001]

The study on the morphology development in blends of PS-Ox with EPM-MA also showed similar results as that of PA6/EPM-MA blends [135]. In fact, the smaller dispersed phase size in the reactive blends compared to the non reactive blends is due to the several different effects:

- reduction of the interfacial tension between the phases.
- inhibition of particle coalescence by the formation of copolymer at the interface.

- differences in the shear stress applied to the blends during melt mixing and
- differences in the viscosity ratio between the two phases caused by the temperature.

The morphology development in the case of EPM/PA6 blends, reactively compatibilised by EPM-g-MA, is reported to be extremely fast [154]. In this study the evolution of the morphology was carefully followed as a function of the mixing time. The mixing was carried out in a co-rotating twin screw mini-extruder. The rotor speed and the mixing temperature were 100rpm and 250°C respectively. The number average domain diameter as a function of the mixing time for the uncompatibilised and reactively compatibilised blends is given in figure 1.13. In the reactively compatibilised blend the morphology development was so fast that within 30 seconds of mixing the morphology was almost completely developed. No major change in morphology could be observed up to 10 minutes.

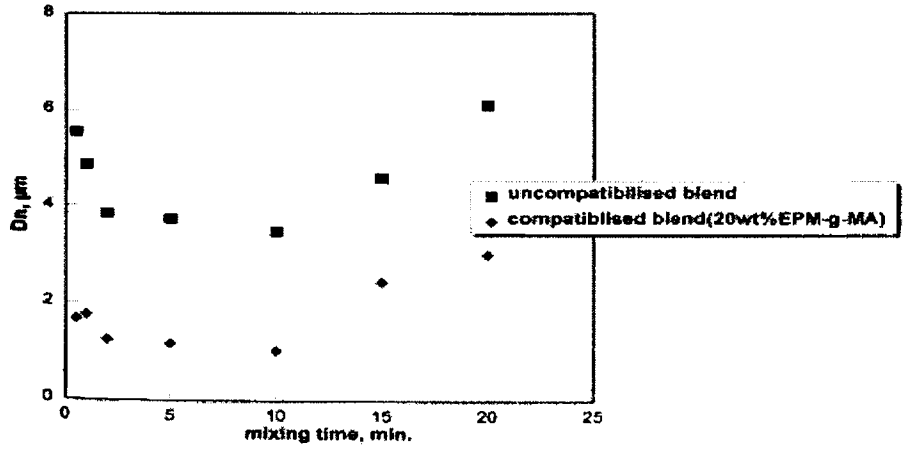

Fig. 1.13: Influence of the mixing time on the number average domain diameter for uncompatiblised and reactively compatiblised 30/70 EPM/PA 6 blends.

[S. Thomas, G. Groeninckx. Polymer, 40, 5799 (1999)]

However, on prolonging the mixing time, there was a strong tendency for phase coarsening both in uncompatibilised and reactively compatibilised blends. The reason for the shear induced coalescence (dynamic coalescence) is attributed to:

- the decrease of the polyamide matrix viscosity on longer mixing and/or
- the removal of the graft copolymer from the interface as a result of shear forces.

Jerome and co-workers investigated the dependence of the phase morphology development on the kinetics of the interfacial reaction [157]. For this purpose, SAN containing 20wt% reactive SAN-X was melt blended with EPDM containing 50 wt% of maleic anhydride grafted EPM chains(EPM-g-MA). Two groups (X) reacting with maleic anhydride at a different rate were randomly attached to SAN (0.028 mole X wt %) ie. a primary amine and a carbamate which actually releases a primary amine at the processing temperature. The SAN/rubber weight composition was kept constant at 75/25. The development of the phase morphology from pellet-sized rubber particles to dispersed submicrometer droplets was analysed for the two types of reactive SAN and found to depend on the rate of the interfacial reaction. In the case of the primary amine, the interfacial reaction took place mainly during the melting and softening step, leading to phase morphology after 2-3 min. mixing which did not change upon further mixing.

When the reactive groups were carbamates, the interfacial reaction was controlled by the carbamate thermolysis into primary amine, which was the rate-determining step. The interfacial reaction was then occurring essentially after the softening/melting of the blend components. It was found that, the highly reactive SAN-NH_2/EPM-g-MA system is much more effective than the slowly reacting SAN carbamate/EPM-g-MA counterpart in stabilising finely dispersed rubber particles of a narrow size distribution even for long mixing times.

It is important to examine the effect of the concentration of the reactive compatibiliser on the blend phase morphology development. In a systematic and detailed study on reactive PA6/(PMMA/SMA) blends by Dedecker and Groeninckx [155,156], it is demonstrated that the concentration of SMA 20 (20 wt% MA), as reactive compatibiliser in the blend has a controlling influence on the phase morphology development. The necessary mixing time required for the generation of equilibrium morphology is presented in figure 1.14 as a function of the SMA 20 concentration.

As can be seen from this figure, the critical time required for the equilibrium morphology development decreased drastically from 30 to 3 min. as the amount of SMA in the blend was increased from 1 to 3 wt %. The points below the indicated line represent morphologies which are still in development; those above the line and on the line represent equilibrium morphologies.

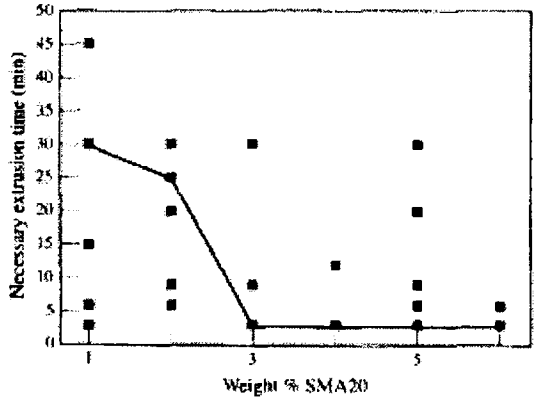

Fig. 1.14: The necessary extrusion time to obtain an equilibrium morphology as a function of the SMA 20 content in the blend PA-6/(PMMA/SMA20) 75/(25-x/x), x = wt% of SMA 20. **[K. Dedecker, G. Groeninckx, Polymer, 39, 4985 (1998)]**

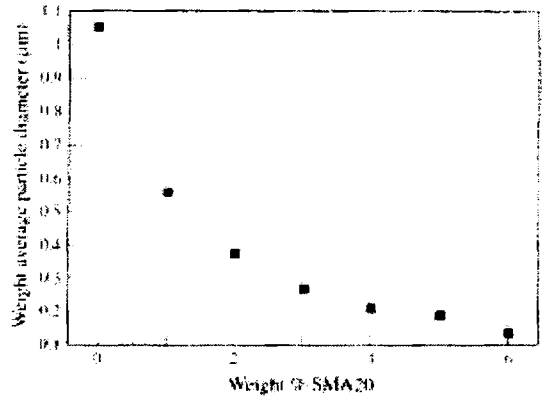

Fig. 1.15: The weight average particle diameter as a function of theSMA20 content in the blend PA-6/(PMMA/SMA20) 75/(25-x/x), x = wt% of SMA 20.
[K. Dedecker, G.Groeninckx, Polymer, 39, 4985 (1998)]

When low contents of SMA 20 are added, the amount of interfacial area will initially be relatively low. Only a very limited amount of SMA 20 will be close enough to the PA6/PMMA interface to react immediately. The remaining amount of SMA 20 will have to diffuse over large distances, which will take a longer time. When larger amounts of SMA 20 are added the amount of SMA 20 which can immediately react will be higher. The reaction of this SMA 20 can already cause a significant particle size reduction. In these smaller particles, the diffusion distance of the remaining SMA 20 towards the interface is decreased and the amount of interfacial area is increased. In this way, the formation of the equilibrium morphology will be very fast. It is important to note that the very fast formation of the equilibrium morphology in blends with minimum 3 wt% SMA 20 is only possible because of the particle size reduction during extrusion. In parallel, the small amount of the compatibiliser, SMA 20, could cause a dramatic reduction of the equilibrium particle size (figure 1.15). It was also observed that the

dispersed particles showed a more spherical shape and a more uniform size as the amount of added SMA 20 was increased. The polydispersity of the particle size also decreased.

Macosko and coworkers compared the reaction rates of aliphatic amine and aromatic amine end-capped PS with anhydride end-capped polyisoprene at 180°C. The reaction of the aliphatic amine was much faster than the aromatic one and resulted in a molecular scale self-assembly into cylindrical micelles within 2 minutes of mixing. In contrast in the case of the slower reactive aromatic amine, the blend did not show this molecular scale morphology even after 90 minutes of mixing [158].

The molecular weight of the reacting polymers has also a direct influence on the yield of the compatibilisation reaction. At a constant weight fraction of the reacting polymers, the concentration of the reactive group attached as an end-group of linear chains increases with decreasing molecular weight. In addition, lower molecular weight chains diffuse faster to the interface and are localised in this region as favourably as the entropic penalty is small [159-164]. Thus any decrease in the molecular weight of the reacting polymers must be in favour of the interfacial reaction.

Koning *et al* [165] studied the reactive compatibilisation of SMA and poly (phenylene oxide) (PPO) blends by mixtures of α-amino-PS and styrene/maleic anhydride random copolymers (SMA) containing 28 wt% maleic anhydride groups. At constant weight faction of the α-amino-PS, the size of the dispersed PPO particles was observed to decrease with decreasing molecular weight of PS, and with the increasing concentration of the end functional groups.

Nevertheless, there is a lower limit for the molecular weight of the reactive polymer below which the in-situ formed compatibiliser may escape the interface where it has been formed. For example, in the reactive blending of PS with PMMA

having end-reactive chains (PS-COOH: MW= 30,000 and PMMA-epoxy: MW = 20,000), large PMMA particles were surrounded by small clouds of micelles, whereas when a copolymer of higher molecular weight was formed in the otherwise identical system, formation of micelles was not observed. Although the mechanism of formation of these micelles is not well understood, it is strongly related to the molecular weight of the copolymer.

1.14 Effect of mode of addition of the compatibiliser

In order to study the influence of mode of addition of EPM-g-MA [154] the blending operations were carried out in four different ways: These include: (i) PA6, EPM and EPM-g-MA were added together into the extruder and then mixed (ii) Both PA 6 and EPM were preblended for three minutes and then EPM-g-MA was added into the blend (iii) EPM-g-MA was preblended with the minor EPM phase for 3 min. and then mixed with the PA 6 phase(iv) EPM-g-MA was preblended with the major continuous PA 6 phase for 3 min. and then mixed with the EPM minor phase.

The morphology of the 20/80 EPM/PA 6 blend containing10 wt.% of EPM-g-MA for the case (i), (ii), (iii); and (iv) are given in figures 1.16 (a-d) respectively. The results are presented in Table 1.2. It is interesting to note that the most finely and uniform dispersion is obtained when the EPM-g-MA was preblended with the minor EPM phase. The size of the domains increases in the order case (iii) , case (i) , case(ii) , case (iv); and case (iv) was the worst. This has been further explained in figure 1.17 with a schematic model. In fact a two-step mixing process in which the EPM-g-MA is mixed with the EPM phase (EPM master batch) gives more opportunity for the EPM-g-MA to diffuse towards the blend interface. In this method of mixing, the EPM-g-MA is forced to be at the blend interface.

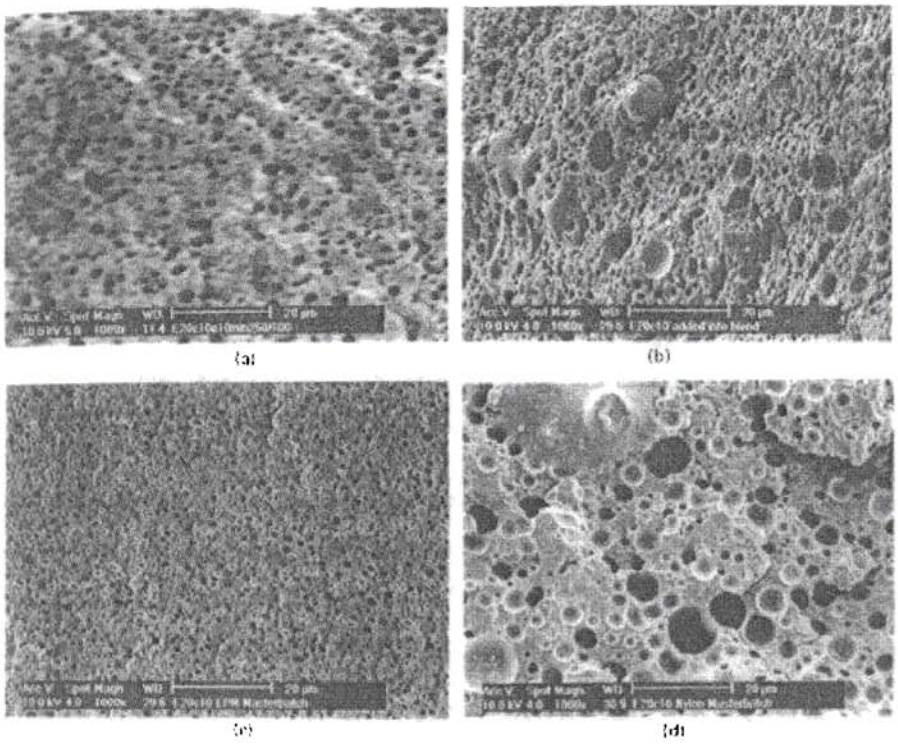

Fig. 1.16: SEM micrographs showing the influence mode of addition on the morphology of 20/80 EPM/PA 6 blend containing 10 wt.% of EPM-g-MA: (a) PA 6, EPM rubber and EPM-g-MA were added together into the extruder and then mixed, (b) both PA 6 and EPM were preblended for three minutes and then EPM-g-MA was added into the blend, (c) EPM-g-MA was preblended with the minor EPM phase for 3 min. (EPM master batch) and then mixed with the PA 6 phase,(d) EPM-g-MA was preblended with the major continuous PA 6 phase for 3 min. (PA 6 master batch) and then mixed with the EPM minor phase. **[S. Thomas, G. Groeninckx. Polymer, 40, 5799 (1999)]**

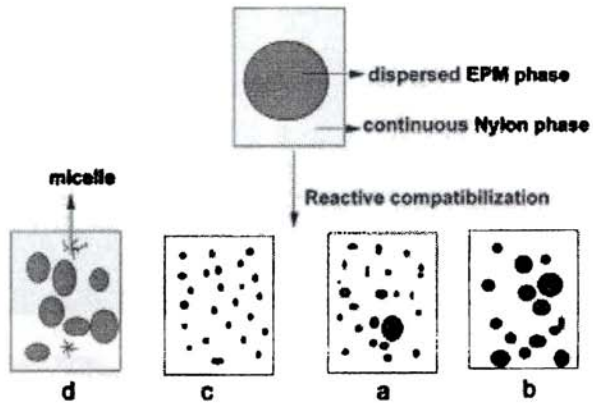

Fig. 1.17: Schematic models illustrating the mode of mixing on blend morphology: (a) mixing all together (simultaneous addition), (b) added into blend, (c) EPM masterbatch, (d) PA 6 masterbatch. **[S. Thomas, G. Groeninckx. Polymer, 40, 5799 (1999)]**

This will lead to a situation where the EPM-g-MA can react with the amino end group of PA 6 at the interface and the resulting graft copolymer will be easily located at the blend interface. Interestingly the polydispersity was lowest in this case (table 1.1). In contrast, when the EPM-g-MA is pre-mixed with the PA 6 phase at high temperature (PA 6 masterbatch), the graft copolymer is already generated as result of the reaction between the amino end group of PA 6 and MA group of EPM-g-MA.

This graft copolymer has to diffuse into the blend interface during the final mixing with the EPM rubber. It is believed that only a very small fraction of the graft copolymer will be able to reach the interface in such a situation. Most of the graft copolymer will be located in the bulk PA 6 phase where they will give rise to micellar aggregation as depicted in figure 1.17 d and results a coarse morphology.

Table 1.1: Effect of order of addition of compatibiliseron the morphology of 20/80/10EPM/PA 6/EPM-g-MA blend. [S. Thomas, G. Groeninckx. Polymer, 40, 5799 (1999)]

Mode of addition	D_n (μm)	D_w (μm)	D_w/D_n
Added into blend	1.02	1.54	1.50
PA 6 masterbatch	2.03	3.42	1.68
EPM masterbatch	0.50	0.62	1.24
Mixed together	0.61	0.92	1.50

1.15 Effect of reactive blending on phase stabilisation in the melt

One of the important advantages of reactive blending is the stabilisation of the blend phase morphology in the melt. The general morphology should be preserved against coalescence during melt processing, on account of the fact that very often polymer blends are annealed during fabrication and processing operations which can lead to coalescence.

The phase instability was shown to be dramatic for blends of PP/PA6, PE/PC and PS/PA6, as reported by White and co-workers [166-168] These studies were carried out in the barrel of a capillary rheometer where annealing was conducted. The influence of reactive compatibilisation on phase stability of blends in the melt can be understood from table 1.2. The study of the phase stability of reactive and non-reactive EPM/PA6 blends indicated that the number average domain diameter is unaffected by annealing the melt in the case of the reactively compatibilised blends. However, for the uncompatibilised EPM/PA6 blends, the domain size increases drastically as a function of time; the rate of growth was

found to be much faster at longer times [154]. Based on this observation, the authors have concluded that the in-situ formed graft copolymer at the interface between the phases stabilise the morphology against coalescence. It is believed that the graft copolymer forms a shell around the dispersed phase, which leads to a broad, stable and less mobile interface, which can resist coalescence.

Table 1.2: Mean dimension of phases in annealed polymer melt blends

[W.E. Baker, C.E. Scott, G.H. Hu, eds., Hanser, Munich, 2001]

Blend System	Blend ratio	Mean phase dimension (μm)		
		30[a]	60[a]	90[a]
PS/PA 6	60/40	90.2	140	310
HDPE/PA 6	50/50	163	248	278
LDPE/PA 6	55/45	251	314	319
HDPE/PA 11	50/50	50.9	202	229
LDPE/PA 11	55/45	162	275	303
PS/PA 6/SAN	57/38/5	131	104	117
PS/PA 6/SMA	57/38/5	4.02	4.65	4.58
HDPE/PA 6/MA-g-PP	47.5/47.5/5	8.81	11.9	10.1
LDPE/PA 6/MA-g-PP	47.5/47.5/5	4.53	6.90	13.0
HDPE/PA 11/MA-g-PP	47.5/47.5/5	11.6	12.5	13.0
LDPE/PA 11/MA-g-PP	47.5/47.5/5	4.76	5.68	4.12

[a] annealing time in minutes

1.16 Effect of Reactive Blending on Phase Co-continuity

A lot of literature deal with the formation of co-continuous phase morphologies in uncompatibilised binary polymer blends [169-172]. However, very few literature deal with the phase co-continuity of reactively compatibilised blends. Hietaoja *et al* [173] have investigated the phase morphology of the blend system PA6/PP compatibilised by PP-MA.

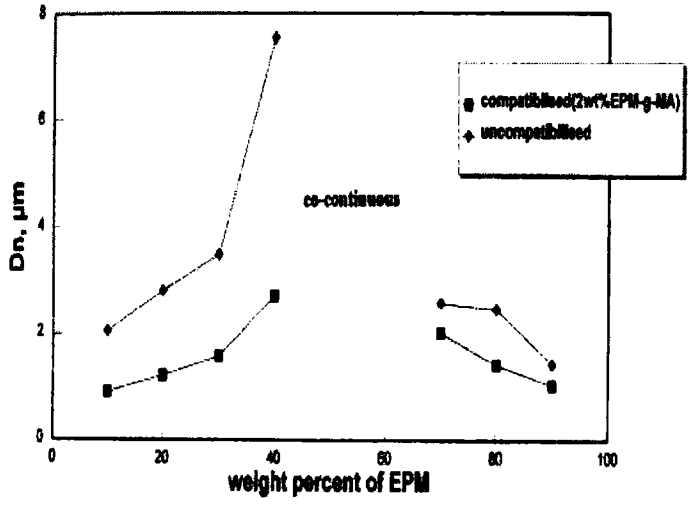

Fig. 1.18: Effect of blend ratio on number average domain diameter for uncompatibilised and reactively (2wt.% EPM-g-MA) compatibilised EPM/PA6 blends [S. Thomas, G. Groeninckx, Polymer, 40, 5799 (1999)

The effect of the addition of the reactive compatibiliser on the location and width of the phase inversion region was also studied; the authors observed only a minor effect upon the addition of the reactive compatibiliser. De Roover [174] has shown that in the case of in-situ compatibilisation, the amount of graft copolymer formed at the interface does not affect the composition at which phase inversion occurs. According to De Roover during the reactive blending of Poly (m-xylene

adipamide) (PAMXD6) and PP-g-MA, the only parameter that determines the phase inversion composition is the viscosity ratio of the blend components at the first stage of the mixing process. The location of the phase inversion region is fixed early during the blending process and does not seem to be influenced by either further modification of the viscosity ratio versus mixing time, or the amount of graft copolymer formed during reactive blending. Recent data of Thomas and Groeninckx [154], which were in agreement with those reported by De Roover, showed that the addition of a reactive compatibiliser, EPM-g-MA does not have any influence on the location of the region of phase co-continuity in EPM/PA 6 blends [154]. This can be understood from figure1.18 where the co-continuity is observed between 40 and 70 wt% of EPM in both uncompatibilised and reactively compatibilised blends.

On the other hand, upon reactive compatibilisation of PA6/PMMA blends by SMA 20, a pronounced change in the region of phase co-continuity was reported [156]. In this study the region of phase co-continuity has been analysed both for the uncompatibilised and reactively compatibilised blends. It is reported that the region of phase co-continuity is much smaller in the compatibilised blends, and that this region is shifted to lower contents of PA6. The narrowing of the region of phase co-continuity is ascribed to the reduced rate of coalescence in the compatibilised blends. However, the observed shift in the region of co-continuity upon reactive compatibilisation was not accounted for. It is believed that factors such as increased viscosity, reduced mobility of the interface and the generation of core-shell morphology have to be considered to explain the observed shift in the region of co-continuity.

1.17 Studies on the toughening of polystyrene

Several methods for incorporating rubber into PS matrix are known. Besides the melt blending technology, the in-situ polymerisation technique has been well proven to be an attractive method for producing HIPS [175,176]. In this process, polymerisation of styrene containing 5–10% of dissolved butadiene based rubber takes place thermally under agitation. While PS is forming, phase separation occurs that finally produces multiphase morphology. The proposed mechanisms for toughening rely mainly on the dispersion of rubber particles within the glassy matrix results in energy absorption by the rubber particles, debonding at the rubber matrix interface and crazing. Factors such as amount of rubber added, type of rubber, size and morphology of the rubber particles, rubber phase volume, degree of adhesion of the rubber to the matrix, relaxation behaviour of rubber, and composition of rubber are believed to play a significant role in the improved impact resistance of HIPS [4, 175, 177 -183].

Natural rubber (NR) latex was also studied for its use as an impact modifier of several polymers [184-186]. Due to its broad particle size distribution, the existence of large size and high molecular weight [187], the NR latex particle might be suitable for the improvement of toughness of glassy polymers including PS. Tangboriboonrat *et al* [188] reported an attractive method for the preparation of HIPS based on NR. The key steps involved the use of γ–radiation vulcanised natural rubber (RVNR) latex/phase transfer /bulk polymerisation. The toughened PS prepared exhibited the HIPS like morphology, and the impact energy was higher than that of the unmodified PS. The phase transfer technique has been successfully used to transfer uncrosslinked, γ–radiation vulcanised and deproteinated NR latex particles from the aqueous phase into the styrene monomer phase [189-191].

Core shell particles containing PS subinclusions are well suited for the toughening of PS [185]. For the fine reinforcement of PS, the NR based particles were coated with a shell of crosslinked PMMA or PS. Core shell particles based on NR containing PS subinclusions toughened PS more effectively. The hard shell assures adequate stress transfer at fast deformation speeds and the rigid subinclusions render the rubber particles capable of stabilising a generated craze since the incorporated rubber particles do not debond from the matrix.

The technological compatibilisation of PS/NBR blend by styrene–acrylonitrile copolymer (SAN) was carried out by M. Mathew *et al* [192]. The incorporation of SAN is effective in reducing the phase size of PS/NBR blends. The domain size of the dispersed phase decreases with the addition of small amounts of the copolymer followed by levelling of at higher concentration. The compatibilised blends showed improved impact toughness and transformed into super tough materials.

PS was toughened with EPDM in the presence of styrene–butadiene–styrene block copolymer (SBS) and the incorporation of SBS into the PS/EPDM blends improved the impact properties [193]. The impact strength of PS can be increased by reactive extrusion with trimethylol propane triacrylate (TMPTA) and dicumyl peroxide (DCP) [194]. The coupling reaction caused by TMPTA increased the molecular weight of PS. The coupling reaction was enhanced in the presence of DCP at high TMPTA/DCP ratio. Toughness, thermal stability and storage modulus of brittle PS could be improved by the addition of some more brittle polyphenyl silsesquioxane (PPSQ) particles [195].

The influence of poly[(ethylene-co-vinylacetate)-g–polystyrene] (EVA-g-PS) on the mechanical properties and morphological properties of PS has been investigated by Soares *et al* [196]. Addition of the graft copolymer enhances the mechanical and impact resistance of the PS matrix. Better results on impact

strength and elongation at break have been achieved by using an EVA-g-PS copolymer with higher EVA proportion by weight. Morphological studies by SEM revealed some interfacial adhesion between the components in the compatibilised blends.

The impact strength of blends consisting of PS and EPDM could be increased by adding poly (styrene/ethylene–propylene) (SEP) compatibiliser and an organic peroxide during reactive extrusion [197]. The enhanced impact strength could be related to the enhanced adhesion between the dispersed EPDM phase and the PS matrix as a consequence of radical graft link between the rubbery part (EP) of the compatibiliser and the dispersed EPDM phase.

S. Shaw *et al* [198] studied the impact modification of PS by EPDM compatibilised by PS/EPDM-g-(styrene-co-methyl methacrylate) and observed that there is improvement in impact strength with subsequent decrease in tensile strength.

The effects of dynamic vulcanisation and blend ratios on mechanical properties and morphology of thermoplastic elastomeric compositions based on blends of NBR and SAN were studied [199]. Dynamic vulcanisation causes a decrease in the size of the dispersed particles and improvement in mechanical properties.

The impact strength of PS was considerably increased by the addition of poly[(n-BA/MMA)/S] core shell structured particles. When the amount of core shell particles added was 15 phr, impact strength was almost six times higher than that of unmodified PS [200].

The size of domains in a series of compatibilised polystyrene-(ethylene-propylene rubber) blends was measured by solid-state NMR spin diffusion measurements. The average diameter of ethylene propylene rubber (EPM) particles in the blends was observed to decrease as the concentration of interfacial agent was increased up

to approximately 15% (weight/volume of EPM) and remained constant upon further addition of interfacial agent. Comparison of the domain sizes obtained from NMR measurements with those obtained from scanning electron microscopy measurements suggests that the NMR technique can be used to confirm large scale phase separation and investigate the trends in domain sizes in immiscible blends [201].

Two triblock copolymers of styrene/ethylene-butylene/styrene (SEBS), of different molecular weights, were used to compatibilise a blend of 80 vol % polystyrene (PS) and 20% ethylene propylene rubber (EPM) [202]. Charpy and Izod impact tests were performed to determine the effect of the compatibilisation on mechanical properties of the blend and to establish links between morphology, interface, and properties. Results suggest that for the lower molecular weight interfacial agent, a transition in fracture mechanisms, from fragile to ductile, occurs around 20% interfacial agent (based on the volume of the minor phase). This transition, however, is not observed with the high molecular weight interfacial agent.

The compatibility of solid blends: PS/SBR, PS/SBR filled with glass fibre and PS/SBR filled with talc were studied using ultrasonic pulse echo technique. Measurements were carried out at room temperature (298 K) and a frequency of 3 MHz. The ultrasonic velocity for the compressional wave and that for shear wave have been measured to obtain the elastic modulus data by knowing the density. The variation of ultrasonic wave velocities and elastic modulus with weight percent of the blend was found to be linear in PS/SBR blend, indicating some degree of compatibility but the drawback of elastic modulus indicate incompatibility of the system blend, while it deviates from linearity in blends of PS/SBR filled with glass fibre and talc but the increase in elastic modulus indicates

that there is an increase in degree of compatibility between PS and SBR due to addition of glass fibre or talc [203].

1.18 Scope and objectives of the work

The objective of this research work is to prepare an ABS (acrylonitrile-butadiene-styrene) type toughened thermoplastic by melt blending polystyrene (PS) and powdered nitrile rubber (NBR). The product may be an interesting class of toughened thermoplastic, which would combine the superior mechanical and processing characteristics of PS and the excellent oil-resistant properties of NBR. PS offers excellent ozone resistance, weather resistance, mechanical properties and easy processability. NBR compounds assume commercial interest due to its excellent oil-resistance, abrasion resistance and elastic properties. Unfortunately, blends of non-polar PS and polar NBR form incompatible mixtures, owing to poor interaction between the two constituent polymers. Powdered NBR offers good flow rate, mixing possibility and fully automatic continuous operation. No serious efforts have been made to develop a technologically compatible toughened thermoplastic from PS and NBR. Several methods have been developed to alleviate the problem of incompatibility in polymer blends. These include (1) addition of a third homopolymer or graft or block copolymer which is miscible with the two phases, non-reactive compatibilisation (2) in-situ generation of graft or block copolymer during melt blending via interfacial reaction of added functionalised polymeric components, reactive compatibilisation, (3) using vulcanised rubbers and (4) dynamic vulcanisation of the elastomeric part. The addition of these interfacial agents or compatibilisers reduces the surface tension between the phases and thereby improves the interfacial adhesion and mechanical properties. In this thesis an attempt has been made to investigate systematically the effect of compatibilisation and dynamic vulcanisation on the morphology and properties of powdered nitrile rubber toughened polystyrene.

The main objectives of the work are:

- **Correlation between morphology and mechanical properties of binary blends**

In a two phase system such as PS/NBR, morphology is a major determinant of properties. Thus the shape, size and distribution of the dispersed phase along with the interfacial characteristics decide the mechanical properties. In an incompatible blend premature failure occurs when subjected to a mechanical load due to lack of adhesion between the two. The tensile measurements give an idea about the maximum load bearing capacity of the material. The influence of blend composition on the mechanical properties has been investigated.

- **Evaluation of the effectiveness of compatibilisation based on phase morphology**

The PS/NBR blend system is incompatible resulting in inferior mechanical properties. Hence it is essential to compatibilise it for satisfactory product performance. Three compatibilisers, maleic anhydride modified polystyrene (MAPS), phenolic modified polystyrene (PhPS) and styrene-co-acrylonitrile (SAN) were used as compatibilisers. The effect of compatibiliser concentration on morphology and mechanical properties were investigated. Dynamic vulcanisation using dicumyl peroxide was also adopted as a compatibilisation technique.

- **Prediction of blend miscibility based on dynamic mechanical analysis and effect of compatibilisation on miscibility.**

The dynamic mechanical analysis of PS/NBR blends provides valuable information regarding the damping characteristics. The viscoelastic properties like storage modulus, loss modulus and tan δ of various blends were determined with special reference to the effect of blend ratio and compatibilisation.

❖ **Evaluation of the processability of binary and compatibilised blends by rheological measurements**

The study of the flow behaviour of toughened thermoplastics is essential to optimise the processing conditions and also to improve the quality of the final product. The effect of blend ratio, compatibiliser concentration and dynamic vulcanisation on flow behaviour was investigated.

❖ **Evaluation of thermal stability by thermogravimetry**

Polymeric materials are subjected to various types of degradation ranging from thermal degradation to biodegradation. Polymer degradation is undesirable as it leads to deterioration of properties. One of the most accepted methods for studying the thermal properties of polymeric materials is the thermogravimetry. The integral (TGA) and derivative (DTG) thermogravimetric curves provide information about nature and extent of degradation of polymeric materials. Thermogravimetric analysis can be used for determining the thermal stability of polymers and polymer blends. The effect of blend ratio, compatibilisation and dynamic vulcanisation on the thermal properties was evaluated.

References

1. R.J. Gaymans, Toughening of semicrystalline thermoplastics. Polymer Blends, Vol. 2; (D.R. Paul and C.B. Bucknall eds.), pp. 177-224, Wiley-interscience, New York (2000)
2. S. Wu, *J. Appl. Polym. Sci.*, **35**, 549 (1988).
3. R.N. Haward, G. Thackaray, *Proc.Roy. Soc. Lond. A*, **302**, 453 (1968)
4. C.B. Bucknall, *Toughened Plastics*, Applied Science, London, (1977).
5. A.M. Donald, E.J. Kramer, Philos. Mag. A. Ser. 8, **43**, 857 (1981).
6. P. Beahan, M. Bevis, D. Hull, *J. Mater. Sci.*, **8**, 162 (1974).
7. H.R. Brown, *J. Polym. Sci., Polym. Phys.*, **17**, 1431 (1979).
8. P. Beahan, M. Bevis, D. Hull, *J. Mater. Sci.*, **8**, 162 (1974).

9. J.D. Moore, *Polymer*, **12**, 478 (1971).
10. J. Silberberg, C.D. Man, *J. Appl. Polym. Sci.*, **22**, 599 (1978).
11. A.M. Donald, E.J. Kramer, *J. Appl. Polym. Sci.*, **27**, 3729 (1982).
12. A.M. Donald, E.J. Kramer, J. *Mater. Sci.*, **17**, 2351 (1982).
13. S. Newman, S. Strella, *J. Appl. Polym. Sci.*, **9**, 2297 (1965).
14. R.J.M. Borggreve, R.J. Gaymans, H.M. Eichenwald, *Polymer*, **30**, 79 (1989).
15. A.F. Yee, R.A. Pearson, J. *Mater. Sci.*, **21**, 2462 (1986).
16. R.A. Pearson, A.F. Yee, J. *Mater. Sci.*, **21**, 2475 (1986).
17. D.S. Parker, H.J. Sue, J. Huang, A.F. Yee, Polymer, 31, 2267 (1990).
18. A.F. Yee, R.A. Pearson, J. *Mater. Sci.*, **21**, 2462 (1986).
19. C.B. Bucknall, I.C. Drinkwater, W.E. Keast, Polymer, **13**, 115 (1972).
20. W.D. Bascom, R.L. Cottington, R.L. Jones, P. Peyser, *J. Appl. Polym. Sci.*, **19**, 2545 (1975)
21. A.F. Yee, J. Du, M.D. Thouless, Toughening of epoxies. Polymer Blends, Vol. 2; (D.R. Paul and C.B. Bucknall eds.), pp. 225–267, Wiley-interscience, New York (2000).
22. A. Lazzeri, C.B. Bucknall, *Polymer*, **36**, 2895 (1995).
23. A. Lazzeri, C.B. Bucknall, *J. Mater. Sci.* **28**, 6799 (1993).
24. C.B. Bucknall, D.S. Ayre, D.J. Dijkstra, Polymer, **41**, 5937 (2000).
25. C.E. Locke, D.R. Paul, *J. Appl. Polym. Sci.*, **17**, 2597 (1973).
26. W. Bartensen, D. Heikens, P. Piet, *Polymer*, **15**, 119 (1974).
27. C.R. Lindsey, D.R. Paul, J.W. Barlow, *J. Appl. Polym. Sci.*, **26**, 1 (1973).
28. S.D. Sjoerdsma, A.C.A.M Bleijenberg , D. Dickens, *Polymer*, **22**, 619 (1981).
29. P. Teyssie, *Makromol. Chem., Macromol. Symp.*, **22**, 83 (1988).
30. G.E. Molau, Colloidal and Morphological Behaviour of Block and Graft Copolymers in *Block Copolymers*, S.L. Aggarwal (ed.), p.70, Plenum Press, New York, (1970).

31. G. Reiss, J. Kohler, C. Tournut, A. Brandert, *Makromol. Chem.*,**101**, 58 (1967).
32. F. Ide, A. Hasegawa, *J. Appl. Polym. Sci.*, **18**, 963 (1974).
33. L. Leibler, *Makromol. Chem., Macromol. Symp.*, **16**, 1 (1988).
34. K.A. Shull, E.J. Kramer, *Macromolecules*, **23**, 457 (1990).
35. K. Sondergaard, J. Lyngaae-Jorgensen, in *Rheo-Physics of Multiphase Systems: characterization by Rheo- optical techniques,* K. Sondergaard, J. Lyngaae-Jorgensen (eds.)Technomic Publishing Company, Lancaster, PA, (1995).
36. J.H. Anastasiadis, J.Gancarz, J.T. Koberstein, *Macromolecules*, **22**, 1449 (1989).
37. D.R. Paul, J.W. Barlow, *Multiphase polymers* , S.L. Copper and G.M Ester, (eds.) p. 315, ACS, Washington D.C., (1979).
38. O. Olabisi, L.M. Robeson, M.T. Shaw, *Polymer–Polymer Miscibility*, p.277, Academic Press, New York, (1979).
39. O. Olabisi, L.M. Robeson, M.T. Shaw, *Polymer–Polymer Miscibility*, p.321, Academic Press, New York, (1979).
40. R. Fayt, R. Jerome, P. Teyssie, *J. Polym. Sci., Polym. Chem.*, ed., **22**, 1633 (1984)
41. T. Ouhadi, R. Fayt, R. Jerome, P. Teyssie, *Polym. Commun.*, **27**, 212 (1986)
42. J. Heuschen,R. Jerome, P. Teyssie, *Polym. Phys.*, **27**, 775 (1989)
43. D.R. Paul, S. Newman, ed., *Polymer Blends*, Ch.2, Vol. I, Academic Press, New York, (1978).
44. M. Aubin, Y. Bedard, M.F. Morrissette, R.E. Prud'homme, *J. Polym. Sci., Polym. Phy.*, **21**, 233 (1983)
45. D. Allard, R.E. Prud'homme, *J. Appl. Polym. Sci.*, **27**, 559 (1982).
46. G. Belorgey, R.E. Prud'homme, *J. Appl. Polym. Sci.*, **27**, 559 (1982).
47. J.M. Jonza, R.S. Porter, *Macromolecules*, **19**, 1946 (1986)

48. I.D. McKay, *J. Appl. Polym. Sci.*, **43**, 1593 (1991).
49. Y. Gnanou, P. Rempp, *Makromol. Chem.*, **188**, 2111 (1987).
50. G.O. Schulz, J. Milkovich, *J. Polym. Sci.,Polym. Chem Ed.*,**22**, 1633 (1984).
51. C.E. Locke, D.R. Paul, *J. Appl. Polym. Sci.*, **13**, 2957(1973).
52. R. Fayt, Ph. Teyssie, *Polym. Eng. Sci.*, **30**, 937 (1990).
53. R. Fayt, R. Jerome, Ph. Teyssie, *J. Polym. Sci.,Polym. Phys.*, **20**, 2209 (1981).
54. D. Braun, M. Fisher, G.P. Hellman, *Makromol. Chem., Macromol. Symp.*, **83**, 77, (1994).
55. H. Keskkula, D.R. Paul, J.W. Barlow, Polymer blends, in *Kirk-Othmer Encyclopaedia of Chemical Technology,* 4th Ed., Vol. 19, John Wiley and Sons, New York, (1996).
56. S. Dutta, D.J. Lohse, *Polymeric Compatibilisers*, Hanser Publishers, Munich, (1996).
57. F. Ide, A. Hasegawa, *J. Appl. Polym. Sci.*, **18**, 963 (1974).
58. L. Leibler, *Makromol. Chem., Macromol. Symp.*, **16**, 1 (1988).
59. R. Greco, M. Maliconico, E. Matruscelli, G. Rogosta, S. Scarzini, *Polymer*, **28**, 1185 (1987).
60. B. Majumdar, H. Keskkula. D.R. Paul, N.G. Harvey, *Polymer*, **35**, 4263 (1994).
61. B. Majumdar, H. Keskkula. D.R. Paul, *Polymer*, **35**, 1386, 1399, 3164, 5453 and 5468 (1994).
62. B. Majumdar, H. Keskkula. D.R. Paul, *J. Appl. Polym. Sci.*, **54**, 339 (1974).
63. R.J.M. Borggreve, R.J. Gaymans, J. Scuijer, J.F. Ingen Houze, *Polymer*, **28**, 1489 (1987).
64. R.J.M. Borggreve, R.J. Gaymans, *Polymer*, **30**, 63, 71, 78, (1989).
65. W.E. Baker, M. Saleem, *Polym. Eng. Sci.*, **27**, 1634 (1987).
66. W.E. Baker, M. Saleem, *Polymer*, **28**, 2057 (1987).

67. N.C. Liu, W.E. Baker, *Adv. Polym. Technol*, **11**, 249 (1992).
68. N.C. Liu, W.E. Baker, *Polymer*, **35**, 998 (1994).
69. V.J. Triacca, S. Ziaee, J.W. Barlow, H. Keskkula, D.R. Paul, *Polymer*, **32**, 1401 (1992).
70. A.J. Oshinski, H. Keskkula, D.R. Paul, *Polymer*, **33**, 268, 284 (1992).
71. Y. Takeda, H. Keskkula, D.R. Paul, *Polymer*, **33**, 3173 (1992).
72. A.R. Padwa, R.E. Lavengood, *ACS Symp. Ser.*,**33**, 600 (1992).
73. S. Wu, *Polym. Eng. Sci.*, **27**, 335 (1987).
74. G. Serpe, J. Jarrin, F. Dawans, *Polym. Eng. Sci.*, **30**, 553 (1990).
75. M. Lu, H. Keskkula, D.R. Paul, *Polymer*, **34**, 1874 (1993).
76. M. Lu, H. Keskkula, D.R. Paul, *Polym. Eng. Sci.* **34**, 33 (1994).
77. M.J. Modie, L.A. Pottick, *Polym. Eng. Sci.* **33**, 819(1993).
78. K. Dijkstra, R.J. Gaymans, *Polymer*, **35**, 323 (1994).
79. A. Gonzalez-Montiel, H. Keskkula, D.R. Paul, *Polymer*, **36**, 4587, 4605, 4621, (1995)
80. J. Rosch, R. Malhaupt, *Makromol. Chem. Rapid Commun.*, **14**, 503 (1993).
81. R. Malhaupt, T. Duschek, J. Rosch, *Polym. Adv. Tech*, **4**, 465 (1993).
82. M. Lu, H. Keskkula, D.R. Paul, *Polymer*, **37**, 625(1996).
83. B. Majumdar, D.R. Paul, A.J. Oshinski, *Polymer*, **38**, 1787 (1997).
84. A.J. Oshinski, H. Keskkula, D.R. Paul, *J. Appl. Polym. Sci.*, **61**, 623 (1996).
85. A.J. Oshinski, H. Keskkula, D.R. Paul, *Polymer*, **37**, 4891, 4909, 4919 (1997).
86. A. Padwa, *Polym. Eng. Sci.* **32**, 1703(1992).
87. J.C. Angola, Y. Fujita, T. Sakai, T. Inoue, *J. Polym. Sci.,Polym. Phys.* **26**, 807 (1988).
88. M. Xanthos, *Polym. Eng. Sci.* **28**, 1392 (1992).
89. C.T. Maa, F.C. Chang, *J. Appl. Polym. Sci.*, **49**, 913 (1993).

90. M.E. Stewart, S.E. George, R.L. Miller, D.R. Paul, *Polym. Eng. Sci.* **33**, 675 (1993).

91. N.C. Beck Tan, S.K. Tai, R.M. Briber, *Polymer*, **37**, 3909 (1996).

92. E.A. Flexman, *Polym. Eng. Sci.* **19**, 564 (1979).

93. N. Dharmarajan, S. Datta, *Polymer*, **33**, 3848 (1992).

94. S. Datta, N. Dharmarajan, G. Ver Strate, L. Ban, *Polym. Eng. Sci.* **33**, 721 (1993).

95. S.Horiuchi, N. Matchariyakul, K. Yase, T. Kitano, H.K. Choi, Y.M. Lee, *Polymer*, **37**, 3065 (1996).

96. S.Horiuchi, N. Matchariyakul, K. Yase, T. Kitano, *Macromolecules,* **30**, 3664 (1997).

97. A.M. Aerdts, G. Groeninckx, H.F. Zirkzee, H.A.M. van Aert, J.M. Geuts, *Polymer*, **38**, 4247 (1997).

98. H. Li, T. Chiba, N. Higashida, Y. Yang, T. Inoue, *Polymer*, **38**, 3921 (1997).

99. K. Yokioka, T. Inoue, *Polymer*, **35**, 1182 (1994).

100. B. Deroover, J. Devaux, R. Legras, *J. Polym. Sci.,Polym. Chem.*, **35**, 901 (1997).

101. B.O. Shaughnessy, U. Sawhney, *Macromolecules,* **29**, 7230 (1996).

102. G.F. Fredickson, S.T. Milner, *Macromolecules,* **29**, 7386 (1996).

103. B.C. Trivedi, B.M. Culbrtson, *Maleic Anhydride*, p. 269 Plenum Press, New York, (1982).

104. N.G. Gaylord, M.K. Mishra, *J. Polym. Sci.,Polym. Lett.*, **21**, 23 (1986).

105. N.G. Gaylord, R. Mehta, *J. Polym. Sci.,Polym. Chem.*, **26**, 1189 (1988).

106. N.G. Gaylord, M.Mehta, R. Mehta, *J.Appl. Polym. Sci.*, **33**, 2549 (1987).

107. W. Heinen, C.H. Rosenmoller, C.B. Wenzel, H.J.M. Degroot, J. Lgtenburg, M. Van Duin, *Macromolecules,* **29**, 1151 (1996).

108. J.M.G. Cowie (ed.) *Alternating Copolymers*, Plenum Press, New York, (1985).

109. I. Park, J.W. Barlow, D.R. Paul, *J. Polym. Sci.,Polym. Chem.* **29**, 1329 (1991).

110. M. Halden-Abberton, *Polym. Mater. Sci. Eng.*,**65**, 361 (1991).

111. M.E. Fowler, D.R. Paul, L.A. Cohen, W.T. Freed, *J.Appl. Polym. Sci.*, **37**, 513 (1989).

112. J.R. Campbell, S.Y. Hobbs, T.J. Shea, V.H. Watkins, *Polym. Eng. Sci.*,**30**, 1056 (1990).

113. J.H. Glans, M.K. Akkapoddi, *Macromolecules,* **24**, 383 (1990).

114. C. Carrot, M. Jaziri, J. Guillet, J.F. May, *Plast. Rubber Process Appl.*, **14**, 245 (1990).

115. D.F. Ferrari, W.E. Baker, *J. Polym. Sci.,Polym. Chem.* **36**, 1572 (1998).

116. S.V. Usachev, N.D. Zhakarov, V.N. Kuleznev, A.B. Ventoshikin, *Int. Polym. Sci. Tech.*, **7** (2), T 48-T 51 (1980).

117. A.Y. Coran, S. Lee, Paper presented at a meeting of the Rubber Division, ACS Nov. 3 – 6 (1992).

118. C. Koning, M. Van Duin, C. Pagnoulle, R. Jerome, *Prog. Polym. Sci*, **23**, 707 (1998)

119. D. Romanini, E. Garagnani, E. Marchetti, *New Polym. Mat.*, Proc. Int. Sem., **56**, (1987).

120. Y. Kikuchi, T. Fukui, T. Okada, T. Inoue, *Polym. Eng. Sci.*,**31**, 1029 (1991).

121. A.Y. Coran in *Thermoplastic Elastomers*, A Comprehensive Review, Ch.7, N.R. Legge, G. Holden, H.E. Schroeder, eds., Hanser, New York, (1987).

122. A.M. Gessler, US patent 3,037, 954, June 5, (1962).

123. W.K. Fischer, US patent 3,758, 643, Sept. 11, (1973).

124. P.L. Ma, B.D. Favis, m.F. Champague, M.A. Huneault, F. Tofan, *Polym. Eng. Sci.*,**42**, 1976 (2002).

125. X. Liu, H. Huang, Z.Y. Xie, Y. Zhang, K. Sun, L.N. Min, *Polymer Testing*, **22**, 9 (2003).

126. X.F. Zhang, H. Hung, Y.X. Zhang, *J.Appl. Polym. Sci.*, **85**, 2862 (2002).
127. Z.J. Wang, X.F. Zhang, Y.X. Zhang, *Polymer Testing*, **21**, 577 (2002).
128. C.R. Kumar, I. Fuhrmann, J. Karger Kocsis, *J. Hydrology*, **261**, 137 (2002).
129. D.K. Setua, C. Soman, A.K. Bhowmick, G.N. Mathur, *Polym. Eng. Sci.*,**42**, 10 (2002).
130. Y. Coran, R. Patel, *Rubber Chem. Technol.*, **53**, 141 (1980).
131. H. J. Radusch, , E. Lammer, T. Liipke, L. Haussler, M. Sandring, *Kautschuk Gummi Kunstst.*, **44**, 1125 (199
132. W.E. Baker, C.E. Scott, G.H. Hu, (eds.), Reactive Polymer Blending, Ch. 4, Hanser, Munich, (2001).
133. Y.D. Lee, C.M. Chen, *J.Appl. Polym. Sci.*, **33**, 1231 (1987).
134. W.E. Baker, C.E. Scott, G.H. Hu, (eds.), Reactive Polymer Blending, Ch. 4 Hanser, Munich, (2001).
135. C.E. Scott, C.W. Macosko, *Polymer*, **35**, 5422 (1994).
136. C.M. Roland, G.G.A. Bohm, *J. Polym. Sci.,Polym. Phys.*, **22**, 79 (1984).
137. J.J. Elmendrop, A.K. Van der Vegt, *Polym. Eng. Sci.*,**26**, 1332 (1986).
138. A.K. Chester, *Trans I Chem*, **61**, 259 (1991).
139. J.L. Jorgensen, A. Valenza, *Makromol. Chem., Makromol. Symp.*, **38**, 43 (1990).
140. G.I. Taylor, *Proc. R. Soc. London*, **A 138**, 41 (1932).
141. G.I. Taylor, *Proc. R. Soc. London*, **A 146**, 501 (1934).
142. W. Bartok, S.G. Manson, *J. Colloid Sci.*, **13**, 393 (1958).
143. H.J. Karan, J.C. Bellingeer, *Ind. Eng. Chem. Fundam.*, **167**, 241 (1986).
144. H.P. Grace, *Chem. Eng. Commun*, **14**, 225 (1982).
145. H.J. Van Oene, *J. Colloid Interface Sci.*, **40**, 448 (1972).
146. S. Wu, *Polym. Eng. Sci.*,**27**, 335 (1987).
147. A.J. Oshinski, H. Keskkula, D.R. Paul, *Polymer*, **37**, 4891 (1996).
148. M.A. Huneault, Z.H. Shi, L.A. Utracki, *Polym. Eng. Sci.*, **35**, 115 (1995).

149. G. Serpe, J. Jarrin, F. Dawans, *Polym. Eng. Sci.*, **30**, 553 (1990).

150. U. Sundararaj, C.W. Macosko, *Macromolecules,* **28**, 2647 (1995).

151. A.P. Plochocki, S.S. Dagli, R.D. Andrews, *Polym. Eng. Sci.*, **30**, (1990).

152. B. Majumdar, D,R, Paul, J. Oshinski, *Polymer*, **38**, 1787 (1997).

153. G.H. Hu, L.J. Kadri, *J. Polym. Sci.,Polym. Phys.*, **36**, 2153 (1998).

154. S. Thomas, G. Groeninckx, *Polymer*, **40**, 5799 (1999).

155. K. Dedecker, G. Groeninckx, *Polymer*, **39**, 4985 (1998).

156. K. Dedecker, G. Groeninckx, *Polymer*, **39**, 4993 (1998).

157. C. Pagnoulle, C. Koning, L. Leemans, R. Jerome, *Macromolecules*, **33**, 6275 (2000).

158. C.A. Orr, A. Adedeji, A. Hirao, F.S. Bates, C.W. Macosko, *Macromolecules,* **30**, 1243 (1997).

159. D. Broseta, G.H. Fredrickson, E. Helfand, L. Leibler, *Macromolecules,* **23**, 132 (1990).

160. E. Helfand, *J. Chem. Phys.*, **62(3)**, 999 (1975).

161. E. Helfand, A.M. Sapse, *J. Chem. Phys.*, **62(4)**, 1327 (1975).

162. J. Kressler, *Macromolecules,* **27**, 2448 (1994).

163. S.K. Kumar, *Macromolecules,* **27**, 260 (1994).

164. J. Reiter, G. Zifferer, O.F. Olaj, *Macromolecules,* **23**, 224 (1990).

165. C.E. Koning, A. Jkker, R. Borggreve, L. Leemans, M. Moller, *Polymer*, **34**, 4410 (1993).

166. J.L. White, K. Min, *Mixing of Polymer* in Comprehensive Polymer Science, S.L. Aggarwal, ed., Pergamon, New York (1989).

167. S. Endo, K. Min, J.L. White, T. Kyu, *Polym. Eng. Sci.*, **26**, 4563 (1985).

168. C.C. Chen, F. Fontain, K. Min, J.L. White, *Polym. Eng. Sci.*, **28**, 69 (1988).

169. D.R. Paul, J.W. Barlow, *J. Macromol. Sci., Macromol. Chem.*, **C18**, 109 (1980).

170. G.M. Jordhamo, J.A. Manson, L.H. Sperling, *Polym. Eng. Sci.*, **26**, 517 (1986).

171. V.I. Metelkin, V.S. Blekht, *J. Colloid,* **46,** 425 (1984).

172. L.A. Utraki, *Polym.Mater. Sci. Eng.*, **65**, 50 (1991).

173. P.T. Hietaoja, R.M. Holsti-Miettinen, J. Seppala, O.T. Jkkala, *J.Appl. Polym. Sci.,* **54**, 1613 (1994).

174. B. De Roover, *PhD Thesis*, University Cotholique de Louvain (1994).

175. A.A. Collyer, Rubber Toughened Engineering Plastics, Chapman and Hall, London, (1994).

176. A. Echte, Rubber Toughened Plastics, pp 15-64, C.K. Riew, ed. ACS, Wasington D.C. (1989).

177. E. Piorkowska, A.S. Argon, R.E. Cohen, *Macromolecules*. **23**, 3838 (1990)

178. A.M.L. Magahaes, J.M. Borggreve, *Macromolecules*, **28**, 5841 (1995).

179. S.G.Turley, H. Keskkula. Polymer, **21**,466 (1980).

180. D.G. Cook, A. Plumtree, A. Rudin, *Plast. Rubber Compos. Process Appl.*, **20**, 219 (1993).

181. D.G. Cook, A. Plumtree, A. Rudin, *J. Appl. Polym. Sci.*, **48**, 75 (1993).

182. G. Dagli, A.S. Argon, R.E. Cohen, *Polymer*, **36**, 2173 (1995).

183. S.Y. Hobbs, *Polym. Eng. Sci.*, 26, 74 (1986).

184. M. Schneider, T. Pith, M. Lambla, *J. Appl. Polym. Sci.*, **62**, 273 (1996).

185. M. Schneider, T. Pith, M. Lambla, *J. Meter. Sci.*, 32, 6331 (1997).

186. M. Schneider, T. Pith, M. Lambla, *Polym. Adv. Technol.*, 7, 577 (1996)

187. K.F. Gazeley, A.D.T. Gorton, T.D. Pendle, Natural Rubber Science and Technology, A.D. Roberts, ed., pp. 63-97, Oxford Science Publications, Oxford, (1988).

188. P. Tangboriboonrat, C. Tiyapiboonchaiya, *J. Appl. Polym. Sci.*, **71**, 1333 (1999).

189. P. Tangboriboonrat,K. Suchiva, S. Kuhakarn, *Polymer*, **35**, 3144 (1994)

190. P. Tangboriboonrat,K. Suchiva, G. Riess, *Polymer*, **36**, 781 (1995)

191. P. Tangboriboonrat,K. Suchiva, S. Kuhakarn, S. Thuchinda, *J. Nat. Rubb. Res.*, **11**, 26 (1996).

192. M. Mathew, S. Thomas, *Polymer*, **44**, 1295 (2003).

193. Z.P. Fang, Z.H. Guo, L. Zha, *Macomol. Meter. Eng.*, **289**, 743 (2004).

194. B.K. Kim, K.H. Shon, H.M. Jeong, *J. Appl. Polym. Sci.*, **92**, 1672 (2004).

195. G.Z. Li, M.L. Ye, L.H. Shi, *J. Appl. Polym. Sci.*, **60**, 1163 (1996).

196. B.G. Soares, R.V. Barbosa, J.C. Covas, *J. Appl. Polym. Sci.*, **65**, 2141 (1997).

197. J.J. Crevecoeur, L. Nelissen, M.C.M. Vander Sanden, P.J. Limstra, *Polymer*, **36**, 1295 (1995).

198. S. Shaw, R.P. Singh, *J. Appl. Polym. Sci.*, **40**, 693 (1990).

199. S. Anandhan, P.P. De, S.K. De, A.K. Bhowmick, *J. Appl. Polym. Sci.*, **88**, 1976 (2003).

200. T.Y. Guo, G.L. Tang, G.J. Hao, M.D. Song, B.H. Zhang, *J. Appl. Polym. Sci.*, **90**, 1290 (2003).

201. Kevin S. Jack, Almeria Natansohn, Jiahu Wang, Basil D. Favis, Patrick Cigana, *Chem. Mater.*, **10**, 1301 (1998).

202. Patrick Cigana, Basil D. Favis, Carolyne Albert, Toan Vu-Khanh, *Macromolecules*, **30**, 4163 (1997).

203. A.A. Higazy, H. Afifi, A.H. Khafagy, M.A. El-Shahawy, A.M. Mansour, *Ultrasonics*, **44**, 1439 (2006)

Chapter 2

Experimental techniques

The materials used for the study, the experimental methods, procedures used for blending, sample preparation and measurement of various properties are discussed in this chapter.

2.1 Materials

2.1.1 Polymers

Polystyrene (PS) was supplied by M/s LG polymers, Mumbai, India. Powdered nitrile rubber (NBR) was purchased from M/s Gujarat Apar polymers Ltd, Mumbai, India.

Polystyrene

Density = 1.05g/cm^3, Melt flow index =10g/10 min.

Uncrosslinked powdered NBR (P 6423)

Acrylonitrile content = 33%, density = 1.0 g/cm^3. Mooney viscosity (1+4) 100^{0}C = 80.

Partially crosslinked powdered NBR (P 3383)

Acrylonitrile content = 33%, density = 1.0 g/cm^3 Mooney viscosity (1+4) 100^{0}C = 60.

2.1.2 Compatibilisers

Maleic anhydride modified polystyrene (MAPS) was prepared by melt mixing PS (100g) with maleic anhydride (6g) and dicumyl peroxide (1g) in a Haake Rheocord at180°C and 60 rpm [1]. The sample was purified by extracting with acetone and dried at 40°C in a vacuum oven for 6 h. The FTIR spectrum of the sample was recorded on a Nicolet Avtar 360 ESP FTIR spectrophotometer at a resolution of 2 cm^{-1} with the spectral range of 4000 -- 400 cm^{-1}

Phenolic modified polystyrene (PhPS) was prepared using a Haake Rheocord by melt mixing process [2-4]. PS (100g) and dimethylol phenolic resin SP 1045 (4g) were mixed at180°C and 60 rpm for 3 min. Stannous chloride (0.8g) was then added and mixing was continued for 2 min. The sample was purified by extracting with acetone. The FTIR spectrum of the sample was recorded on a Nicolet Avtar 360 ESP FTIR spectrophotometer with the spectral range of 4000–400 cm^{-1}

Styrene-co-Acrylonitrile (SAN) was purchased from Anoopam plastics India Ltd, New Delhi.

2.2 Experimental procedure

2.2.1 Blending

Blends were prepared by melt mixing in Haake Rheocord 600 for 10 min., at 40 rpm rotor speed and 180°C. PS was first melted for 4 min. followed by the addition of powdered NBR. Mixing was continued for 6 min. In compatibilised blends, compatibilisers were added 4 min. after the melting of PS and mixed for another 2 min. followed by the addition of NBR. The compatibiliser concentration was varied from 1 to 10 wt%.

2.2.2 Dynamic crosslinking

Dynamic vulcanisation was carried out with dicumyl peroxide (40% active DCP). The concentration of the DCP was varied from 0.5 to 2 phr. Representative sample codes with composition are given in table 2.1

2.3 Moulding

The hot mix was sheeted out using a two roll mill and granulated. The test specimens were prepared using a semiautomatic plunger type injection moulding machine at a barrel temperature of 180^0C.

Table 2.1: Representative sample codes with composition

P_{100}	100 PS
P_{95}	95 PS/5 NBR
P_{90}	90 PS/10 NBR
Px_{95}	95 PS/5 XNBR
Px_{90}	90 PS/10 XNBR
$P_{90}D_{1.5}$	P_{90} vulcanised using 1.5 phr DCP
$P_{90}M_2$	P_{90} containing 2% MAPS
$P_{90}H_2$	P_{90} containing 2% PhPS
$P_{90}S_2$	P_{90} containing 2% SAN

2.4 Scanning electron microscopy

Scanning electron microscopy is a very useful tool to gather information about topography, morphology, composition and microstructural information of materials. The image is formed by scanning a probe of focused electron beam

across the specimen. The electron beam interacts with a thin film surface layer of the specimen resulting in back scattering of electrons of high energy, generation of secondary electrons of low energy and X-rays. These signals are monitored by detectors and magnified. An image of the investigated microscopic region of the specimen is thus observed in cathode ray tube and photographed using photographic film. SEM image has characteristic three dimensional appearance and are useful in judging the surface structure of the sample.

In the present study, morphological characterisation of the fractured surfaces of the tensile test specimens was carried out using scanning electron microscope (Cambridge Stereoscan S 360) after sputter coating the surface with gold/palladium alloy. The domain size was measured from the scanning electron photomicrographs. Several micrographs were taken for each blend and about 100 domains were taken for number average domain diameter measurements. The apparent domain diameter was obtained from the measurement of hole diameter.

2.5 Mechanical properties

Tensile testing was done using dumb-bell shaped samples at a cross-head speed of 50mm/min. with a Universal Testing Machine (UTM)-Shimadzu AG 1 according to the ASTM D-638 test method. One grip is attached to a fixed and the other to a movable (power-driven) member so that they will move freely into alignment as soon as any load is applied. Test specimen was held tight by the two grips, the lower grip of which was fixed. The output data in the form of stress-strain graph and elongation, modulus and energy absorbed at various stages of the test directly appears on the console of the microprocessor and as a print out. The area under the stress-strain curve provides an indication of the overall toughness of the material at the particular temperature and rate of loading. The energy absorbed by the sample is also a measure of the toughness.

Izod impact strength was measured on a Zwick Impact Tester as per ASTM D 256-88 specifications. Impact strength is the energy absorbed by the specimen during the impact process and is given by the difference between the potential energy of the hammer or striker before and after impact.

The specimens were tested on the impact tester having 4J capacity hammer and striking velocity of 2.2 m/s. A sample is clamped vertically in the base of the machine. The pendulum is released. The impact resistance or strength is evaluated from the impact values directly read from the tester.

The flexural properties were tested on a Shimadzu Autograph (AG-1 50 kN) Universal Testing Machine (ASTM D 790) at a constant rate of traverse of the moving grip of 1.3 mm/min. The cast specimens in the form of rectangular bars were polished using emery paper prior to testing. The depth and width of the specimen was measured nearest to 0.01 mm. The support span should be 16 times the depth of the specimen. The specimen was centred on the supports with the long axis of the specimen perpendicular to the loading nose and supports. The load was applied to the specimen and flexural strength and modulus were recorded. The load-deflection curve was also obtained. It is calculated at any point on the stress strain curve by the following equation

$$S = \frac{3PL}{2bd^2}$$

where S = stress in the outer fibres at midpoint (MPa), P = Load at any point on the load–elongation curve (N), L = support span (mm), b = width of specimen tested (mm), d = depth of specimen (mm).

Flexural modulus is the ratio of stress to corresponding strain and is expressed in MPa. It is calculated by drawing a tangent to the steepest initial straight line portion of the load- deflection curve and using the equation

$$E_B = \frac{L^3 m}{4db^3}$$

where E_B = modulus of elasticity in bending (MPa), L = support span (mm), b = width of specimen tested (mm), d = depth of specimen (mm), m = slope of the tangent to the initial straight line portion of the load – deflection curve (N/mm of deflection)

2.6 Dynamic mechanical analysis

The dynamic mechanical analysis of the samples was carried out using a dynamic mechanical analyzer (TA instrument Q 800). Rectangular 50x12x3 mm^3 samples were subjected to a frequency of 1 Hz over a temperature range of 35 to 120°C at a heating rate of 3°C/ min.

2.7 Melt flow measurements

Rheological measurements were carried out using a capillary rheometer attached to an Universal Testing Machine. A capillary of length 40 mm and diameter 1.0 mm was used. The angle of entry was 90° so as to minimise end effects. Samples for testing were cut into small pieces and packed inside the barrel of the extrusion assembly without air entrapment. The melt height before extrusion was kept the same in all the experiments. The material was extruded at 170, 180 and 190°C through the capillary at six pre-selected cross-head speeds. The force corresponding to different plunger speeds was recorded. The force and cross-head speeds were converted into apparent shear stress (τ_w) and shear rate (γ_w) at the wall respectively, using the following equations involving the geometry of the capillary and plunger:

$$\tau_w = \frac{F}{4A_p(l_c / d_c)}$$

$$\gamma_w = \frac{3n'+1}{4n'} \frac{32Q}{\pi d_c^3}$$

where F the force applied at a particular shear rate, A_p the cross-sectional area of the plunger, l_c the length of the capillary and d_c the diameter of the capillary, Q the volume flow rate and n' the flow behaviour index.

The flow behaviour index n' was determined by regression analysis of the values of τ_w and γ_w obtained from the experimental data. The shear viscosity, η was calculated from τ_w and γ_w using the relation

$$\eta = \frac{\tau_w}{\gamma_w}$$

2.8 Die swell measurements

Extrudates emerging from the die of the capillary were collected for die-swell measurements taking maximum care to avoid any further deformations. The die swell ratio was calculated by measuring the diameter of the extrudate (d_e) at several points using a travelling microscope. The swelling index is the diameter of the extrudate to that of the capillary (d_c).

$$\text{Die - swell ratio} = \frac{d_e}{d_c}$$

2.9 Determination of crosslink density

The crosslink density (CLD) of vulcanised samples was determined by the equilibrium swelling method. To estimate the extent of crosslinking, the volume fraction, Vr, of the rubber in chloroform swollen specimens was determined after 48 hours using the relation [5]

$$Vr = \frac{(D\text{-}fT)\rho_r^{-1}}{(D\text{-}fT)\rho_r^{-1} + A_O\rho_s^{-1}}$$

where D the weight of the sample after drying out, f the fraction of insoluble components, T the weight of the sample, A_o the weight of the absorbed solvent, ρ_r the density of the rubber and ρ_s the density of the solvent.

2.10 Thermogravimetric analysis

Thermogravimetric analysis of the samples was carried out using a thermogravimetric analyzer (TA instrument Q 50). A small amount (1-3 mg) of sample was taken for the analysis and the samples heated from 30 to 800°C at a heating rate of 20°C/min in nitrogen atmosphere. The TGA and DTG curves are drawn for each sample.

2.11 Fourier transform infrared spectroscopy

Fourier transform infrared spectra (FTIR) are generated by the absorption of electromagnetic radiation in the frequency range 400 to 4000 cm^{-1} by organic molecules. Different functional groups and structural features in the molecules absorb energy at characteristic frequencies. The frequency and intensity of absorption are the indication of the bond strength and structural geometry in the molecule. The FTIR spectrum of the sample was recorded on a Nicolet Avtar 360 ESP FTIR spectrophotometer with the spectral range of 4000–400 cm^{-1}.

References

1. K. Dedecker, G. Groeninckx, *Macromolecules*, **32**, 2472 (1999)
2. A.Y. Coran, R. Patel, *Rubber Chem. Technol.*, **56**, 1045 (1983)
3. A.Y. Coran, R. Patel, *US 4299931* (Nov. 10, 1981) (to Monsanto Co.)
4. A.Y. Coran, R. Patel, *US 4355139* (Oct. 19, 1982) (to Monsanto Co.)
5. P.E. Cassidy, T.M. Aminabhavi, C.M. Thompson, *Rubber Chem. Tech.*, **56**, 594 (1983)

Chapter 3

Toughening of polystyrene with uncrosslinked and partially crosslinked powdered NBR

Plastic/rubber blends have been commercialised as rubber toughened plastics or as thermoplastic elastomers [1, 2]. Generally if a relatively large portion of the hard plastic is used, the composition can be used as an impact resistant plastic; whereas, if a relatively large amount of rubbery phase is used, the blend will be soft and have at least some of the properties of an elastomer. Polymer blends vary greatly in morphological complexity. Rubber toughened plastics are typically two phase systems consisting of a rubbery impact modifier dispersed in a thermoplastic matrix. Small changes in the size and arrangement of these dispersed particles can produce large variation in the physical performance and aesthetic qualities of the blend.

The main physical factors that determine the final morphology of the blends are composition, rheological and physical characteristics of the components, relative compatibility, and rate of shearing during the melt mixing. Detailed investigations on phase morphology development, phase co-continuity and phase stability of polymer blends [3, 4] have been undertaken. The correlations between morphology and mechanical properties have been established [5, 6]. In fact, it is well known that by using different mixers, and/or by varying the mixing parameters, it becomes possible to control phase morphology [7-9].

Morphology development is the evolution of the blend morphology from pellet-sized or powder sized particles to the sub micrometer droplets, which exists in the final blend. Final morphology has a controlling influence on the properties and end use of the blend. Knowledge of mechanism of morphology development is useful for design of intensive mixers with better dispersive mixing capabilities for reactive blending and also to understand the kinetics of creation of interfacial area during blending. The mechanism governing morphology developments are; fluid drops stretching into threads, break-up of the threads into smaller droplets [9] and coalescence of droplets into larger ones. Balance of these competing processes determines the final particle size, which is formed upon solidification of the blend. While drop break-up is not dependent on the content of the dispersed phase [10], coalescence [9] is strongly influenced by the blend composition [8, 11, 12]. There are several good reports depicting the relationship between morphologies and these factors [13-18].

Thomas *et al* [19] studied the effect of processing conditions on the morphology development of PA6/EPM blends. The dispersed phase morphology as a function of mixing time was investigated for aromatic amorphous PA6/Zytel (Zytel 330)/EPM and PS/EPM by Scott and Macosko [20]. In this study most of the reduction in the dispersed phase size was observed at shorter mixing times in conjunction with the melting and softening process. At intermediate mixing time, the morphology consisted of a large number of small particles along with a small number of very large particles in the size distribution. The effect of subsequent mixing reduced the size of the largest particles in the size distribution. Other reports in the literature regarding the influence of mixing time on the dispersed phase size include the studies of Karam and Bellinger [21], Karger-Kocsis *et al* [22], Schreiber *et al* [23] and Laokijcharoen *et al* [24].

The influence of time of mixing in a Haake Rheocord on the size of dispersed phase has been studied by a number of workers. Particle size reduction is the first step in morphology development for a poly blend. Favis [25] observed that for polypropylene/polycarbonate (PP/PC) blends, the most significant particle size deformation and disintegration process took place within the first 2 min. of mixing. After 2 min. very little reduction in the size of the dispersed phase was observed up to 20 min. mixing time. Based on these results it was suggested that melting process might be important in generating the final morphology of an immiscible blend. Plochocki *et al* [26] studied the processing of PS/LDPE blends in several industrial mixers and observed that the initial dispersion mechanism might be due to abrasion of solid or partially softened pellets on the wall of the processing equipment. Sundararaj *et al* [27] studied the processing of both polyamide/PS and polypropylene/PS blend systems in a twin screw extruder and showed that major reduction in domain size occurred during the melt softening step. Continued mixing reduces the size of large particles and rounds off the particles. Morphology of the dispersed phase is rapidly modified under dynamic conditions in the melt.

Numerous studies were carried out to investigate the toughening of PS by the effects of dispersed rubber phase properties such as rubber concentration, particle size, shape, spatial packing of the rubber particles and the degree of functionalisation. However there were few studies concerned with crosslinking of the rubber phase. Bucknall [1] reported that crosslinking of rubber particles is desirable since during impact the rubber phase is subjected to a very large tensile strain giving craze like structure. A moderate degree of crosslinking allows the rubber particles to reach high strain by fibrillation and at the same time renders mechanical strength to the fibrils. Dao [28] found that crosslinked ethylene propylene diene terpolymer (EPDM) is more effective as an impact modifier for polypropylene than uncrosslinked EPDM. A moderate degree of crosslinking allows the rubber to reach high strains by fibrillation and at the same time renders

mechanical strength to the fibrils. Crosslinking increases the rubber viscosity, which will affect the blending process and particle size of rubber. The particle size, in turn, strongly influences the impact behaviour of the blends [29]. Crosslinked EPDM did not seem to have any effect on the impact properties of polyamide6/EPDM blends [30]. Mehrabzadeh *et al* [31] studied the effect of crosslinking on the impact properties of PA 11/NBR blends. They found that static and dynamic crosslinking do not significantly improve the impact strength. Several recent articles deal with the optimisation of processing parameters based on morphology and mechanical properties [32-35].

Miscibility between two polymers is usually characterised by dynamic mechanical analysis or viscoelastic data. The viscoelastic properties like storage modulus, loss modulus and tan δ of polymer depend on structure, crystallinity and extent of crosslinking [36]. The effect of polychloroprene content on the storage modulus of ABS was reported by Kang *et al* [37]. They found that the storage modulus of the blends increases with increase in rubber content. The effect of blend ratio on the dynamic mechanical properties of PP/NBR blends was investigated by George *et al* [38]. Mas *et al* [39] studied the effect of blend ratio on the dynamic mechanical properties of PC/ABS blends.

The usual processing techniques for polymeric materials are injection moulding, extrusion etc. Therefore, it is very important to study their rheological properties to optimise the processing conditions. The importance of rheological studies in predicting the flow behaviour of polymer systems at high temperatures and shear conditions of extrusion and injection moulding processes has been described by several authors [40-42]. Danesi and Porter [43] have reported on the rheological behaviour of polypropylene and ethylene propylene rubber blends.

In order to develop durable industrial products it is necessary to investigate the thermal stability of these blends. Thermogravimetric analysis can be used as a way to measure the thermal stability of polymer due to the simplicity of this weight loss method [44, 45]. The thermal degradation of polymer blends was investigated by various researchers using the thermogravimetric method [46]. The blending of a polymer with other polymers has stabilising as well as destabilising effects. Grassie *et al* [46] reviewed these stabilising effects of blending. The complete degradation of PMMA into monomers on heating can be considerably reduced by blending with other polymers. The destabilising effect of PVC on the degradation of polymers was also investigated. Varughese *et al* [47] reported that, the blending of ENR with PVC reduced the rate of HCl elimination in the first degradation step of PVC. The thermal degradation behaviour of blends has been used to identify SBR/BR blends from SBR based compounds by Amraee *et al* [48] from the ratio of the peak heights of DTG. The effect of miscibility of polymer blends on thermal degradation behaviour was investigated by Lizymol *et al* [49].

This chapter focuses on the preparation of toughened thermoplastic polymer by melt blending polystyrene with uncrosslinked and partially crosslinked nitrile rubber powder (NBR and XNBR) and to evaluate mechanical properties, morphology, dynamic mechanical properties, melt rheology and thermogravimetric analysis of the resulting blends.

3.1 Processing characteristics

The processing characteristics of the blends have been studied from the torque-time plots. Figure 3.1 shows the torque-time plots of PS/NBR and PS/XNBR blends. All the blends show a higher mixing torque than PS and the torque is found to increase with NBR content. This is due to higher melt viscosity of NBR as compared to PS. The XNBR blends register higher torque than blends

with uncrosslinked NBR. In these blends the crosslinked rubber particles exert greater resistance to rotation.

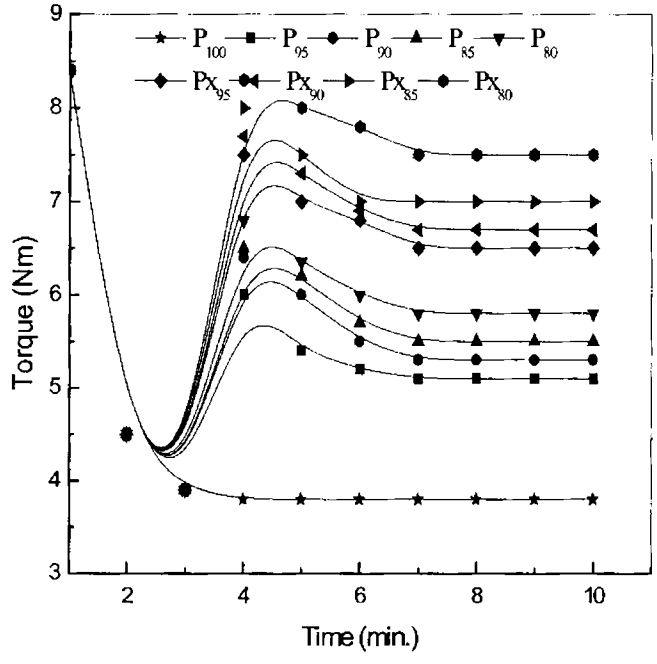

Fig.3.1: Variation of torque with time of mixing for various PS/NBR blends

3.2 Effect of blend ratio on mechanical properties and morphology

Figures 3.2 and 3.3 show the variation of tensile strength and Young's modulus as a function of weight percentage of NBR. From the figures it is clear that for the two blend systems, tensile strength and Young's modulus decrease with increase in NBR content.

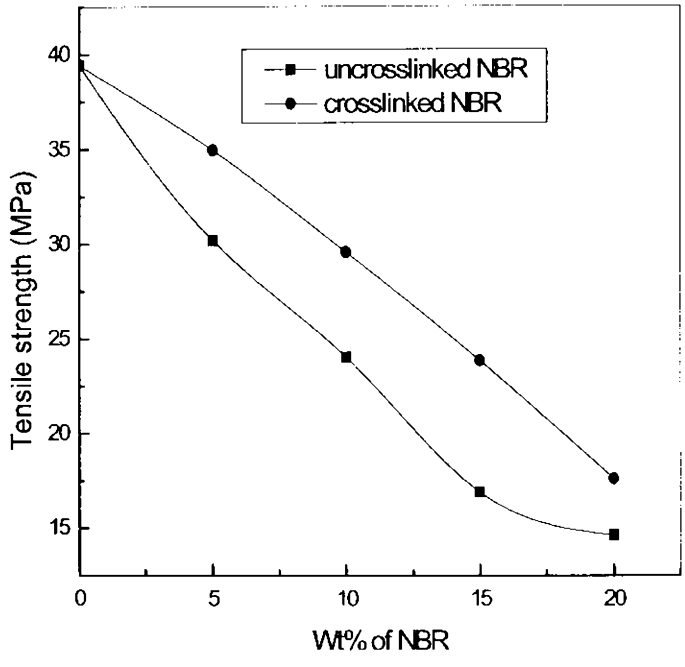

Fig. 3.2: Variation of tensile strength of PS/NBR blends with wt% of NBR

The observed decrease in tensile strength and Young's modulus is due to the presence of soft rubber phase and poor interfacial adhesion between the non-polar PS and polar NBR phases which causes poor stress transfer between the matrix and the dispersed phase. Blends with XNBR display higher values than

blends with NBR. This is due to better interfacial adhesion between PS matrix and XNBR.

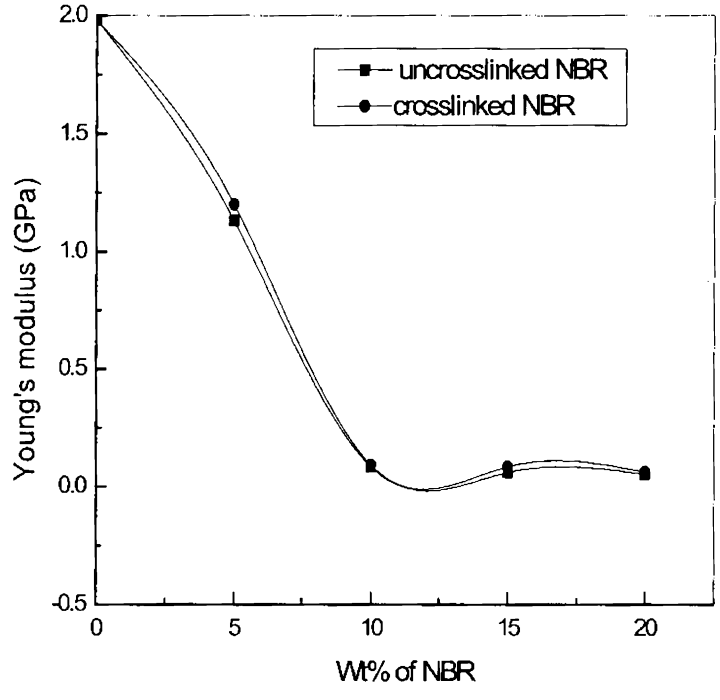

Fig. 3.3: Effect of blend ratio on Young's modulus of PS/NBR blends

The variation of elongation at break with rubber content is shown in figure 3.4. Blends with XNBR have higher elongation at break. This is because the

craze fibrils are stabilised by molecular entanglements and can sustain high stresses for long periods. In unvulcanized systems the molecular entanglement is unable to prevent rapid flow and fracture, in response to applied stress.

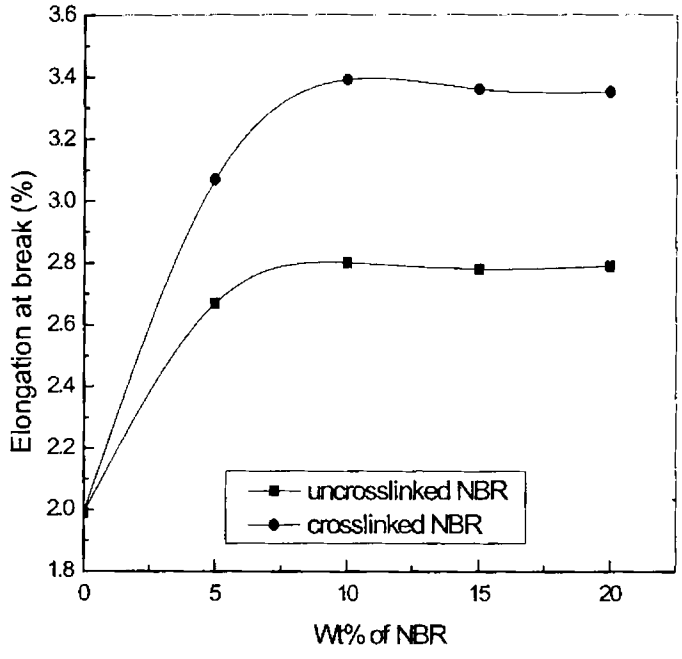

Fig. 3.4: Variation of elongation at break with wt% of NBR

The variation of tensile toughness and Izod impact strength (unnotched) of the blends with NBR content is shown in figures 3.5 and 3.6 respectively. The tensile toughness and impact strength of pure PS are very low. The failure is due to the brittle fracture initiated by crazes. The mechanical behaviour of polymeric system depends on viscoelastic and plastic deformation, which lead to macroscopic failure of the specimen.

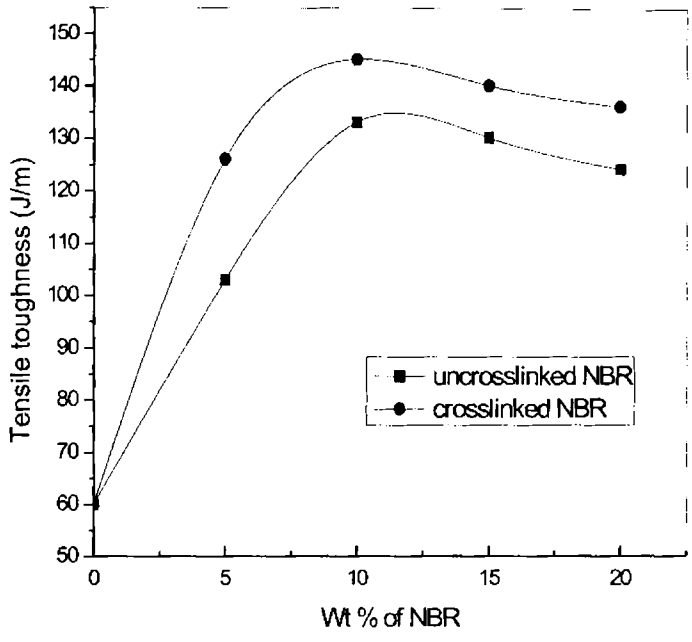

Fig.3.5: Variation of tensile toughness with wt % of NBR

The two main mechanisms responsible for the plastic deformation are crazing and shear yielding, which can operate separately or simultaneously. The plastic deformation mechanism and material toughness will be predicted from molecular parameters (chain flexibility and entanglement density) and from blend morphology (rubber particle size and inter particle distance). In the plastic deformation of brittle plastics like polystyrene, a craze is initiated as a precursor to brittle fracture. This micro mechanism of brittle fracture is often highly localized and confined to a very small volume of the material. Shear yielding consists of a change in shape of the specimen at constant specimen volume. It was considered as due to the molecular slip, flow or molecular motion of different types. A bulk shear yielding mechanism leads to ductile fracture. The intrinsic brittleness or ductility of

polymeric systems is controlled by entanglement density and chain stiffness. Crazing is initiated by chain scission, which is not favoured in the case of high entanglement density polymers [50]. Craze initiation and craze growth can be reduced by increasing the matrix entanglement density. Shear yielding is directly related to chain mobility and is temperature dependent. The competition between crazing and shear yielding determines which mode of fracture will predominate. Crazing occurs when crazing stress is lower than yield stress whereas shear yielding occurs when yielding stress is lower than crazing stress. Both crazing and yielding occurs when crazing stress and yielding stress are comparable.

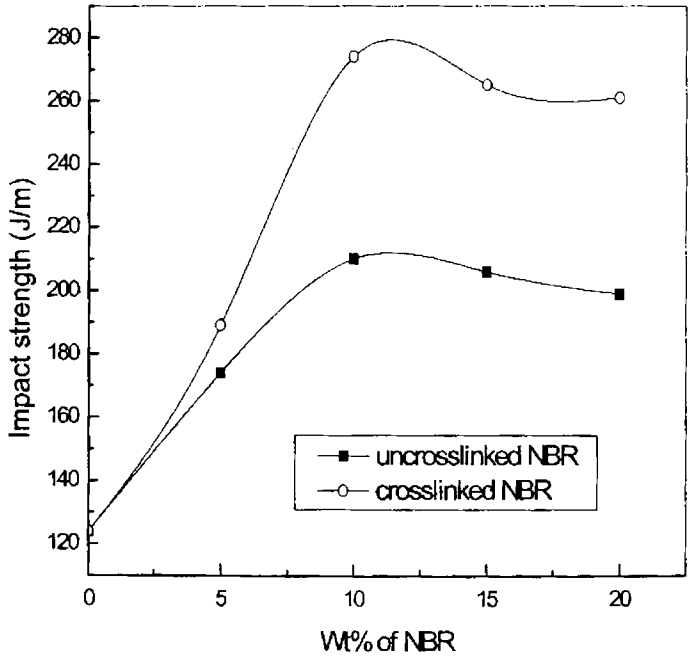

Fig.3.6: Variation of impact strength with wt % of NBR

The tensile toughness and impact strength increases as the NBR content increases from 5 to 10% in both blend systems. This is attributed to the fact that rubber domains act as stress concentration sites for the dissipation of impact energies by controlling and promoting matrix deformation. The addition of rubber leads to relaxation of the stress concentration due to release of constrains of strain by Poisson's contraction between voids at the PS-NBR interfaces. As a result nucleation of catastrophic cracks at the sites of crazes is suppressed and impact strength is improved.

The low impact strength for bends of PS with uncrosslinked NBR compared with blends of PS with XNBR is due to the coalescence of rubber domains during static cooling. This gives rise to irregularly sized rubber domains which are larger than the critical size desired for impact toughening. The size enlargement and shape irregularity results in a reduction of stress concentration sites and interfacial adhesion. In the blends with XNBR, the crosslinked structure of rubber particles inhibits the chance of rubber cohesion during cooling and also the interfacial adhesion is increased by physical interlocking [51].

The flexural strength and flexural modulus results are given in figures 3.7 and 3.8. Flexural strength and flexural modulus show a decrease with increase in rubber content. This is mainly caused by poor interfacial adhesion. The decrease in flexural strength with increase in rubber content indicates an elastomeric nature of the blend. The blends with XNBR have higher flexural strength and flexural modulus than the corresponding blends with NBR. The crosslinked structure enhances the interfacial adhesion. This is accompanied by an increase in flexural strength and flexural modulus.

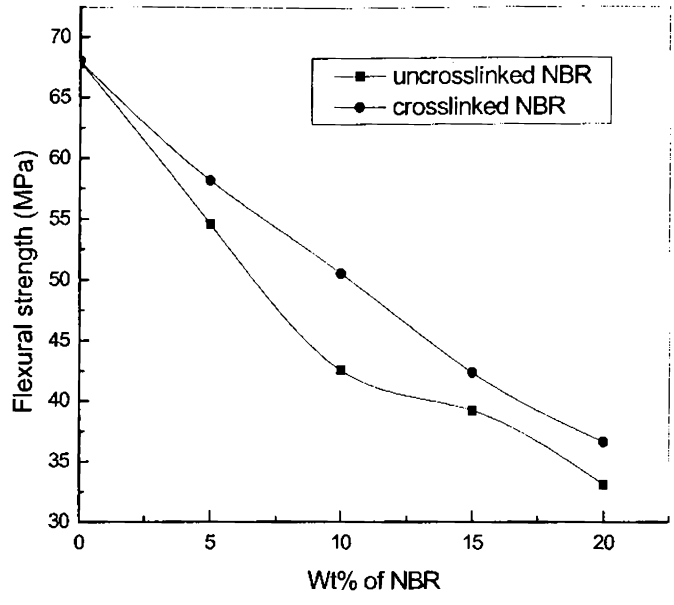

Fig.3.7: Variation of flexural strength with wt% of NBR

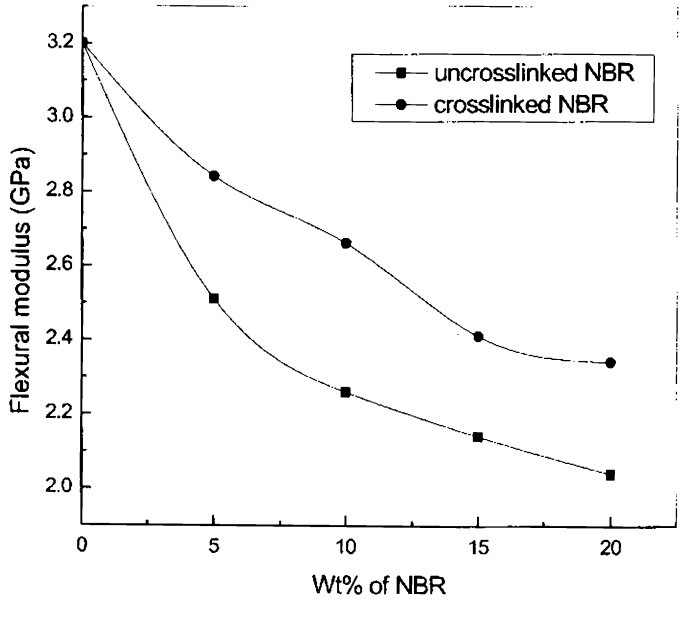

Fig.3.8: Variation of flexural modulus with wt% of NBR

Figure 3.9-1 (a) is the scanning electron micrograph of the fracture surface of pure PS. It contains plane areas with sharp brittle fracture in various planes. The white stress stripes are traces of stress in a propagating process for unmodified PS. The scanning electron micrographs of P_{90}, P_{85} and P_{80} are shown in figures 3.9-1 (b) to (d). These micrographs show the irregular shapes of NBR domains which are more pronounced in P_{85} and P_{80}. The fracture surface observation of blends with XNBR [figures 3.9-2 (a) to (c)] by SEM reveals that, in Px_{90}, the crosslinked rubber particles exist as spherical domains.

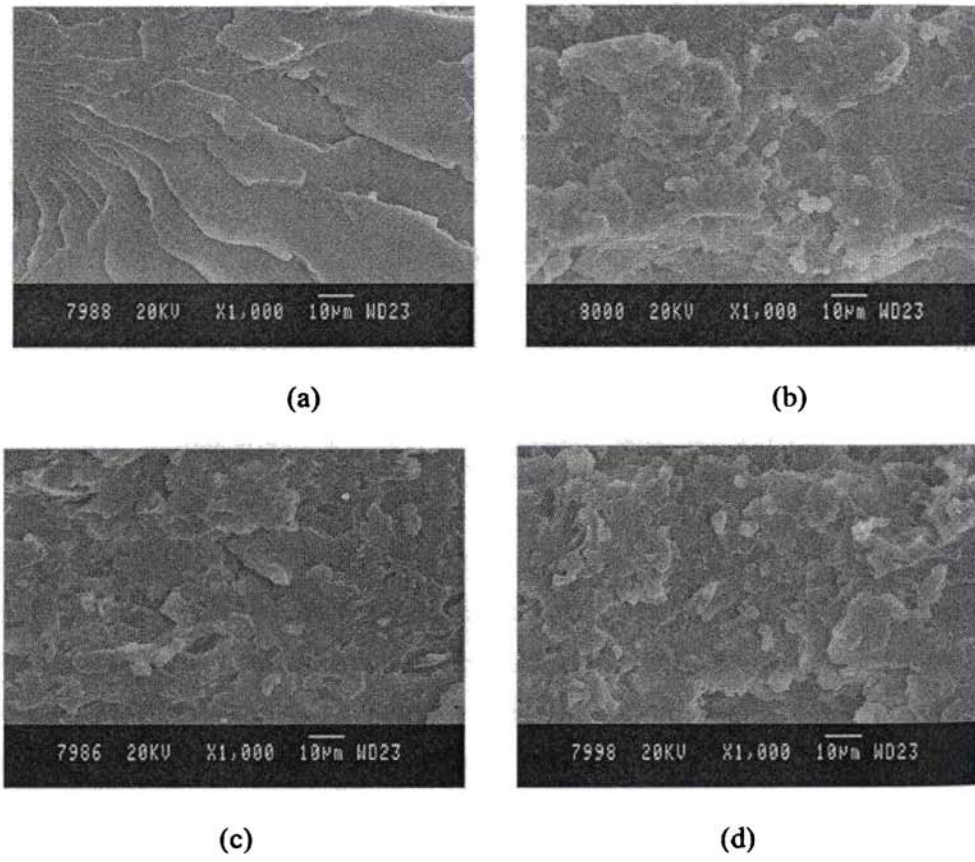

(a) (b)

(c) (d)

Fig. 3.9-1: Scanning electron micrographs of fracture surfaces of PS/NBR blends (a) P_{100}, (b) P_{90}, (c) P_{85} and (d) P_{80}.

As the rubber content increases the average size of the dispersed NBR phase increases. This is attributed to the reagglomeration or coalescence of rubber particles. The occurrence of coalescence at higher concentrations has been reported by many authors [52, 53]. Heikens and Barentsen [53] have reported that in PE/PS blends, the increase in particle dimension of PE at higher concentrations is caused by coalescence

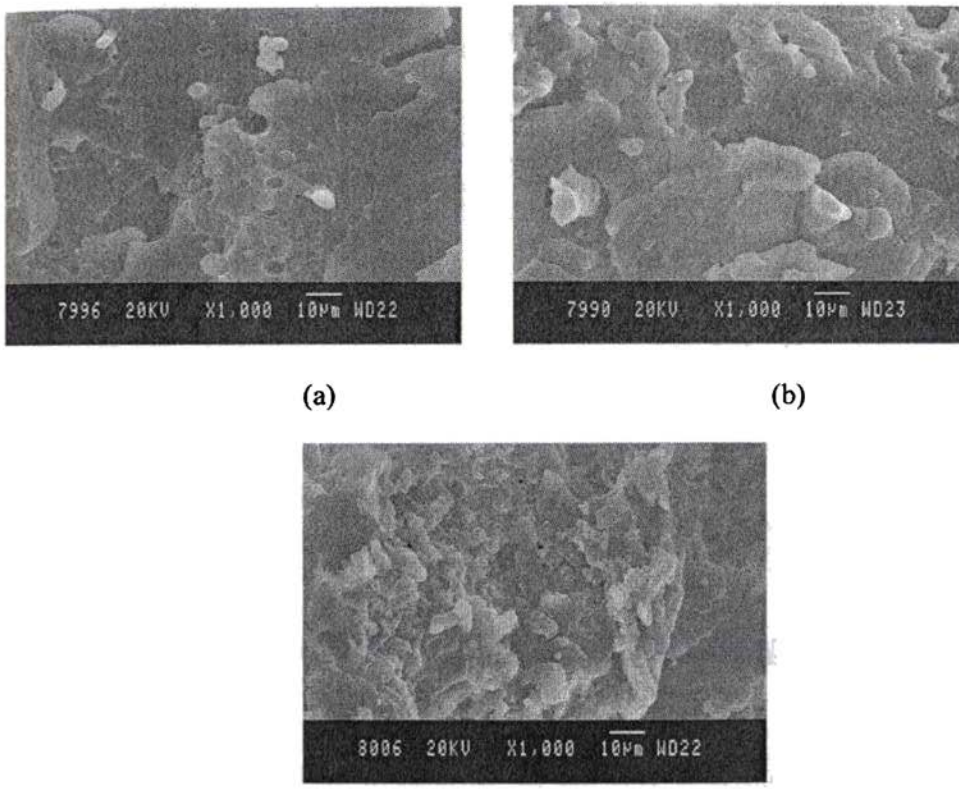

(a) (b)

(c)

Fig. 3.9-2: Scanning electron micrographs of fracture surfaces of PS/XNBR blends (a) Px_{90}, (b) Px_{85} and (c) Px_{80}

3.3 Dynamic mechanical analysis

The variation of storage modulus (E') of various blends as a function of temperature is shown in figures3.10 and 3.11 respectively.

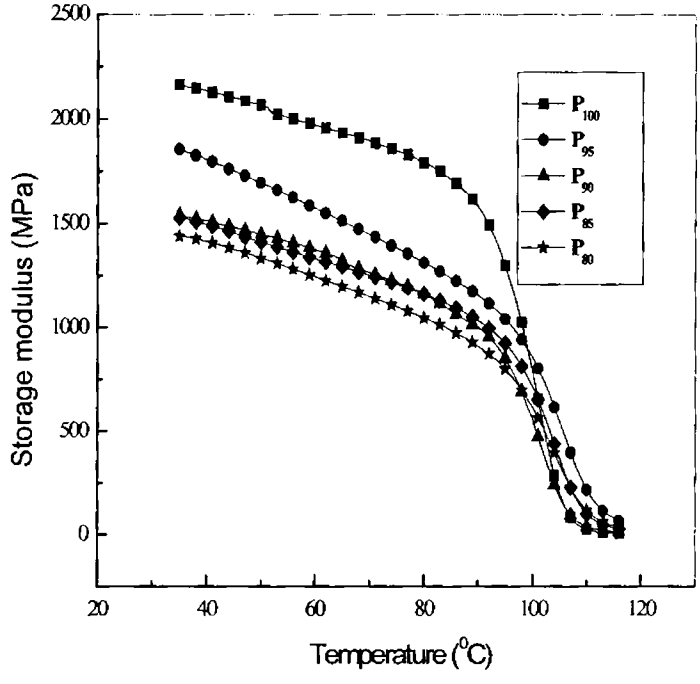

Fig. 3.10: Effect of temperature on the storage modulus of PS/NBR blends

The value of E' signifies the stiffness of the material. The curves for all compositions have the following regions: a glassy region, a transition region and a rubbery region. In the glassy region all the blends show a high modulus. At any fixed rate of deformation, the temperature at which E' starts to decrease rapidly corresponds to the glass transition temperature (T_g). At the transition zone there is drastic decrease in modulus with temperature. This is because at the transition zone segmental mobility sets in followed by a corresponding decrease in the E' values.

The storage modulus is dependent on the rubber content. It is seen from the figures that the modulus of the blends decreased with increase in the rubber content.

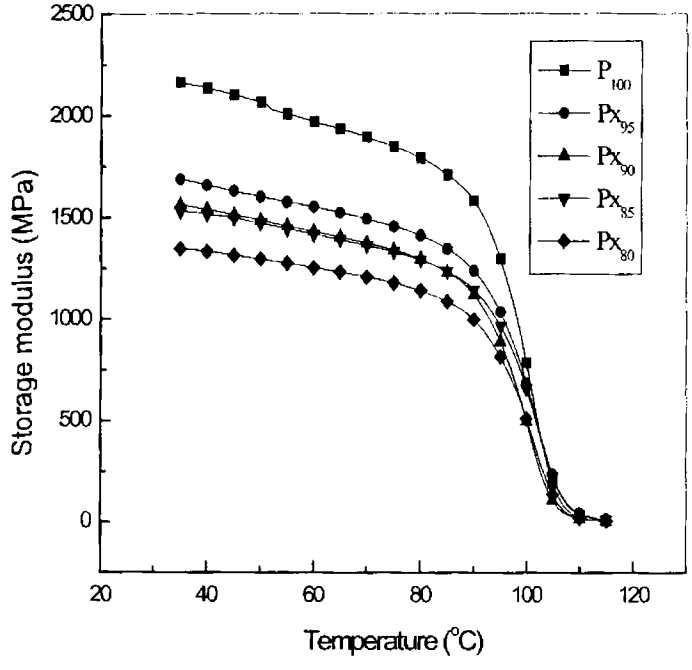

Fig.3.11: Effect of temperature on the storage modulus of PS/XNBR blends

Figure 3.12 shows the variation of storage modulus at 35°C as a function of NBR content. As we have already discussed, the storage modulus decreases with increase in rubber content. The storage modulus of PS/XNBR blends is higher than that of PS/NBR blends at 35°C.

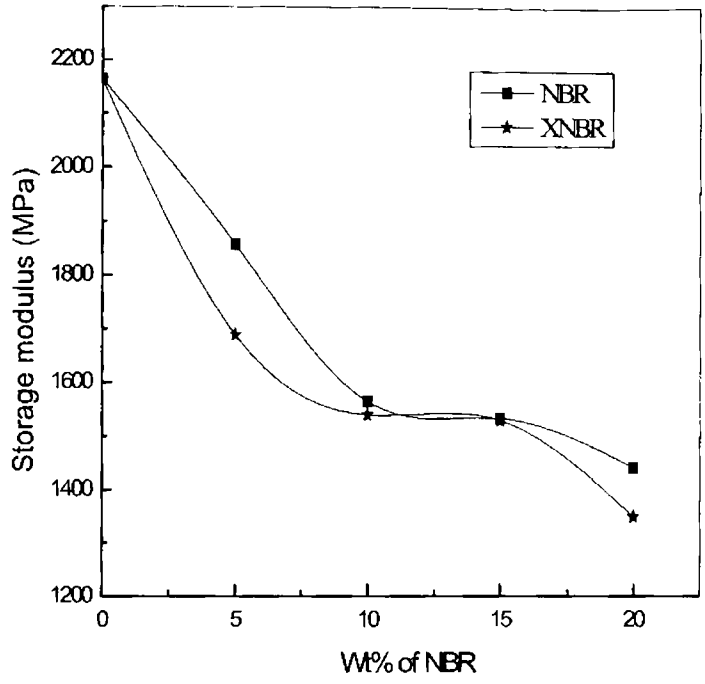

Fig.3.12: Variation of storage modulus of PS/NBR and PS/XNBR blends with wt% of NBR at 35°C

The variation of loss modulus (E") and tan δ with temperature of P_{100}, P_{90} and Px_{90} are shown respectively in figures 3.13and 3.14. In both figures, peaks corresponding to the T_g of polystyrene can be observed. It is evident from figure 3.14 that in Px_{90} the temperature corresponding to the second order transition of PS is unaffected. The tan δ value of Px_{90} is less compared to P_{90} is due to the fact that the three dimensional network of the rubber phase restricts the mobility of the chain segments. As a result, the system becomes more elastic and the dissipation of energy as heat is minimised.

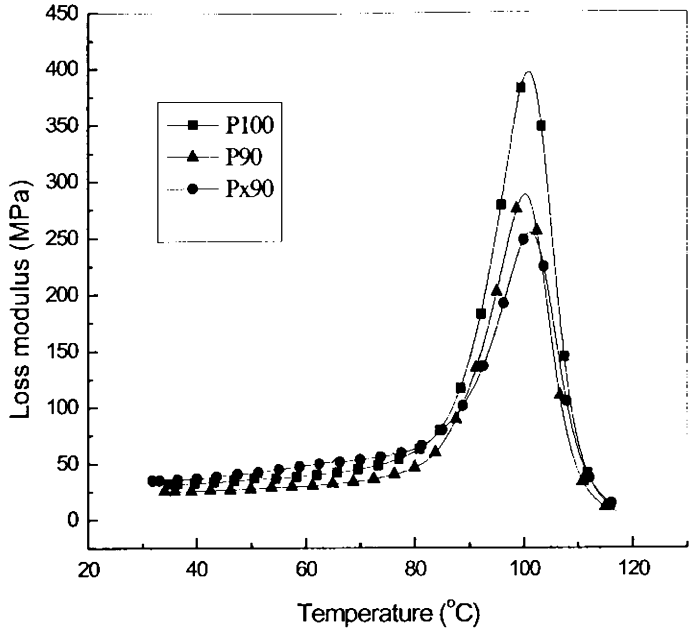

Fig.3.13: Variation of loss modulus of P_{100}, P_{90} and Px_{90} with temperature

The main relaxation process in PS can also be detected in the damping curves presented in figure 3.14. As temperature increases, damping goes through a maximum, near T_g in the transition region and then a minimum in the rubbery region. This type of behaviour can partially be explained on a molecular basis. The damping is low below T_g because the chain segments are frozen in. Below T_g, the deformations are thus primarily elastic and molecular slip resulting to viscous flow is low. Above T_g, where rubbery region exists, the damping is also low because molecular segments are very free to move about and there is little resistance to their flow. Hence, when the segments are frozen in or are less free to move, damping is low. In the transition region, a part of the segments are free to move about and remainder are not so free.

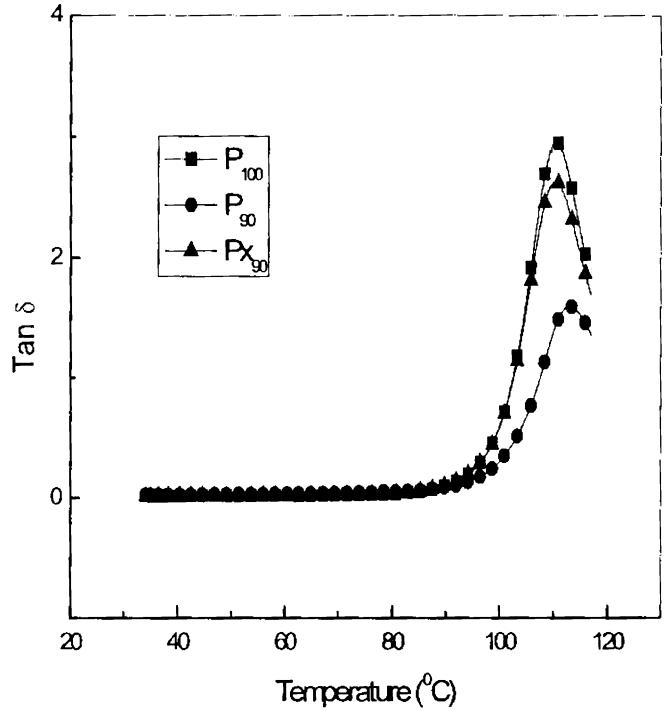

Fig.3.14: Variation of tan δ of P_{100}, P_{90} and Px_{90} with temperature

3.4 Melt rheology

Melt viscosity data of the PS/NBR and PS/XNBR binary blends are given in figures 3.15 and 3.16 respectively as the variations of melt viscosity (η) with the shear stress at 180°C. It is seen from the figures that the viscosity decreases with

the increase in shear stress, showing a pseudoplastic behaviour of the blend systems.

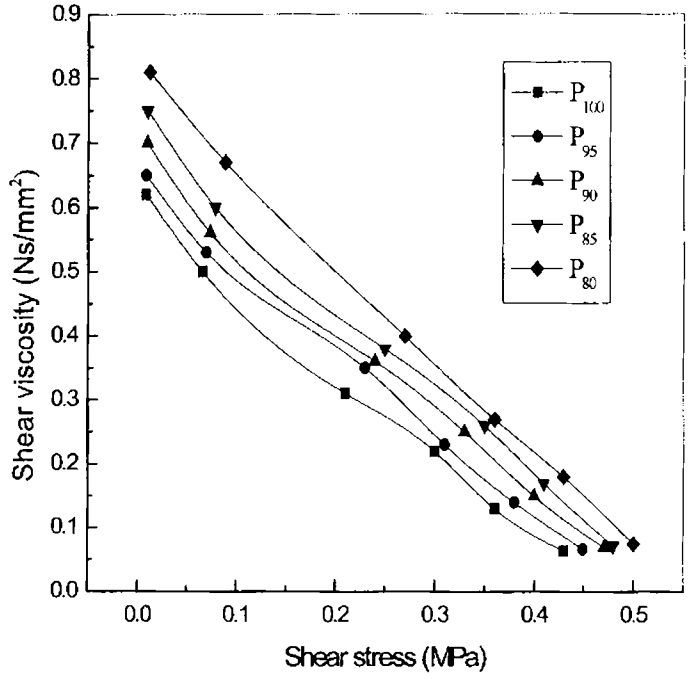

Fig. 3.15: Effect of blend ratio on the shear viscosity/shear stress plots of PS/NBR blends

The pseudoplastic nature of polymers arises from the randomly oriented and entangled nature of polymer chains which on application of higher shear rates, become oriented and disentangled [40]. At any given shear stress, the melt viscosity is lowest for PS. When NBR is added to the PS, viscosity increases with NBR content at all shear rates. PS/XNBR blends have higher shear viscosity than PS/NBR blends

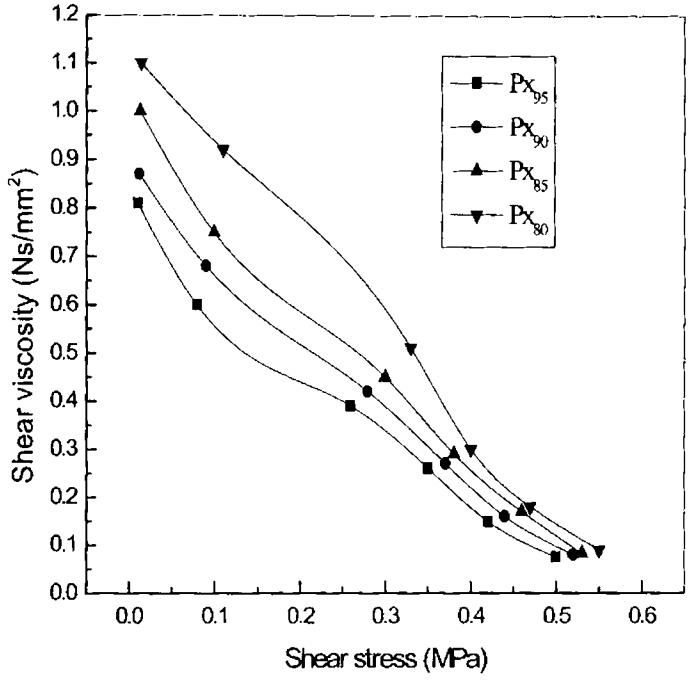

Fig. 3.16: Effect of blend ratio on the shear viscosity/shear stress plots of PS/XNBR blends

Variations of melt viscosity as a function of blend composition at different shear rates for PS/NBR blends are shown in figure 3.17. As the rubber content in the blend increases, the viscosity of the blend is increased. Such an increase in viscosity on incorporation of rubber phase has been reported for several systems [54-58]. In polymer blends, the viscosity depends on interfacial thickness and interface adhesion in addition to the characteristics of the component polymers. This is because, in polymer blends, there is interlayer slip along with orientation and disentanglement on the application of shear stress. When a shear stress is applied to a blend it undergoes an elongational flow.

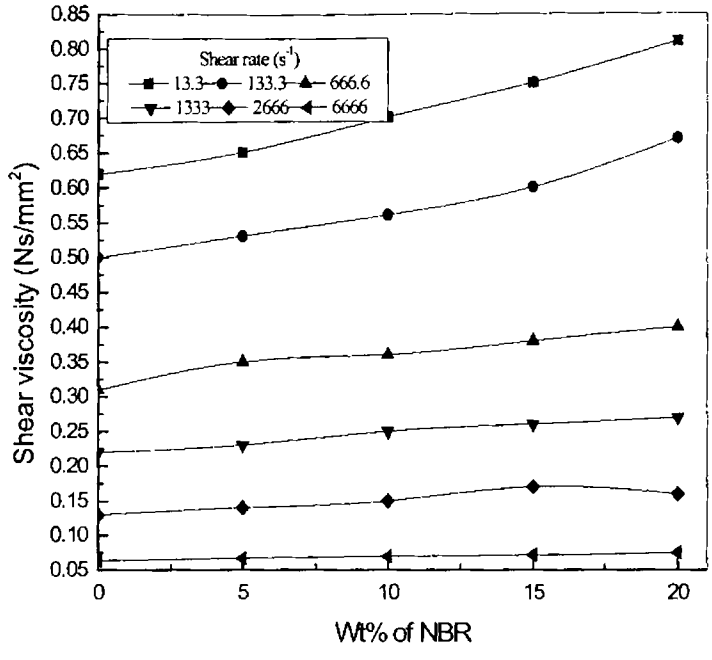

Fig. 3.17: Variation of shear viscosity with wt% of NBR in PS/NBR blends at different shear rates

When the interface is strong, deformation of the dispersed phase would be effectively transferred to the continuous phase. However, in the case of weak interface, interlayer slip occurs and, as a result, the viscosity of the system decreases. The extent of negative deviation is more prominent at the high-shear-rate region than at the low-shear-rate region.

From the figure it is clear that the increase of viscosity with rubber content becomes prominent only at lower shear rates. At high shear rates, only a marginal increase of the viscosity with rubber content occurs. This is also the case with PS/XNBR blends (figure 3.18). This can be explained on the basis of relaxation

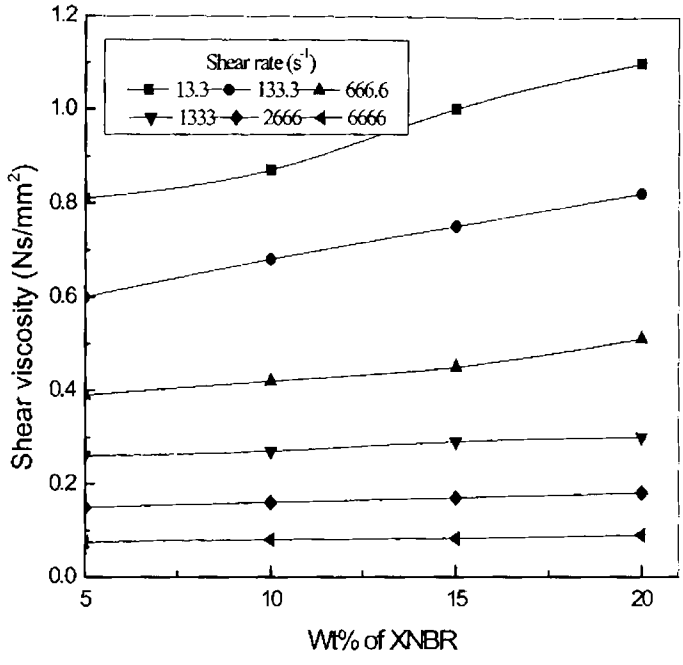

Fig. 3.18: Variation of shear viscosity with wt% of XNBR in PS/XNBR blends at different shear rates.

process and structure build up which are prominent only conditions of low shear. Munstedt [59] had extensively studied on the flow behaviour of ABS with different rubber contents and found that the yield stress increases with increase in rubber content. His conclusion was that, in the range of low shear stresses where relaxation process takes place, a remarkable influence of the rubber was observed on the flow behaviour. Another reason for the observed behaviour is structure build up occurring at regions of low shear. White [60] and Metzner [61] have reported that particle-particle interactions begin to dominate at progressively lower deformation rates. Lewis and Nielsen [62] have studied on particle agglomeration

occurring at lower shear rates. They correlated the viscosity increase with reduced packing fraction resulting from particle agglomeration. As the shear rate increases, the agglomerated structure is broken down and the flow curves follow the behaviour of virgin polymers.

In polymer blends, the viscosity depends on interfacial thickness and interfacial adhesion in addition to the characteristics of the component polymers. This is because in polymer blends there is interlayer slip along with the orientation and disentanglement on application of shear stress. When a shear stress is applied to a blend it undergoes an elongational flow. If the interface is strong, deformation of the dispersed phase would be effectively transferred to the continuous phase. However in the case of weak interface, interlayer slip occurs and as a result the viscosity of the system decreases.

The melt elasticity of polymers leads to different phenomena like extrudate swell, melt fracture, shark skin, etc. during flow through a capillary [56] In the capillary the polymer molecules undergo orientation under the action of shear. On emerging from the die, the oriented molecules have a tendency to recoil. As a result, lateral expansion takes place which leads to extrudate swell. At low shear rate, the deformation of the extrudates is less, whereas at high shear rate the deformation is very prominent. This is associated with melt fracture which occurs at high shear forces, where the shear stress exceeds the strength of the melt. As the concentration of rubber increases, the surface of the blend exhibits more roughness and the extrudates have a non-uniform diameter since the elastic response increases with increase in concentration of the rubber phase

The die-swell ratio of the extrudates of PS/NBR blends as a function of the blend ratio is shown in figure 3.19. It is clear from the figure that the die-swell increases with the shear rate. This is because at high shear rates, the polymer molecules cannot respond to the rapidly changing stresses and the stored elastic

energy is greater. Once the material is extruded out from the die, the excess energy is released and manifested as die swell. It is also evident from the figure that the die-swell increases with NBR content at a particular shear rate.

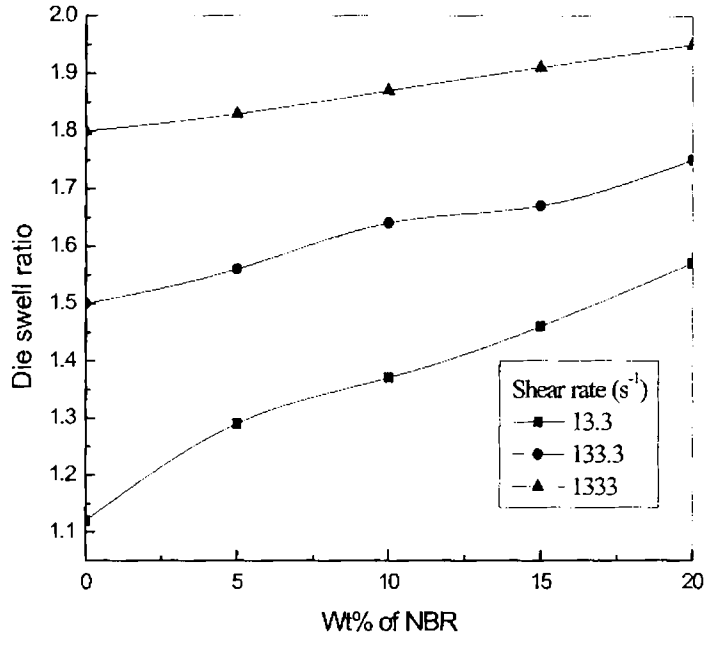

Fig. 3.19: Effect of blend ratio and shear rate on the die swell values of PS/NBR blends

The effect of temperature on the melt viscosity of P_{100}, P_{95}, P_{90}, P_{85}, P_{80} is shown in figure 3.20. The viscosity reduction with increase in temperature in the case of blends is lower compared with that of pure polystyrene. This may be due to crosslinking of the NBR phase in the blend. In fact, reactions take place during the melt blending at higher temperatures are crosslinking of the NBR phase, degradation of the PS phase and the formation of graft polymers.

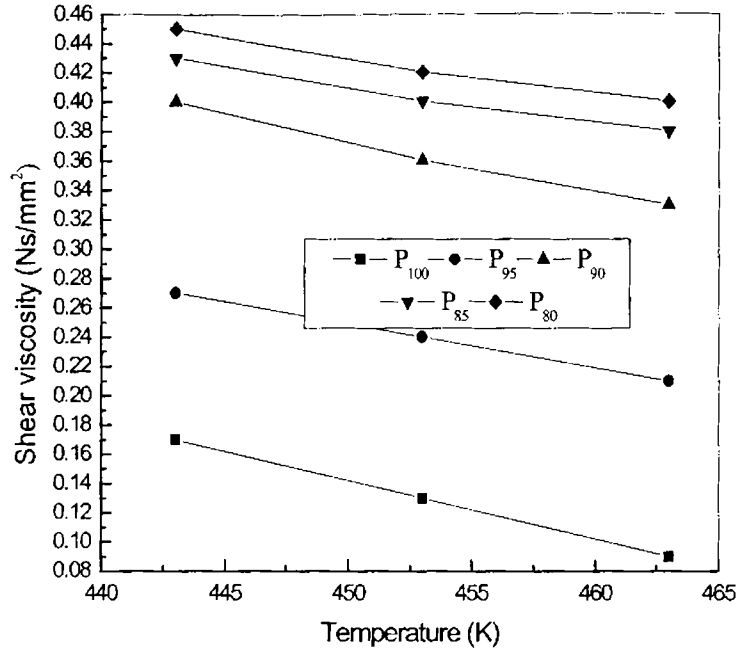

Fig.3.20: Effect of temperature on the melt viscosity of P_{100}, P_{95}, P_{90}, P_{85} and P_{80}

The activation energy was calculated from the plot of log η versus 1/T at three different temperatures 170, 180 and 190°C and at a shear rate of 666.6/s forP_{100}, P_{95}, P_{90}, P_{85} and P_{80}. The plots of log η versus 1/T for these blends are shown in figure 3.21. The results are given in table 3.1. It is seen from the table that the activation energy decreases on blending PS with NBR. The activation energy values are useful in choosing the temperature to be used during processing routes such as injection moulding, calendaring and extrusion.

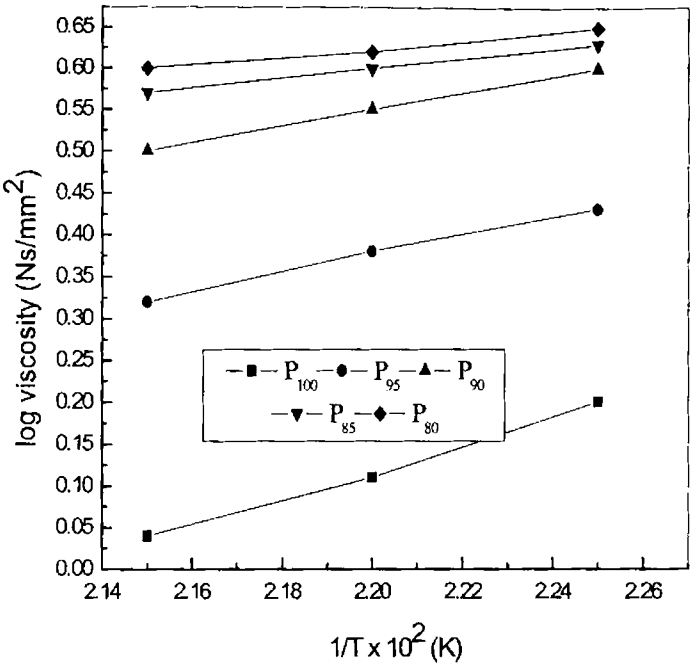

Fig. 3.21: Arrhenius plots for P_{100}, P_{95}, P_{90}, P_{85} and P_{80}.

Table 3.1: Activation energies of PS/NBR blends

Sample	E (KJ/mole)
P_{100}	13.47
P_{95}	11.23
P_{90}	10.71
P_{85}	6.35
P_{80}	4.72

The flow behaviour index (n') of polymers gives an idea about the nature of flow, i.e., whether it is dilatent or pseudoplastic. Most polymers show pseudoplastic behaviour with flow behaviour index (n') less than 1. For Newtonian liquids, n' is 1. The effect of blend ratio on the flow behaviour index is shown in figure 3.22. The low values of n' for PS, and PS/NBR blends indicate pseudoplastic behaviour. The incorporation of NBR shows only a slight increase in flow behaviour index. Thus the addition of NBR to PS does not vary its processing characteristics.

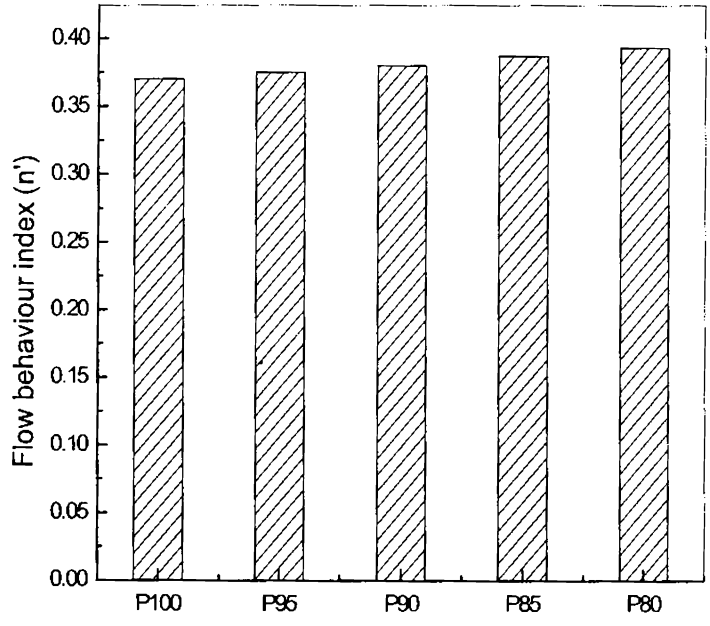

Fig.3.22: Effect of blend ratio on flow behaviour index (n')

3.5 Thermogravimetric analysis

The result obtained from the thermogravimetric analysis of PS is given in figure 3.23. In the case of polystyrene, degradation is observed in a single step. Up

to 267°C the sample is stable and thereafter sharp weight loss occurs. Degradation is completed at 454°C and during this stage the weight loss observed is 98.74%. The weight loss at 300°C is 0.98% and at 400°C is 14.5%. The major peak in the DTG curve is at 426.9°C, which corresponds to the complete chain scission to volatile monomer along with minute amounts of dimer, trimer, tetramer and pentamer. Polystyrene degrades at elevated temperatures (above 300°C) to a mixture of low molecular weight compounds. These include styrene (40%), toluene (2.4%), methyl styrene (0.5%) and other products having an average molecular weight of 264 [63].

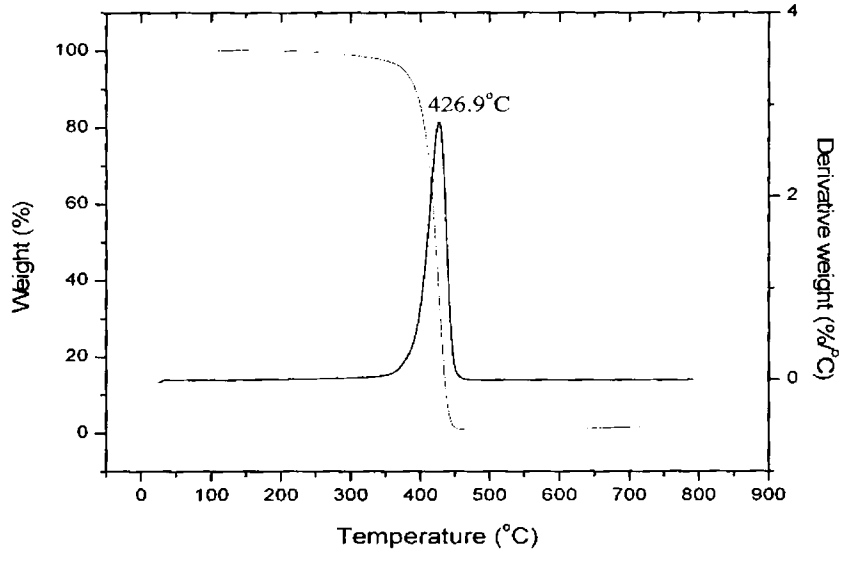

Fig. 3.23: TG trace of polystyrene

From 200 to 300°C the molecular weight of polystyrene drops, but no volatile products are given out. Random scission of polymer chains occurs below 300°C in the following manner [64].

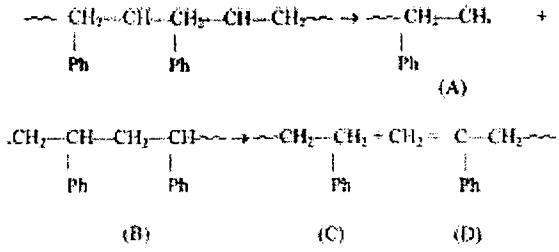

Since below 300°C, no volatile products result, (A) and (B) undergo disproportionation to give (C) and (D) which are stable up to 300°C.

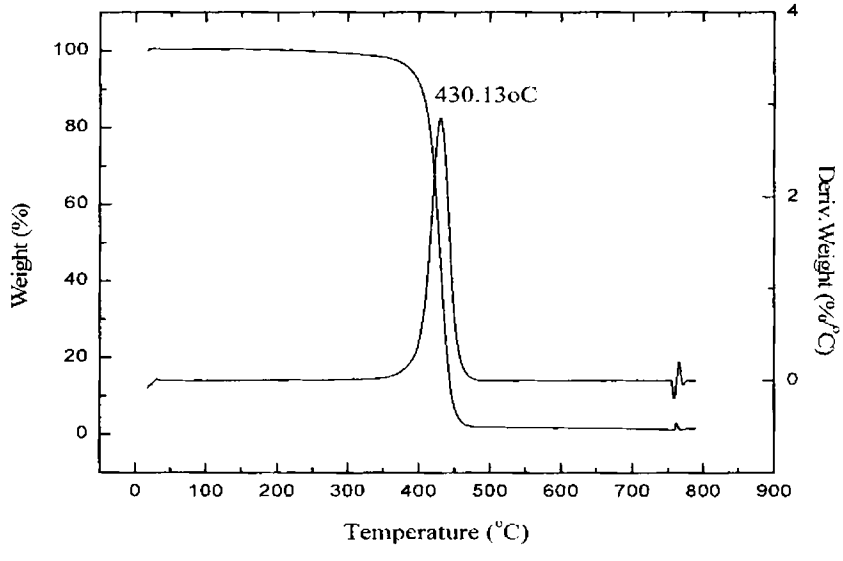

Fig. 3.24: TG trace of 90/10 blend of PS/NBR

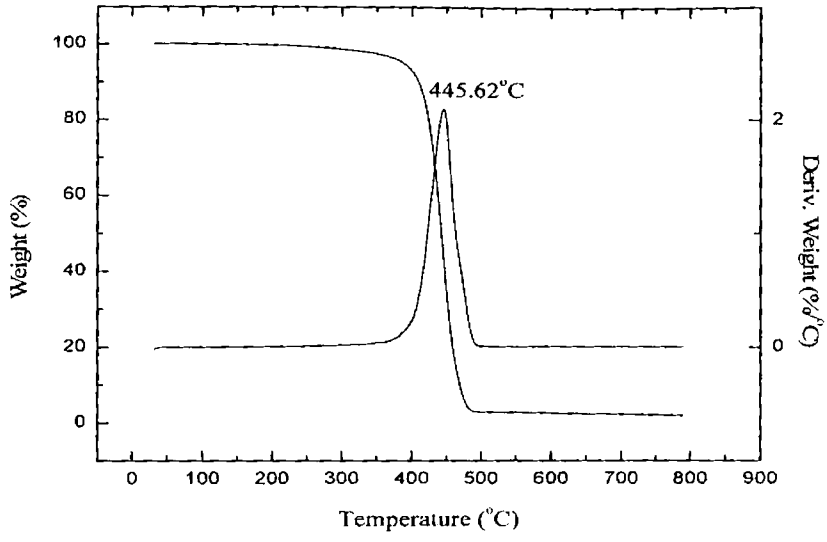

Fig. 3.25: TG trace of 90/10 blend of PS/XNBR

The degradation behaviour of P_{90} is slightly different from polystyrene. In the case of P_{90} the incorporation of NBR into PS is found to improve the thermal stability of PS (figure 3.24). In P_{90} the degradation is in one step. This indicates the better interaction between PS and NBR. The weight loss at 300°C is 0.72% and at 400°C is 8.22%. In the DTG curve, the major peak is observed at 430.13°C which is slightly higher than that for PS.

The vulcanisation of rubbers, generally improve the degradation resistance, since more energy is required to break the bonds formed during vulcanisation. Figure 3.25 shows the TG and DTG plots of Px_{90}. Here also the degradation is in one step. The weight loss at 300°C is 1.26% and at 400°C is 7.07%. In the DTG curve, the major peak is observed at 445.62°C. Px_{90} is thermally more stable than P_{90}.

3.6 Conclusion

The mechanical properties and morphology of powdered nitrile rubber (uncrosslinked and crosslinked) toughened polystyrene have been studied with reference to the effect of blend ratio. The torque-time graphs of various blends showed that the viscosity of PS/NBR blends increases with increase in NBR content and blends with crosslinked NBR registered higher torque than blends with uncrosslinked NBR. The morphology of the blends indicates a two phase structure in which the rubber phase is dispersed as domains in the continuous PS matrix. The mechanical properties of the blends are found to be strongly influenced by blend ratio. The tensile strength, Young's modulus, flexural strength and flexural modulus of the blends decreased with increase in rubber content. The elongation at break and Izod impact strength increased up to 10 wt% NBR and after that no considerable change. The mechanical properties of the blends with crosslinked NBR showed higher values than blends with uncrosslinked NBR. This is attributed to the presence of crosslinked rubber particles. The effect of blend ratio on the dynamic mechanical properties was investigated in the temperature range 35 to 120°C. As the concentration of the rubber increases, storage modulus decreases. Melt rheological studies revealed that the viscosity of the blends decreases with shear stress indicating pseudoplastic nature of the mixes and also showed that the blends are processable. Thermogravimetric analysis was carried out to study the thermal behaviour of the blends. It was found that blending of PS with powdered NBR improved the thermal stability of the blends.

References

1. C.B. Bucknall, *Toughened Plastics*, Applied Science, London, (1977).
2. A.Y. Coran, in *Thermoplastic Elastomers*, N.R. Legge, G. Holden, H.E. Schroeder, Eds., Hanser Publishers, New York, (1987)
3. U. Sundararaj, C.W.Macosko, *Polym. Eng. Sci.*,**32**,1814 (1992)

4. V. Bordereau, Z.H. Shi, L.A. Utracki, P. Sammut, M. Carrega *Polym. Eng. Sci.*, **32**, 1846 (1992)
5. D.R. Paul, S. Newman, *Polymer blends*, Academic Press, New York, (1978).
6. L.A.Utracki, Two-*phase polymer* systems, Hanser Publishers, New York, (1991).
7. U. Sundararaj, C.W. Macosko, *Macromolecules*, **28**, 2647 (1995)
8. S. Wu, *Polym. Eng. Sci.*, **27**, 335 (1982)
9. L.A. Utracki, Z.H. Shi, *Polym. Eng. Sci.*, **32**, 1824 (1992)
10. G.I.Taylor, *Proc. R. Soc. London A*, 138(41), 501 (1932)
11. J.J. Elmendorp, A.K. Van der Vegt, *Polym. Eng. Sci.*, **30**, 553 (1986)
12. J.M. Willis, B.D. Favis, *J. Polym. Sci., Polym Phys.*, **28**, 1416 (1988)
13. H. Varghese, S.S. Bhagawan, S. Someswara Rao, S.Thomas *Eur. Polym. J.*, **31**, 957 (1995)
14. R. Asaletha, M.G. Kumaran, S.Thomas, *Eur. Polym. J.*, **35**, 253, (1999)
15. J. George, K.T. Varughese, S. Thomas, *Polymer*, **57**, 449 (1995)
16. I . Fortelny, J. Kovar, *Polym. Compos.*, **9**, 119, (1998)
17. E. Martuscelli, F. Riva, C. Sellitti, C. Silvestre, *Polymer*, **26**, 270 (1985)
18. B. Majumdar, H. Keskkula, *J. Appl. Polym. Sci.*, **54**, 339 (1994)
19. S. Thomas, G. Groeninckx, *J. Appl. Polym. Sci.*, **71**, 1405 (1999)
20. C.E. Scott, C.W. Macosko, *Polymer*, **35**, 5422 (1994)
21. H.J. Karam, J.C. Bellinger, *Ind. Eng. Chem. Fundam.* **7**, 576 (1986)
22. J. Karger-Koscis, K. Csikai, *Polym. Eng. Sci.*, **27**, 24 (1987)
23. H.P. Schreiber, A. Olguin, *Polym. Eng. Sci.*, 23, 129 (1983)
24. P. Laokijcharoen, A.Y. Coran, Presented at the meeting of the rubber division. Louisville, KY, 8–11 October 1996.
25. B.D. Favis, *J. Appl. Polym. Sci.*, **39**, 285 (1990).
26. A.P. Plochocki, S.S. Dagli, R.D. Andrews, *Polym. Eng. Sci.*, **30**, 741 (1990).

27. U. Sundararaj, C.W. Macosko, R.J. Rolando, H.T. Chan, *Polym. Eng. Sci.*, **32**, 1814 (1992).
28. K.C. Dao, *J. Appl .Polym. Sci.*, **27**, 4799 (1982).
29. R.J.M. Borggreve, R.J. Gaymans, J.Schuijer and J.F. Ingen Housz, *Polymer*, **28**, 1489 (1987).
30. R.J.M. Borggreve and R.J. Gaymans, *Polymer*, **30**, 63 (1989).
31. M. Mehrabzadeh and R.P. Buford, *J. Appl. Polym. Sci.*, **64**, 1605 (1997).
32. S. Joseph, S. Thomas, *Eur. Polym. J.*, **39**, 115 (2003).
33. C. Serra, G. Schlatter, M. Bougquey, R. Muller, J. Terrisse, *Canad. J. Chem. Eng.*, **80**, 1036 (2002).
34. C.P. Fung, *J. Reinf. Plast. Comp.*, **22**, 51 (2003).
35. S.J. Liu, C.F. Chen, *J. Reinf. Plast. Comp.*, **21**, 723 (2002).
36. T.M. Murayama, Ed., *Dynamic Mechanical Analysis of Polymeric Materials*, Elsevier, New York, 1978.
37. D.L. Kang, C.S. Ha, W.J. Cho, Eur. Polym. J., **28**, 565 (1992).
38. S. George, N.R. Neelakantan, K.T. Varughese, S. Thomas, *J. Polym. Sci., Part B: Polym. Phys.*, **35**, 2309 (1997).
39. J. Mas, A. Vidaurre, J.M. Mesegner, F. Romero, M.M. Pardas, J.L.G. Ribelles, M.L.L. Maspoch, O.O. Santana, P. Pages, J.P. Folch, *J. Appl. Polym. Sci.*, **83**, 1507 (2002).
40. J.A. Brydson, *Flow properties of Polymer Melts*, 2nd ed., George, Godwin: London, (1981).
41. J.L. White, *Rubber Chem. Tech.*, **42**, 257 (1969).
42. J.L. White, *Rubber Chem. Tech.*, **50**, 163 (1977).
43. S. Danesi, R.S. Porter, *Polymer*, **19**, 448(1978).
44. I.C. McNeill. In: G. Allen, editor, *Thermal degradation in comprehensive polymer science*, ch. 15, New York, Pregamon Press, (1989).

45. W. Schnabel, *Polymer degradation principles and applications*. New York, Hanser, (1981).
46. N. Grassie, editor, *Developments in polymer degradation*, Applied Science, London, (1998).
47. K.T. Varughese, *Kaustschuk Gummi Kunststoffe*, **41**, 114 (1988).
48. I.A. Amraee, A.A. Kathab, S.A. Jollah, *Rubber.Chem.Technol.*,**69**, 130 (1995).
49. P.P. Lizymol, S. Thomas, *Polym. Degrad. Stab.* **41**, 59 (1993).
50. S.M. Aharoni, *Macromolecules*, **18**, 2624 (1985)
51. A.K. Jain, A.K. Nagpal, R. Singhal, Neeraj. K. Gupta, *J. Appl. Polym. Sci.*, **78**, 2089 (2000).
52. K.C. Dao, *Polymer*, **25**, 1527 (1984).
53. D. Heikens, W.M. Barentsen, *Polymer*, **18**, 69 (1977).
54. K.T. Varughese, P.P. De, G.B. Nando, S.K. De, *J. Vinyl Technol.*, **9**, 161 (1987).
55. K.T. Varughese, *J. Appl. Polym. Sci.*, **39**, 205(1990).
56. S. Akhtar, B. Kuriakose, P.P. De, S.K. De, *Plast. Rubber Process Applic.*, **7**, 11 (1987).
57. B. Kuriakose, *Kaustschuk Gummi Kunststoffe.*, **37**, 1044 (1984).
58. L. Duvdevani, P.K. Agarwal, R.D. Lundberg, *Polym. Eng. Sci.*, **22**, 499 (1982).
59. H. Munstedt, *Polym. Eng. Sci.*, **21**, 5 (1981).
60. J.L. White, L.Czarneck, H. Tanaka, *Rubber Chem. Tech.*, **53**, 823 (1980).
61. A.B. Metzner, *J. Rheol.*, **29**, 739 (1985).
62. T.B. Lewis, L.E. Nielsen, *Trans. Soc. Rheol.*, **12**, 421 (1968).
63. R. Asaletha, M.G. Kumaran, S. Thomas, *Polymer Degradation and Stability*, **61**, 431 (1998).
64. M. Guaita, O. Chiantore, L. Costa, *Polymer Degradation and Stability*, **12**, 315 (1985).

Chapter 4

Compatibilisation by dynamic crosslinking

Dynamic crosslinking is the process of vulcanizing the elastomer during its melt mixing with a non-vulcanising thermoplastic polymer. The introduction of crosslinks into one of the phases increases the viscosity of this phase leading to a change in the morphology of the blend [1]. For blends with similar polarities a fine morphology is seen during dynamic vulcanisation. However a coarse morphology is developed in the case of incompatible blends [2]. Fischer [3] introduced the method of dynamic crosslinking to vulcanise the rubber phase in a thermoplastic elastomer blend while it is being mixed in the molten state. The dynamic crosslinking of PVC/ENR was reported by Varughese *et al* [4]. The micro-heterogeneity between ENR and PVC was reduced due to the improved interfacial adhesion. Both thermal stability and elastic deformation are improved upon dynamic crosslinking. Several studies were carried out to investigate the toughening of PS by the effects of dispersed phase properties such as the rubber concentration, particle size, shape and packing of the rubber particles. However few studies were concerned with the crosslinking of the rubber particles. Bucknall [5] reported that crosslinking of rubber particles is desirable since during impact the rubber phase is subjected to a very large tensile strain giving craze like structure. A moderate degree of crosslinking allows the rubber particles to reach high strain by fibrillation and at the same time renders mechanical strength to the

fibrils. Dao [6] found that crosslinked ethylene – propylene - diene terpolymer (EPDM) was more effective than uncrosslinked EPDM. The brittle – tough transition depends on particle size and Wu [7] stated that a sharp brittle – tough transition occurred at a critical rubber particle size. Because of the fixed morphologies of dynamic vulcanized blends, they have improved property profiles.

Several articles are quoted in the literature on the dynamic crosslinking of rubber/plastic blends. Pesneau [8] reported on the dynamically crosslinked blends of PP/EPM prepared in a twin screw extruder. Mousa [9] studied the effect of sulphur dosage on the dynamic crosslinking of plasticised poly (vinyl chloride) / nitrile rubber blends. The influence of dynamic crosslinking on the morphology–mechanical property relationship in poly (butylene terphthalate)/poly (ethylene–co-glycidyl methacrylate) blends was studied by Okamoto [10]. Inove and Suzuki [11] reported the influence of dynamic crosslinking on PP/EPDM blends. It was found that EPDM particles were crosslinked selectively without degradation of polypropylene. George [12] carried out dynamic crosslinking on 50/50 blend of HDPE and NBR using DCP and reported that DCP dosage has a significant effect on the extent of crosslinking.

The effect of dynamic crosslinking on the dynamic mechanical properties of PP/NR blends was reported by Kuriakose *et al* [13]. They found that the increase in storage modulus and decrease in loss modulus becomes more remarkable as the extent of crosslinking increases. Thomas *et al* [14] investigated the effect of dynamic crosslinking on the dynamic mechanical properties of NR/EVA blends. The damping behaviour of dynamically crosslinked butyl rubber/polypropylene blends was studied by Liao *et al* [15].

Rheological properties of dynamically cured EPDM/PP/HDPE ternary blends were studied by Ha [16]. He found that the curing agent has influence on the melt viscosity especially in blends of EPDM rich compositions. The effect of shear intensity on the melt viscosity of dynamically cured EPDM rich ternary blends was also investigated. Akhtar *et al* [17] reported on the Rheological behaviour and extrudate morphology of thermoplastic elastomers from NR and HDPE with reference to blend ratio and dynamic crosslinking. The morphology was found to depend on the blend ratio and shear rate.

This chapter discusses the effects of dynamic crosslinking on the morphology, mechanical properties, flexural properties, dynamic mechanical properties, melt rheology and thermal properties of powdered nitrile rubber toughened polystyrene.

4.1 Processing characteristics

The torque- time graph of different mixes is shown in figure 4.1. From the figure it is clear that the initial high mixing torque is due to introduction of cold material into the mixing chamber. Once the material attains the set temperature and gets melted, the torque comes down. Again it increases with the addition of NBR and comes down upon melting and levelling off can be observed in the torque values of the blend containing no crosslinking agent. However DCP containing mixes show a small increase in torque with time and levelling off can be observed. The increase in torque is due to the crosslinking of the rubber phase and thereby exerting greater resistance to rotation.

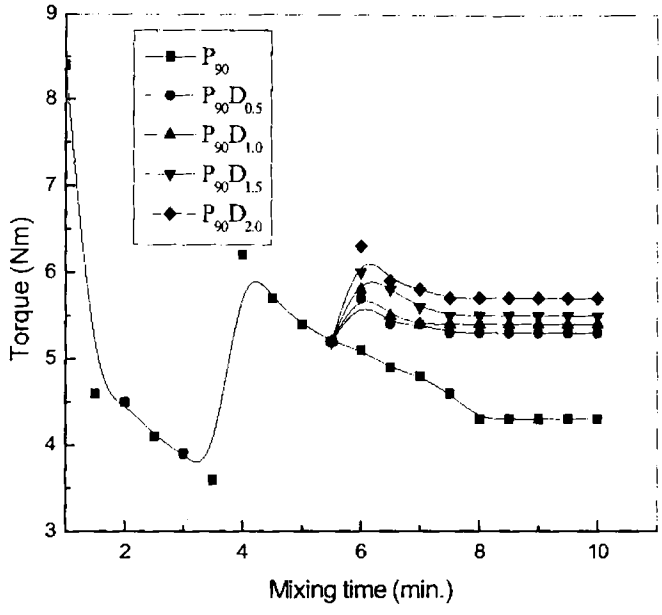

Fig. 4.1: Torque-time plots of 90/10 blend of PS and NBR (P_{90}) containing different amounts of DCP

The effect of DCP concentration on the final torque values of P_{90} is shown in figure 4.2. Form the figure it is clear that the final torque values increase with DCP content. The effect of DCP on polyolefines is determined by the structure of the base polymer. Peroxide initiated reactive extrusion of polyolefin may lead to oxidative degradation, crosslinking or chain scission depending on the type of polymer, compounding conditions and partial pressure of oxygen [18]. In the case of polystyrene, the tertiary macroradical formed will undergo chain scission even under a low partial pressure of oxygen. At high oxygen pressure, oxidative degradation predominates. In addition, the pendant phenyl groups provide steric hindrance for the coupling of two macroradicals. These polystyrene macroradicals combine with the NBR radicals formed by reaction with DCP, results NBR-g-PS

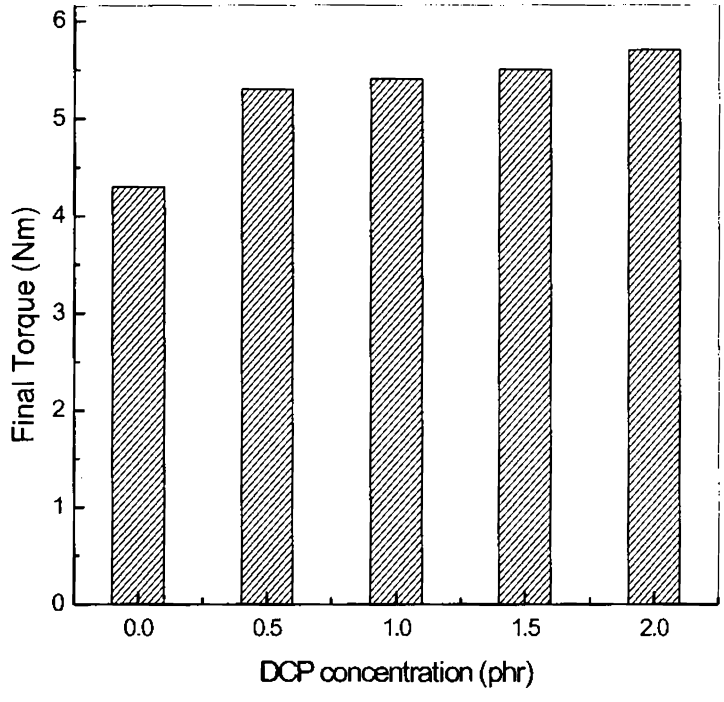

Fig.4.2: Effect of DCP concentration on the final torque values of P_{90}

4.2 Variation of crosslink density

The extent of crosslinking of the rubber phase in the blends containing different levels of DCP can be studied by measuring V_r values. The variation of V_r values with DCP concentration is shown in figure. 4.3. The V_r values increase with

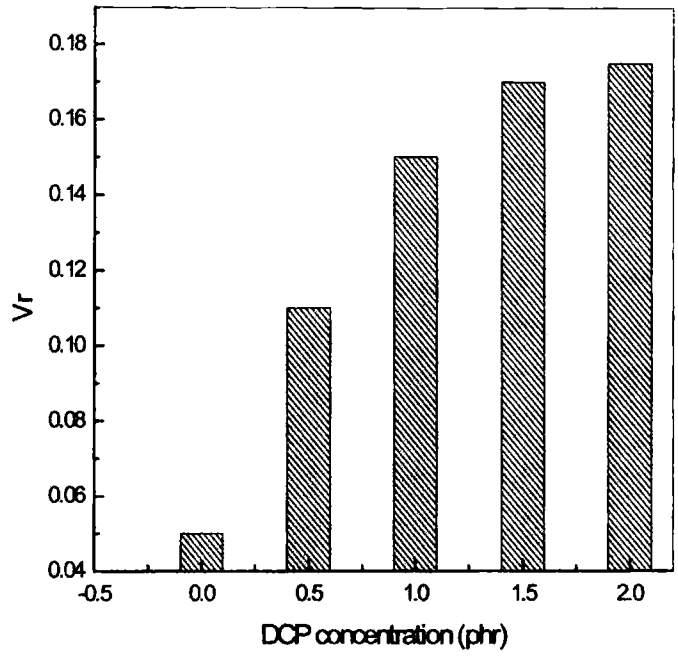

Fig. 4.3: Variation of Vr with DCP concentration showing the effect of extent of crosslinking on Vr values of P_{90}

extent of crosslinking as the restriction to swelling increases with increased network formation. From the figure, it is clear that the crosslink density increases with DCP content.

4.3 Effect of DCP content on the morphology and mechanical properties

The morphology of heterogeneous polymer blends depends on blend composition, viscosity of individual components and processing history. Danesi and Porter [19] have shown that for blends with the same processing history, the morphology is determined by the melt viscosity ratio and composition. The scanning electron micrographs of $P_{90}D_{0.5}$, $P_{90}D_{1.0}$, $P_{90}D_{1.5}$ and $P_{90}D_{2.0}$ are shown in figure 4.4 (a) to (d) respectively. The morphological changes

accompanying the addition of DCP are evident from the figures. Dynamic crosslinking results in crosslinking of the rubber phase. The crosslinked particles exert more torque and leads to particle break-up. A more or less spherical morphology can be seen in $P_{90}D_{1.5}$

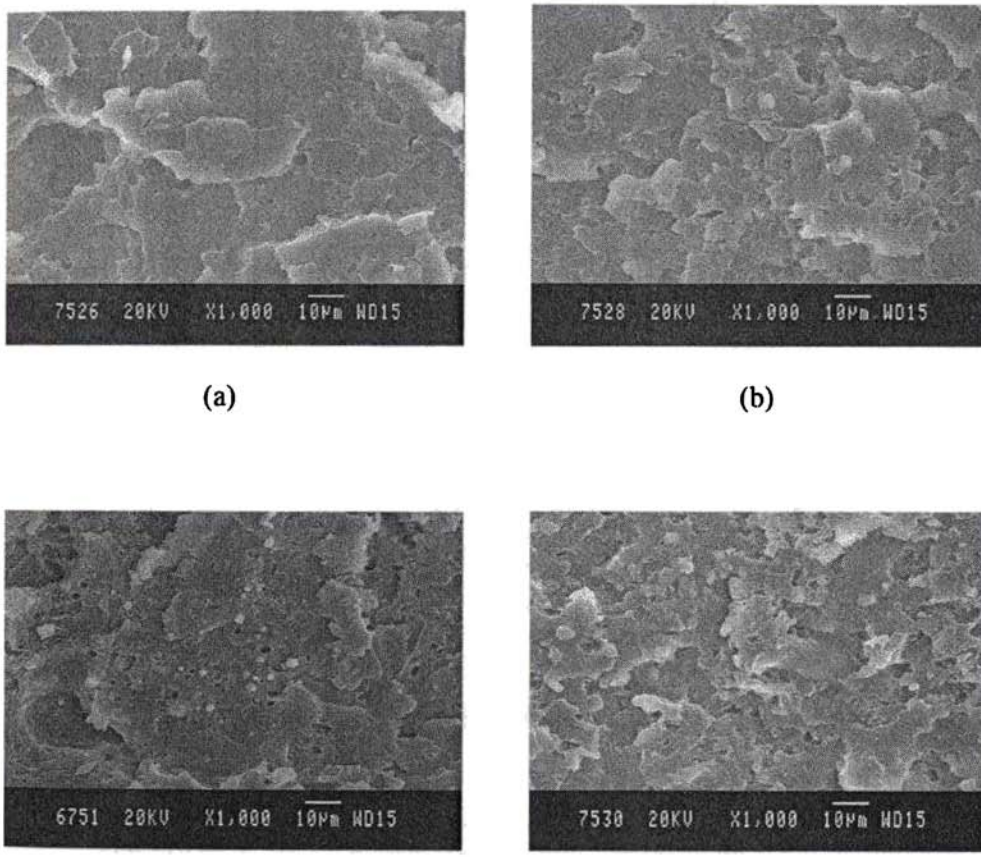

Fig. 4.4: Scanning electron micrographs of fractured surface of (a) $P_{90}D_{0.5}$ (b) $P_{90}D_{1.0}$ (c) $P_{90}D_{1.5}$ and (d) $P_{90}D_{2.0}$

The properties of plastic rubber blends are determined by material properties of plastic and rubber, plastic rubber proportions, the phase morphology and the interaction at the interface [20]. The effect of DCP content on tensile strength and Young's modulus of P_{90} is shown in figures 4.5 and 4.6 respectively. The tensile strength and Young's modulus increase continuously as the DCP content increases up to 1.5 phr. This may be due to the increased crosslink density at higher levels of DCP and better interfacial adhesion.

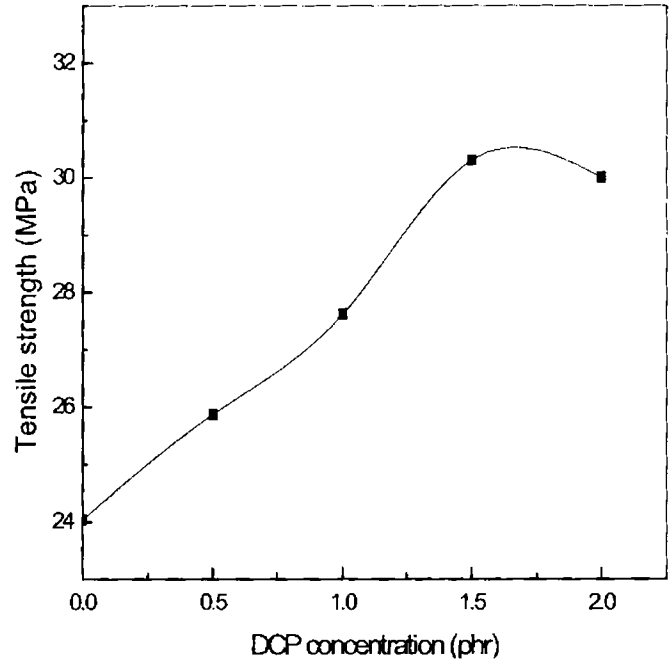

Fig. 4.5: Variation of tensile strength with DCP concentration

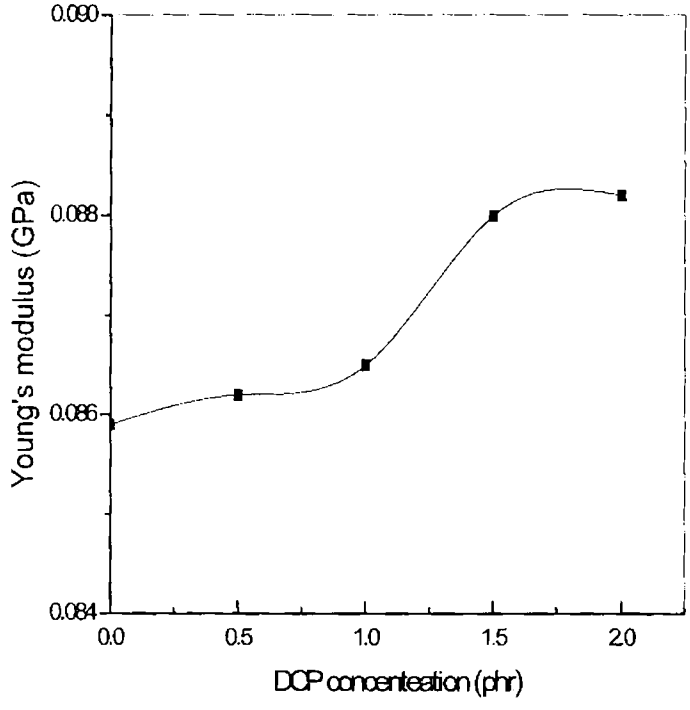

Fig. 4.6: Variation of Young's modulus with DCP concentration

The effect of DCP content on elongation at break is given in figure 4.7. The elongation at break of P_{90} is very low as the blend is incompatible and it increases with increasing crosslink density, as the crosslinked rubber particles can be strained to very large extensions before failure.

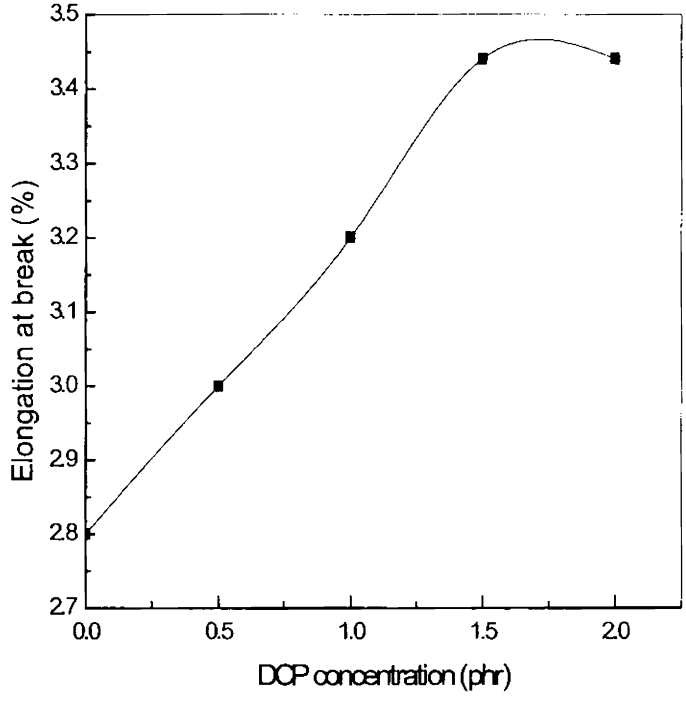

Fig. 4.7: Effect of DCP concentration on elongation at break of 90/10 blend of PS and NBR

The variation of impact strength and toughness with DCP content on the P_{90} are given in figures 4.8 and 4.9 respectively. The impact strength and toughness increase with the addition of DCP up to 1.5 phr. The improvement in mechanical

properties with dynamic crosslinking can be explained on the basis of the morphological changes accompanying dynamic crosslinking.

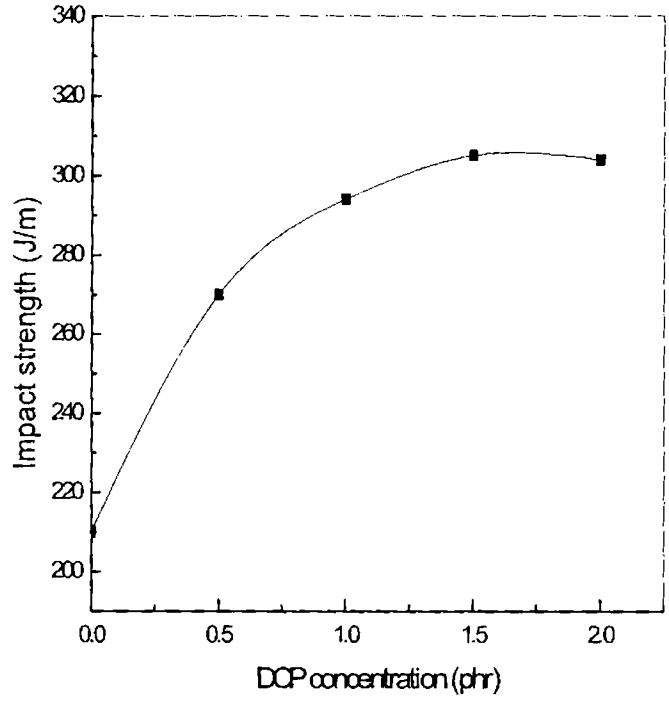

Fig. 4.8: Effect of DCP concentration on impact strength of 90/10 blend of PS and NBR

In the SEM picture (figure 4.4 (c)) of crosslinked P_{90} there is drastic reduction in particle size and most of the dispersed particles are spherical. Also in crosslinked P_{90} there is more effective mixing of the rubber particles with the matrix as the dispersed domains are small.

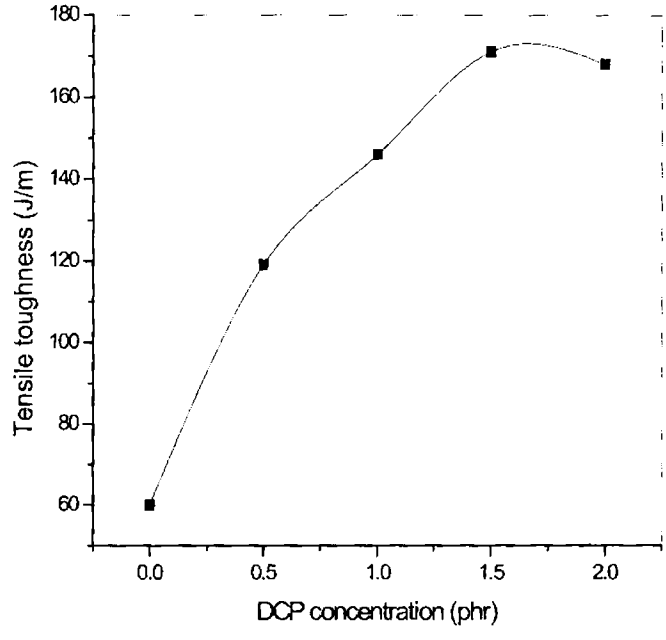

Fig. 4.9: Effect of DCP concentration on impact strength of 90/10 blend of PS and NBR

The effect of DCP content on the flexural strength and flexural modulus is shown in figures 4.10 and 4.11 respectively. The crosslinked blends have higher flexural modulus and flexural strength than the uncrosslinked blend. This is an effect of crosslinking that forms a network structure. The network structure strengthens the interfacial adhesion and improves the mechanical properties.

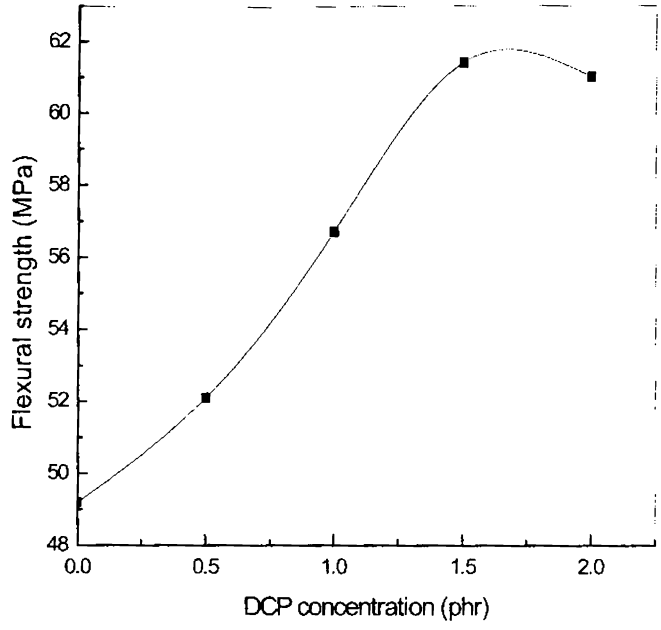

Fig. 4.10: Variation of Flexural strength with DCP concentration

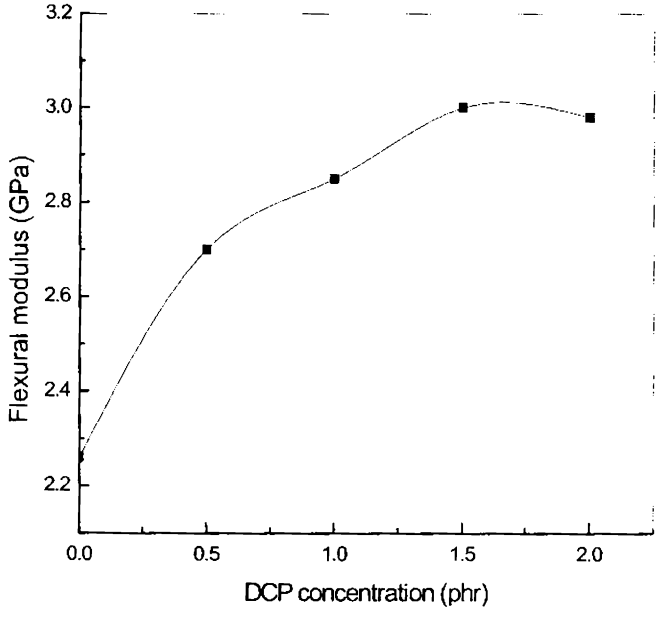

Fig. 4.11: Variation of flexural modulus with DCP concentration

4.4 Dynamic mechanical analysis

The molecular level changes that occur in a polymer under the application of a sinusoidal stress are reflected in dynamic mechanical measurements. The variation of storage modulus (E') with temperature of dynamically vulcanised P_{90} with varying DCP content is shown in figure 4.12. Three distinct regions of mechanical behaviour can be observed: (a) a glassy region; (b) a glass–rubber transition region; and (c) a flow region. In the glassy region at low temperatures the chain conformations are frozen into rigid network yielding high E' values and low loss. Some limited movement either within the main chain or within side groups attached to the chain is however possible giving rise to one or more secondary transitions of low magnitude.

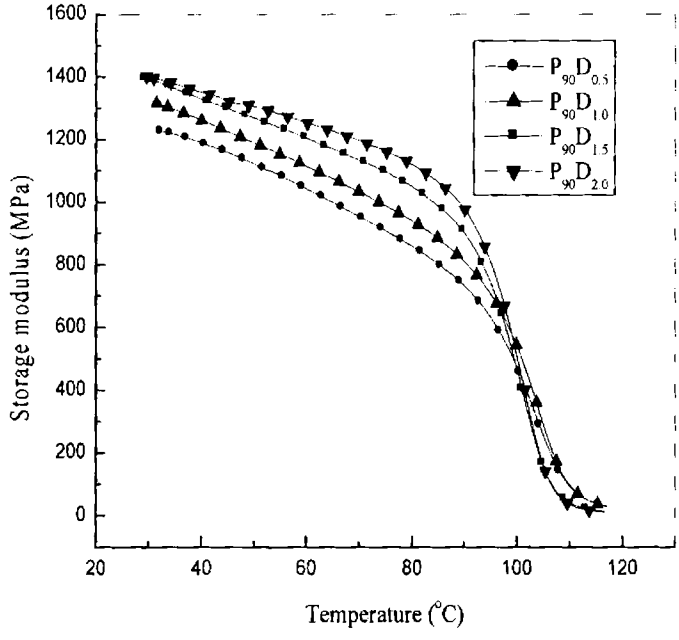

Fig.4.12: Variation of storage modulus with temperature of dynamically crosslinked 90/10 blends of PS and NBR.

The glass–rubber transition marks the onset of long range motions of amorphous polymer chain segments and is characterised by a large drop in modulus and a pronounced loss factor peak. The last region is the flow region, where the amorphous chains undergo net translatory motions relative to each other and a terminal fall off in modulus is accompanied by a continuous increase in loss factor. It can be seen from the figure that the initial storage modulus is highest for $P_{90}D_{2.0}$ and it is due to the maximum crosslinking of the rubber particles.

The variations of loss modulus (E") of dynamically crosslinked P_{90} as a function of temperature are shown in figure 4.13. A distinct peak can be observed

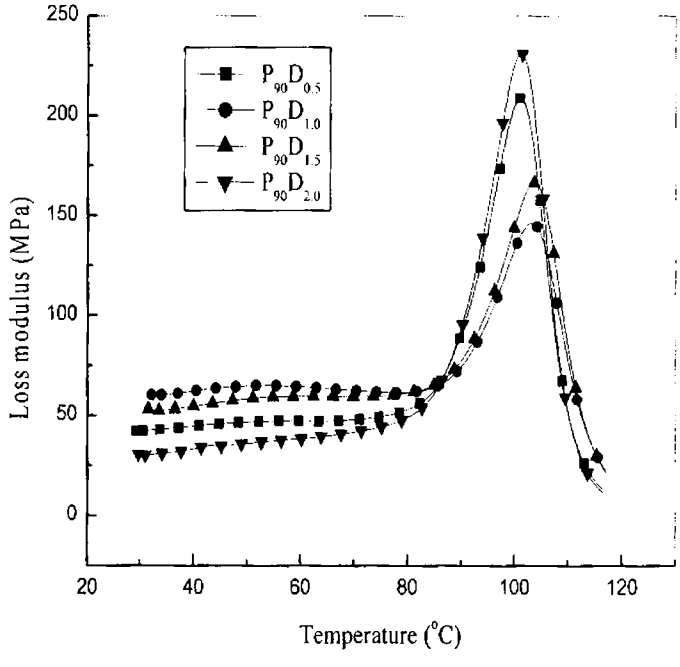

Fig. 4.13: Loss modulus- temperature plots of dynamically vulcanized 90/10 blends of PS and NBR

at the glass transition temperature (T_g) region of PS. Below the T_g values the polymer chains are in tact and stress transfer is possible. When the temperature is approaching the T_g, energy dissipation takes place and a corresponding peak is observed in the E" values. $P_{90}D_{2.0}$ registers maximum loss modulus which is attributed to the increased extent of crosslinking.

The variation of tan δ values of dynamically crosslinked P_{90} as a function of temperature is shown in figure 4.14. The peak between 111°C and 113°C corresponds to the glass transition of polystyrene. The peak temperature values of PS in both crosslinked and uncrosslinked samples are more or less the same indicating that the plastic phase is unaffected by dynamic crosslinking. From the tan δ values it is clear that the interfacial adhesion is better in $P_{90}D_{1.0}$ and $P_{90}D_{1.5}$

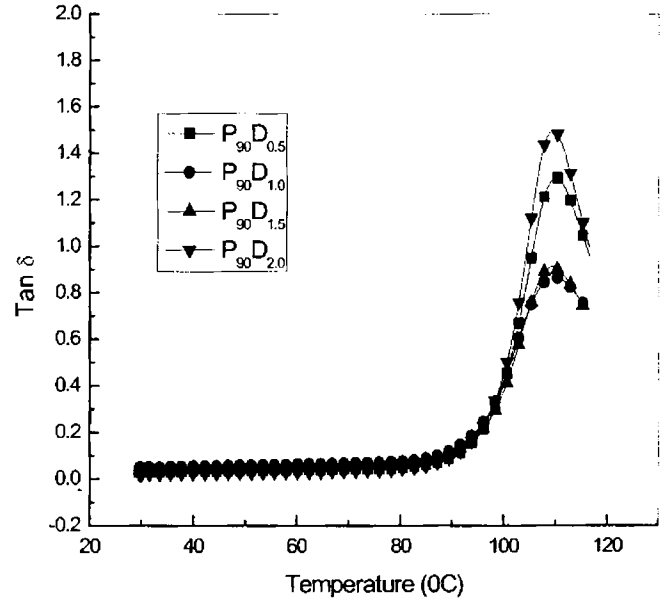

Fig. 4.14: Tan δ-temperature plots of dynamically crosslinked 90/10 blends of PS and NBR

4.5 Rheological studies

The usual processing techniques for toughened plastics are extrusion, injection moulding, blow moulding and thermoforming. Hence a thorough understanding of the flow behaviour of the polymer melts under high shearing action is important to make articles having good finish and dimensional tolerances. The melt elasticity and viscosity are two opposing factors that decide the overall processability.

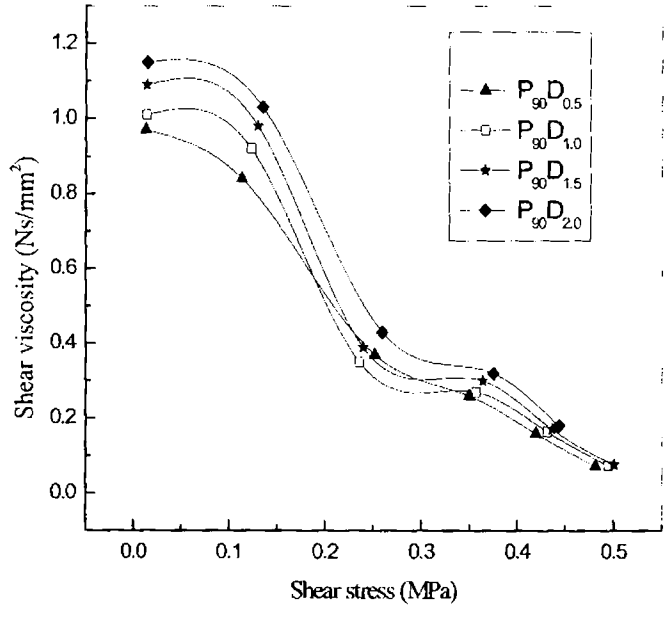

Fig. 4.15: Shear rate-viscosity plots of P_{90} containing different levels of DCP

The effect of shear stress on shear viscosity of the mixes containing different DCP concentration at 180°C is shown in figure 4.15. In all the cases the viscosity decreases with shear stress indicating the pseudoplastic nature of the mixes. The viscosity increases with increasing concentration of DCP over the

entire range of shear stresses. The increase in viscosity with DCP content is more pronounced at low shear regions than at high shear regions as observed from the converging behaviour of the flow curves at high shear stresses. These results show that the dynamically crosslinked samples can be processed like thermoplastics by extrusion or injection moulding technique.

Figure 4.16 shows the effect of DCP dosage on the viscosity of the mixes at different shear rates. At all shear rates there is a gradual increase of viscosity with the concentration of DCP indicating increased extent of crosslinking at higher levels of DCP. At a particular DCP content, the viscosity decreases as the shear rate increases.

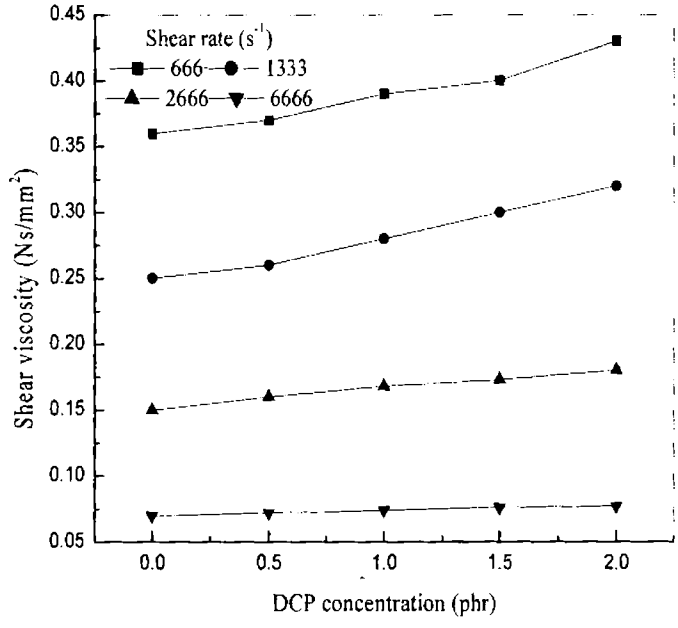

Fig. 4.16: Effect of DCP concentration on the shear viscosity of P_{90} at four different shear rates.

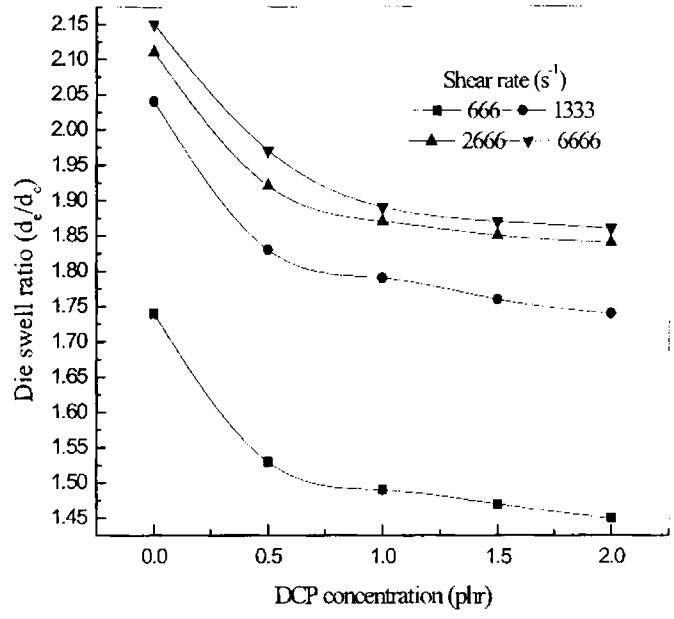

Fig. 4.17: Variation of die-swell with DCP concentration

The die-swell of the blend at four different shear rates is shown in figure 4.17. In all the cases the die-swell shows a substantial reduction even with 0.5% DCP and thereafter a levelling off is observed. The die swell occurs due to molecular relaxation upon emergence of the extrudate from the capillary die. The results of the present study reveal that crosslinking leads to network formation and thereby restricting the relaxation process. In a crosslinked sample, the molecules cannot slip past each other as in uncrosslinked material. As expected, the die swell of vulcanized samples also increases with increase in shear rate.

4.6 Thermogravimetric analysis

Polymeric materials are subjected to various types of degradation ranging from thermal degradation to biodegradation. Polymer degradation is undesirable as it leads to deterioration of properties. One of the most accepted methods for

studying the thermal properties of polymeric materials is the thermogravimetry. The integral (TGA) and derivative (DTG) thermogravimetric curves provide information about nature and extent of degradation of polymeric materials.

The vulcanisation of rubbers, generally improve the degradation tresistance, since more energy is required to break the bonds formed during vulcanisation. The TG and DTG plots of different dynamically crosslinked P_{90} blends are given in figures 4.18 to 4.21. The weight loss and DTG peaks of dynamically crosslinked blends are given in table 4.1. It can be seen that at 300°C and 400°C, the weight loss $P_{90}D_{1.5}$ is lower than other blends.

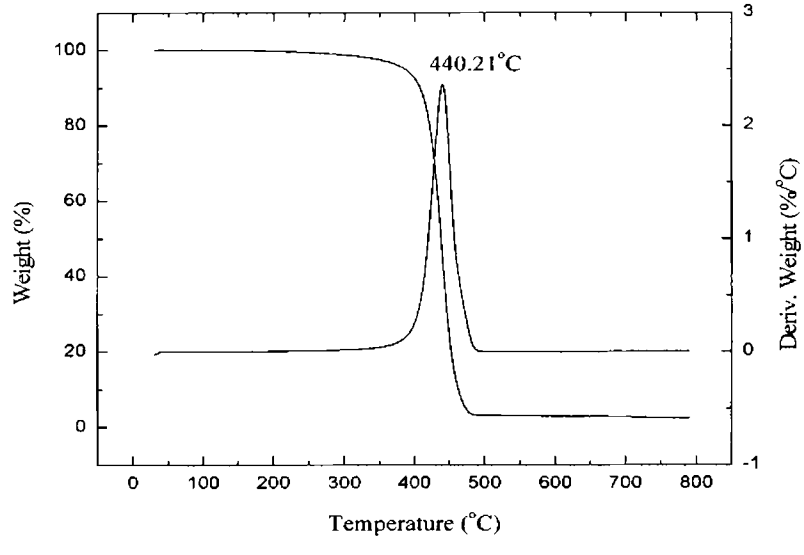

Fig. 4.18: TG trace of 90/10 blend of PS and NBR with 0.5 phr DCP

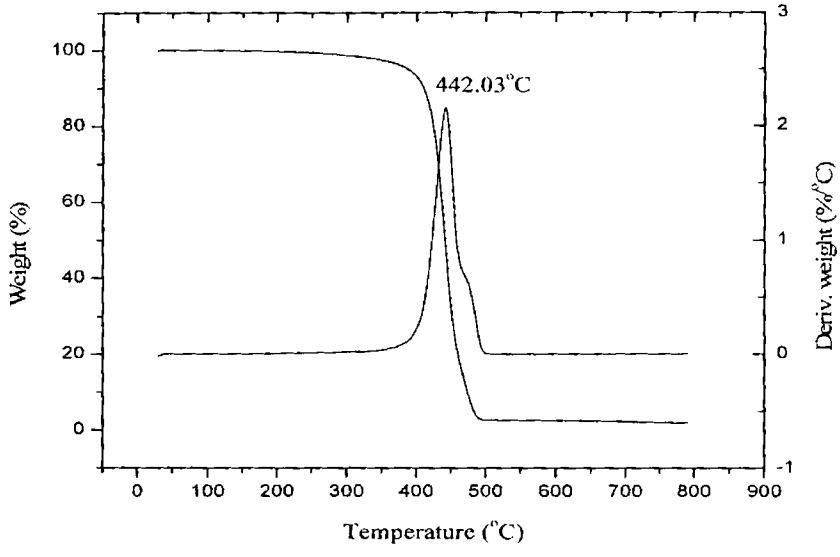

Fig. 4.19: TG trace of 90/10 blend of PS and NBR with 1.0 phr DCP

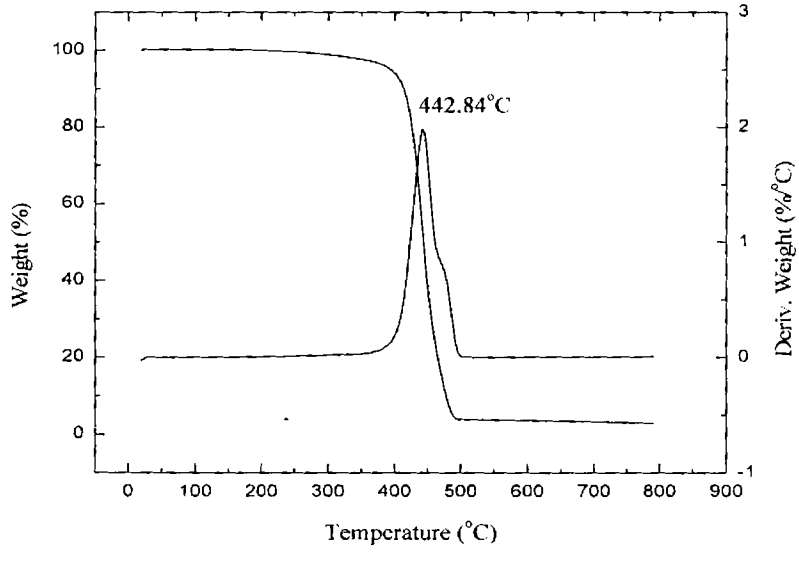

Fig. 4.20: *TG trace of 90/10 blend of PS and NBR with 1.5 phr DCP*

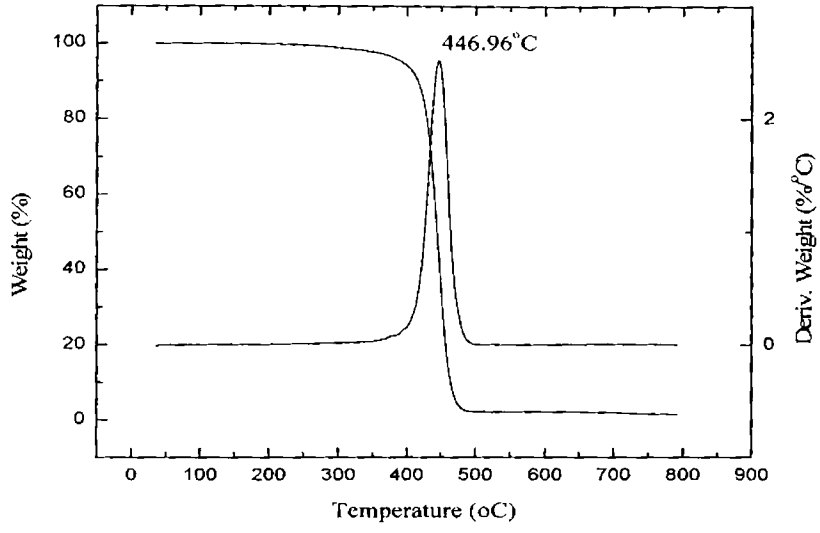

Fig. *4.21: TG trace of 90/10 blend of PS and NBR with 2.0 phr DCP*

Table 4.1. Weight loss and DTG peaks of dynamically crosslinked PS/NBR blends

Sample	Weight loss at 300°C (%)	Weight loss at 400°C (%)	Total weight loss (%)	DTG peak (°C)
$P_{90}D_{0.5}$	1.46	7.40	96.72	440.21
$P_{90}D_{1.0}$	1.20	7.21	97.19	442.03
$P_{90}D_{1.5}$	1.09	5.95	95.30	442.84
$P_{90}D_{2.0}$	1.10	5.98	95.12	446.96

4.7 Conclusion

Dynamic crosslinking of powdered nitrile rubber toughened polystyrene (90/10 PS/NBR blend) was carried out with dicumyl peroxide. As the DCP content increases, the crosslink density also increases as observed from the increase in Vr values. The morphology of the blend changed drastically as a result of dynamic crosslinking. A large number of small crosslinked rubber particles could be observed in vulcanised blend. The impact strength, tensile strength, Young's modulus, elongation at break showed improvement upon dynamic crosslinking with DCP which is due to the presence of crosslinked rubber particles. The rheological studies revealed that the viscosity decreases with shear stress indicating the pseudoplastic nature of the mixes. The viscosity increases with increasing concentration of DCP over the entire range of shear stresses. The increase in viscosity with DCP content is more pronounced at low shear regions than at high shear regions as observed from the converging behaviour of the flow curves at high shear stresses. These results showed that the dynamically crosslinked samples can be processed like thermoplastics by extrusion or injection moulding technique. Die-swell ratio decreases with increase in DCP concentration indicating better dimensional stability of the extrudate. Dynamic mechanical studies indicated separate transition for polystyrene in dynamically crosslinked blends. Although miscibility cannot be brought about by dynamic crosslinking, the overall improvement in properties suggests that dynamic crosslinking can be employed as a means of compatibilisation of PS/NBR blends. The thermal degradation behaviour of dynamically crosslinked PS/NBR blends was studied as a function of the concentration of DCP. The dynamically crosslinked blends were found to be more thermally stable than uncrosslinked blends.

References

1. S.V. Usachev, N.D. Zakharov, V.N. Kuleznev, A.B. Ventoshkin, *Int. polym. Sci. Tech.*, 7, T48 (1980).

2. C. Koning, M.V. Duin, C. Pagnoullie, R. Jerome, *Prog. Polym. Sci.*, **23**, 707 (1998).
3. W.K. Fischer, *Rubber World*, **167**, 49 (1973).
4. K.T. Varughese, P.P. De, S.K. Sanyal, *Angew. Makromol. Chem.* **182**, 73 (1990)
5. C.B. Bucknall, In: *Polymer blends*, D. R. Paul and S. Newman (Ed)., Academic press, New York, (1978)
6. K.C. Dao, *J. Appl. Polym. Sci.*, **27**, 4799, 1982.
7. S. Wu, *Polymer*, **26**, 1855, 1985.
8. I. Pesneau, M.S. Champagne, M.A. Huneault, *Polym. Eng. Sci.*, **42**, 2016 (2002).
9. A. Mousa, U.S. Ishiaku, *Polym. Intl.*, **52**, 120 (2003).
10. M. Okamoto, K. Shioni, T. Inove, *Polymer*, **35**, 4618 (1994).
11. T. Inove, T. Suzuki, *J. Appl. Polym. Sci.*, **56**, 1113 (1995).
12. J. George, K.T. Varughese, S. Thomas, *Polymer*, **41**, 1507 (2000).
13. B. Kuriakose, S.K. De, S.S. Bhagawan, R. Sivaramakrishnan, S.K. Anithan, *J. Appl. Polym. Sci.*, **32**, 5509 (1986).
14. A.T. Koshy, B. Kuriakose, S. Varghese, S. Thomas, *Polymer*, **34**, 3428 (1993).
15. F.S. Liao, A.C. Su, Tzu-Chien J. Hsu, *Polymer*, **35**, 2579 (1994).
16. C.S. Ha, *J. Appl. Polym. Sci.*, **35**, 2211(1988).
17. S. Akhtar, B. Kuriakose, P.P. De, S.K. De, *Plast. Rubber Process Appl.*, **7**, 11 (1987).
18. S. Al Malika, E.J. Amir, *J. Nat. Rubb. Res.*, **1 (2)**, 104 (1986).
19. S. Danesi, R.S. Porter, *Polymer*, **19**, 448 (1978).
20. A.Y. Coran, *Handbook of Elastomers- New Development and Technology.*, Bhowmick A.K., Stephens H.L., eds., p. 249, Marcel Dekker, New York, (1988).

Chapter 5

Compatibilisation by the addition of modified polystyrene

Blending of polymers is a popular method of improving their end-use properties [1]. However, most polymers are thermodynamically incompatible and phase separation occur on blending. Compatibilisation of polymer blends is carried out to reduce the scale of dispersion and to stabilise the morphology. This can be achieved by addition of a premade block copolymer to the system or by carrying out an in-situ reaction between the complementary groups of the blend components. Both techniques promote dispersive mixing which leads to a reduced particle size. There has been much interest in combining the attractive features of incompatible polymers through interfacial reaction that is, adding reactive polymers to form block or graft copolymers in-situ during blend processing. This reactive compatibilisation has been demonstrated to be an effective and cost-efficient route for controlling the properties of various immiscible blend systems [2-5].

Usually, reactive polymers can be generated by free-radical copolymerisation or by the melt grafting of functional groups onto chemically inert polymer chains. Copolymers containing epoxy or oxazoline functional groups have been widely investigated because of their high reactivity to low nucleophilic active hydrogen such as those found in carboxyl, hydroxyl, and anhydride groups [6, 7].

The efficiency of reactive compatibilization of immiscible polymers pairs has already been studied in relation to the content of reactive groups of at least one polymer. De Roover *et al* [8] have studied the effect of maleic anhydride (MA) grafted polypropylene (PP-g-MA) on the average size of the PP phases dispersed in nylon 6. The size decreases rapidly with increasing content of grafted anhydride. However, beyond a critical content, the size levels off. Since maleic anhydride reacts almost quantitatively with the amine end groups of PA 6, a direct relationship between size of the dispersed PP phase and extent of the grafting reaction has been proposed. A Monsanto patent by Lavengood [9] has reported on the influence of the MA content of MA grafted SAN on the notched Izod impact strength of acrylonitrile-butadiene-styrene terpolymer/PA 6 blends. When 6wt % reactive SAN is used as compatibiliser, the impact strength is the highest in the case of SAN containing approximately 1 wt% MA. At higher MA contents, the PA6-g-SAN copolymer formed at the interface becomes rich enough in PA6 for leaving the interface in favour of the PA6 phase. Baker *et al* [10] have studied the compatibilisation capability of glycidyl methacrylate grafted polypropylene (PP-g-GMA) copolymers of different glycidyl methacrylate (GMA) contents in PP/poly(acrylonitrile-co-butadiene-co-acrylic acid) blends. Although the impact energy depends on the total amount of the GMA groups in the blend, it appears that this energy decreases when the average number of GMA groups per PP-g-GMA chain is increased at constant total GMA content. This observation has been discussed on the basis of both number and effectiveness of the interfacial entanglements in relation to the molecular structure of the PP-g-MA compatibiliser. Duvall *et al* [11] have compared the compatibilisation efficiency of PP-g-MA of high and low anhydride content in PP/PA6 blends. Higher fracture strain was observed for the compatibiliser with the low anhydride content. It thus appears from these studies that there is an optimum degree of functionalisation, beyond which the efficiency of the reactive compatibiliser decreases. There are

several reports on the grafting of MA on to PE in the presence of peroxide [12-14] Coran and Patel [15] have functionalised polyolefin with dimethylol phenolic resin (SP-1045) to enhance the compatibility of polyolefines with other polymers.

This chapter discusses the compatibilisation of powdered nitrile rubber toughened polystyrene with maleic anhydride modified polystyrene (MAPS) and phenolic modified polystyrene (PhPS). The effect of compatibilisation on morphology, mechanical properties, dynamic mechanical properties rheological characteristics and thermogravimetric analysis of nitrile rubber toughened polystyrene is given in this chapter.

5.1 Morphology of compatibilised blends

The effect of MAPS and PhPS as compatibilisers on the morphology of 90/10 PS/NBR blend is shown by figures 5.1 and 5.2 respectively. From the scanning electron micrographs, it is seen that the size of the dispersed NBR phase decreases with the addition of compatibilisers. This reduction in particle size with the addition of compatibilisers is due to the reduction in interfacial tension between dispersed NBR phase and the PS matrix.

The average domain size of the compatibilised blends as a function of the compatibiliser concentration is shown in figure 5.3. The average particle size of the unmodified blend is 4.03 μm. In the case of MAPS compatibilised blends, addition of 5% MAPS causes a reduction in domain size of 57%. Further addition of maleic anhydride grafted PS does not change the domain size considerably, but a levelling off is observed. In PhPS compatibilised blends, the average diameter of the dispersed NBR phase decreases with the addition of up to 2 wt% PhPS. The domain size of the uncompatibilised blend is reduced by 68.4% on the addition of 2 wt% PhPS. However further addition of the compatibiliser increases the domain size. The equilibrium concentration at which the domain size levelled off can be considered as the critical micelle concentration (CMC) [16]. The CMC was

estimated by the intersection of the straight lines at the low and high concentration regions [17, 18]

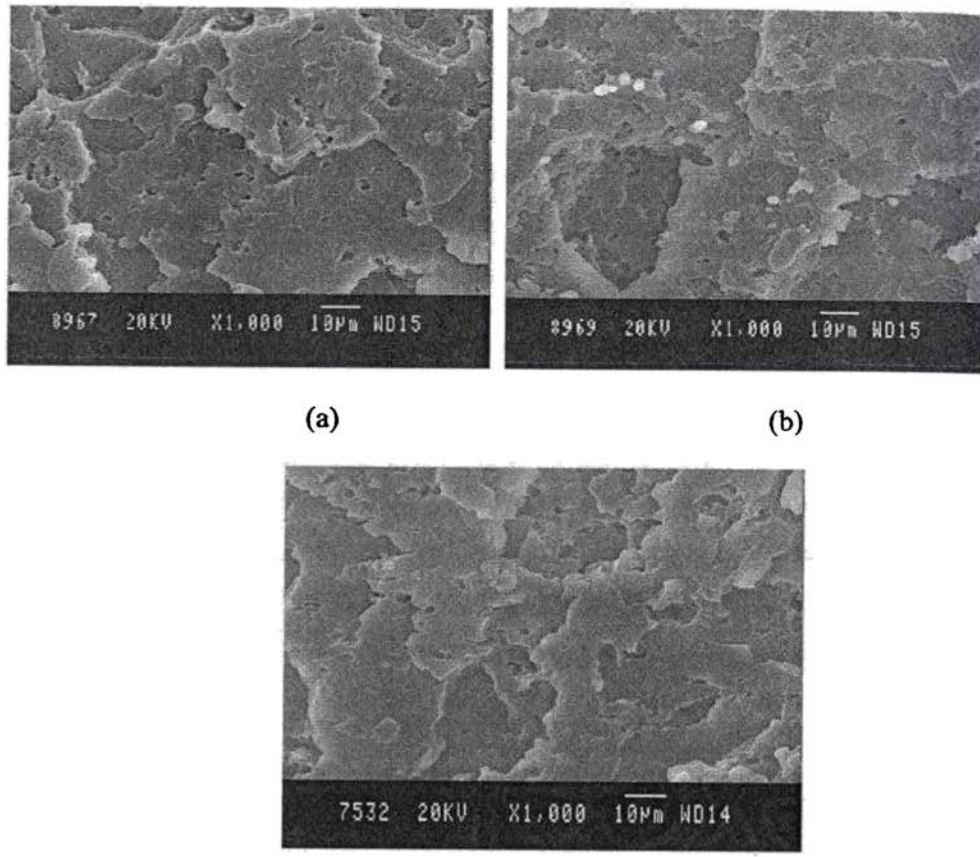

Fig. 5.1: Scanning electron micrographs of the fractured surface of compatibilised P_{90} with (a) 2 wt% (b) 5 wt% and (c) 10 wt% MAPS.

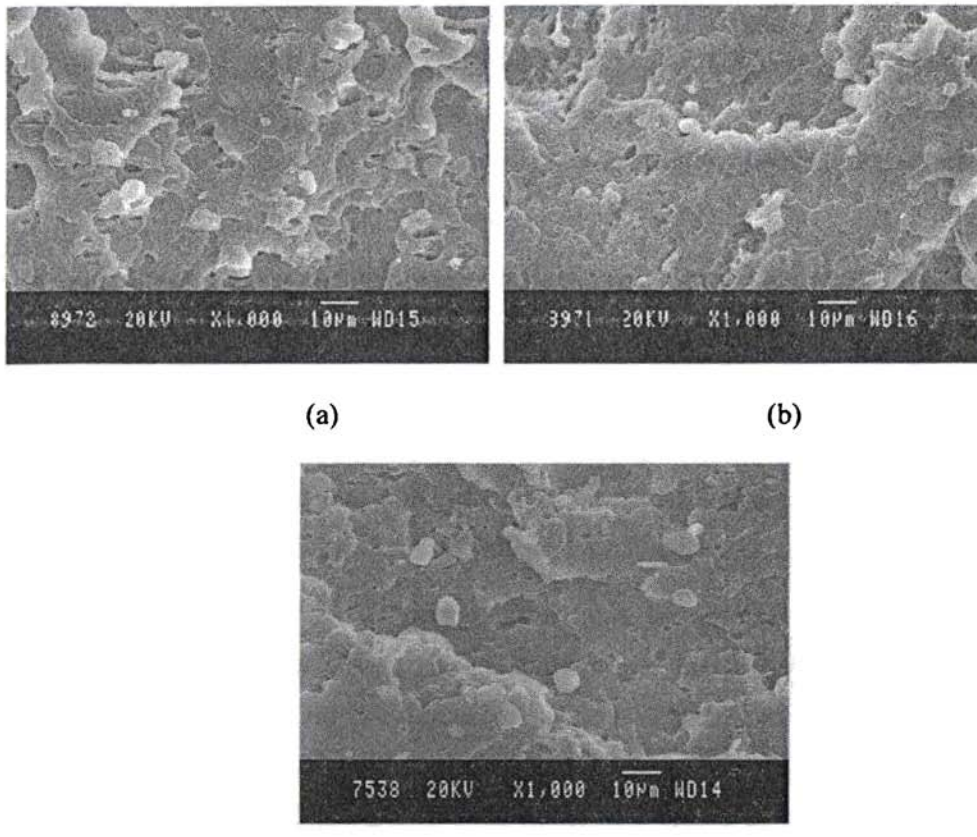

Fig. 5.2: Scanning electron micrographs of the fractured surface of compatibilised P_{90} with (a) 1 wt% (b) 2 wt% and (c) 5 wt% PhPS

The CMC values for MAPS and PhPS are 3.0 and 2.0 % respectively. The CMC value indicates the amount of compatibiliser required to saturate the unit volume of the interface. The increase in domain size above CMC may be due to the formation of micelles of the compatibiliser in the continuous PS matrix. As the micelle formation starts, some of the compatibiliser already at the interface leaves the interface. This leads to an increase in domain size. Several authors have

reported on the interfacial adhesion of binary blends by the addition of compatibilisers [19-21]. Noolandi and Hong [22, 23] theoretically predicted that there is a critical concentration of the block copolymer at which micelles are formed in the homopolymer phases.

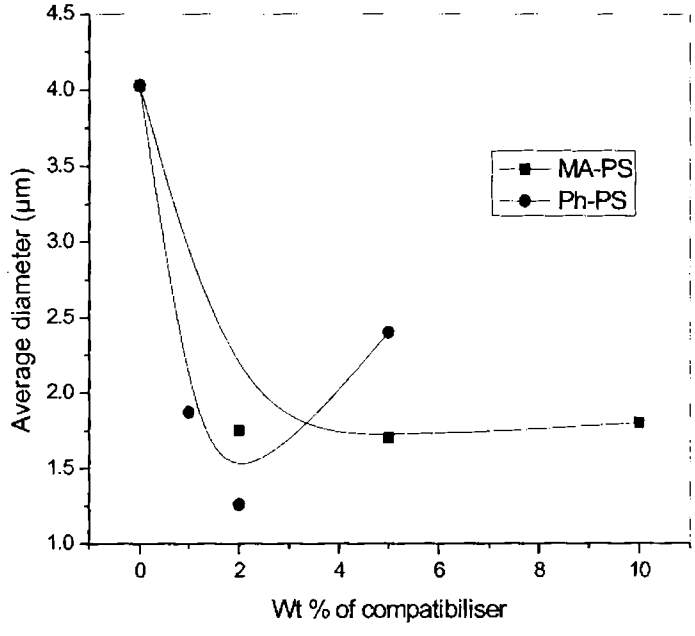

Fig. 5.3: Variation of the average size of dispersed NBR domains as a function of compatibiliser concentration.

These experimental observations and the present study suggest that there is a critical concentration of compatibiliser required to saturate the interface of a binary blend. The compatibiliser concentration above the critical value does not improve the interfacial adhesion.

The interfacial saturation point can be further explained by Taylor's theory. In Taylor's theory [24] of particle deformation, the critical Weber number, W_e, is given by the equation:

$$W_e = \frac{\eta_m d_n \gamma_w}{2\tau_{12}}$$

where η_m is the viscosity of the matrix, *dn* is the number average diameter of the dispersed phase, γ_w is the shear rate and τ_{12} is the interfacial tension. From the equation it is clear that there is a critical value of W_e below which there is no particle deformation and no interfacial tension. At critical particle size, the compatibiliser attains the maximum possible interfacial area and therefore there must be a maximum quantity of compatibiliser available to saturate the interface.

The theories of Noolandi and Hong can be applied to these highly incompatible PS/NBR blends for concentrations less than CMC. According to them the interfacial tension is expected to decrease linearly with the addition of compatibiliser below CMC, and above the CMC a levelling off is expected. The expression for interfacial tension reduction (Δr) in a binary blend A/B upon the addition of divalent copolymer A-b-B is given by [23]

$$\Delta r = \frac{x\Phi_c[(1/2\chi + 1/Z_c) - 1}{Z_c \exp(Z_c\chi/20)}$$

where x is the width at half-height of the copolymer profile given by the Kuhn statistical segment length, Φ_c is the bulk volume fraction of the copolymer in the system, χ is the Flory-Huggins interaction parameter between A and B segments of the copolymer, and Z_c is the degree of polymerisation of the copolymer. According to this equation, the plot of interfacial tension reduction versus ϕ_c should give a straight line. Since interfacial tension reduction is directly proportional to the particle size reduction, as suggested by Wu [25], we can replace the interfacial

tension reduction term by the particle size reduction (Δd) term in Noolandi and Hong's equation. Therefore

$$\Delta d = \frac{K d \phi_c [(1/2\chi + 1/Z_c) - 1}{[Z_c \exp(Z_c \chi / 2)]}$$

where K is a proportionality constant.

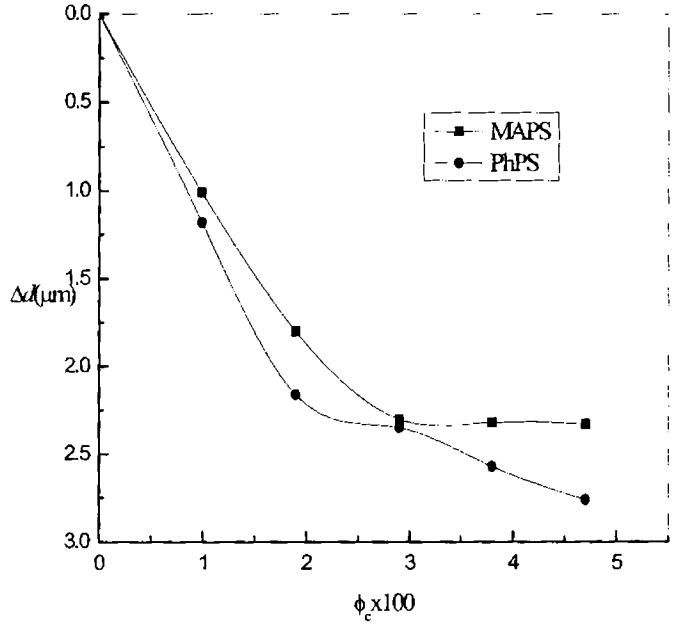

Fig. 5.4: Effect of volume fraction of compatibiliser on the particle size reduction of P_{90}

The plot of particle size as a function of the volume percentage of compatibiliser is shown in figure 5.4. It can be seen that at low copolymer concentrations, below CMC, Δd decreases linearly with increase in copolymer volume fraction.

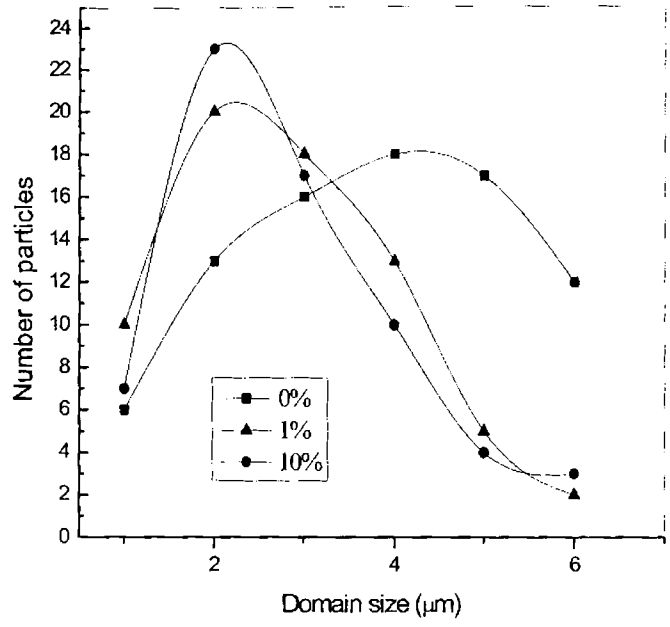

Fig. 5.5: Effect of MAPS concentration on domain size distribution of P_{90}.

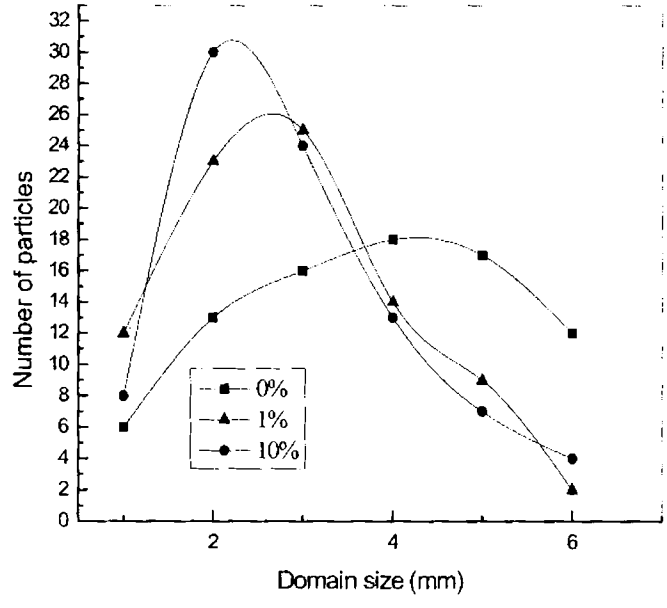

Fig.5.6: Effect of PhPS concentration on domain size distribution of P_{90}.

The domain size distribution curves for the MAPS and PhPS compatibilised blends are shown in figures 5.5 and 5.6 respectively. In the case of unmodified blend, a high degree of polydispersity is evident by the large width of the distribution curve. With increasing concentration of compatibiliser (MAPS and PhPS), the polydispersity decreases, as evident by the decrease in the width of the distribution curve. A narrow distribution is obtained by the addition of 10% compatibiliser. Willis and Favis [26] have also shown that the addition of compatibiliser to polyolefin/PA 6 system not only reduces the dimensions of the minor phase, but also results in uniform distribution of the minor phase.

5.2 IR Spectra of modified polystyrenes

Figure 5.7 shows the FTIR spectrum of MAPS compared with FTIR spectrum of polystyrene. The absorption bands at 1790 cm^{-1} and 1855 cm^{-1} can be assigned to the grafted anhydride, which are due to symmetric and asymmetric C=O stretching vibration of succinic anhydride rings grafted on the PS backbone respectively.

Figure 5.8 shows the FTIR spectrum of phenolic modified polystyrene. The absorption band at a wave number of 3415 cm^{-1} can be assigned to symmetric -OH stretching of phenolic compound.

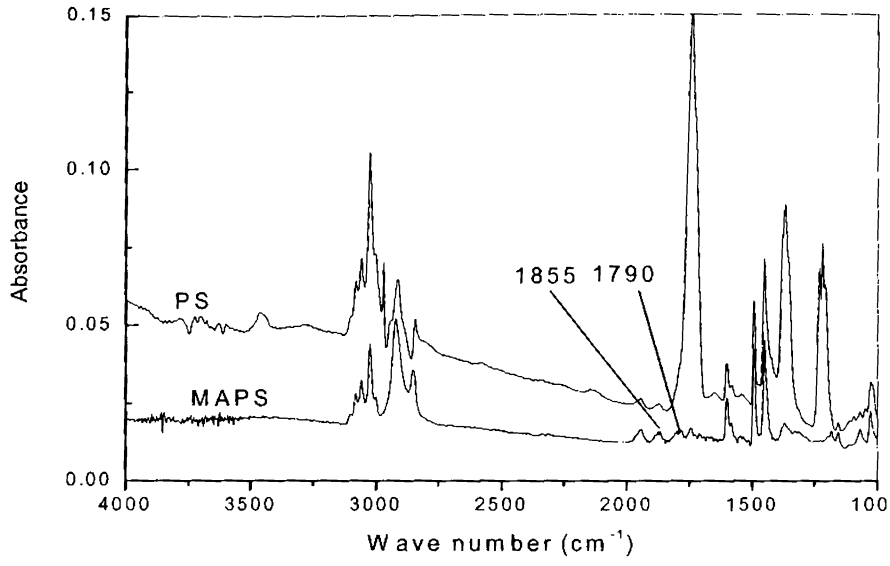

Fig. 5.7: FTIR spectra of MAPS and PS

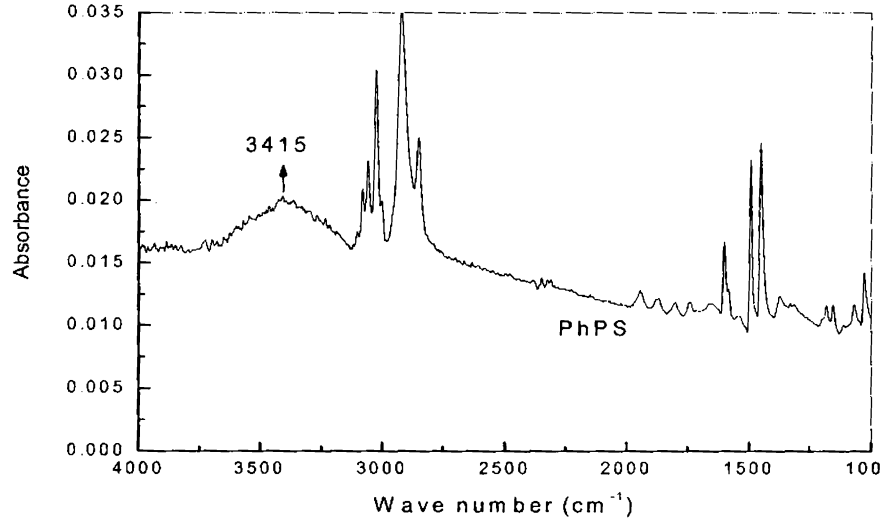

Fig. 5.8: FTIR spectrum of PhPS

5.3 Mechanism of grafting

The mechanism of the compatibilising action and the difference in behaviour of MAPS and PhPS as compatibilisers in nitrile rubber toughened polystyrene can be explained as follows. In MAPS, maleic anhydride groups are grafted on PS back bone [27] as shown in figure 5.9. The compatibilising action of MAPS is due to the dipolar interaction between the anhydride groups of MAPS and NBR. This causes a reduction in interfacial tension, which reduces the domain size of the dispersed phase.

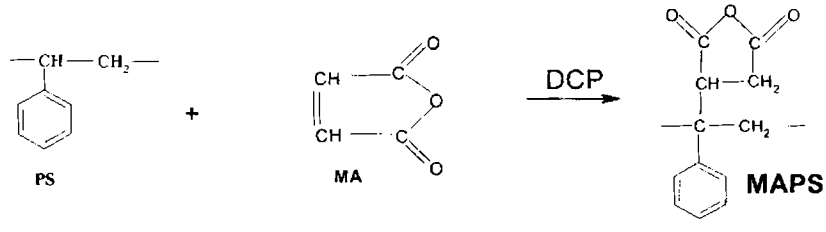

Fig. 5.9: Grafting reaction of MA onto PS during melt reactive process

In phenolic modified polystyrene, dimethylol groups are grafted on polystyrene chain [27] as shown in figure 5.10. Here the compatibilising action is due to the dipolar interaction between the phenolic groups PhPS and NBR and also due to the emulsifying action of the graft copolymer between PS and NBR. Figure 5.10 explains the mechanism of action of PhPS on PS/NBR blend.

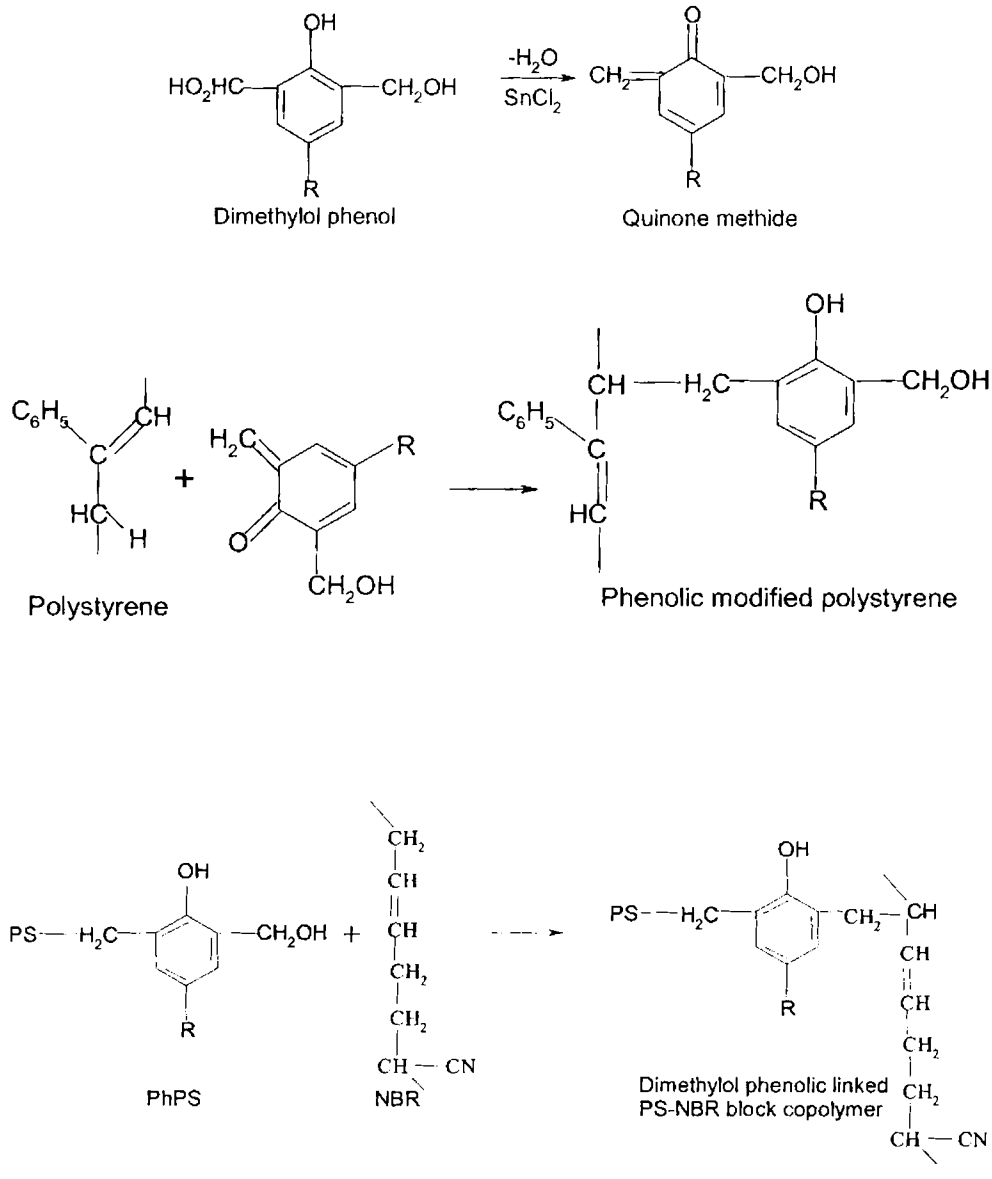

Fig. 5.10: Reaction scheme for phenolic modification on PS and formation of the block copolymer with NBR

5.4 Effect of compatibilisers on mechanical properties

Properties of immiscible polymer blends are affected by the addition of compatibilisers. Figures 5.11 and 5.12 show the variation of tensile strength and Young's modulus of the 90/10 PS/NBR blend with weight percentage of the two compatibilisers MAPS and PhPS respectively. With increase in compatibiliser concentration, the tensile strength and Young's modulus are found to increase up to 5 wt% for MAPS and 2 wt% for PhPS and then levels off for both compatibilisers.

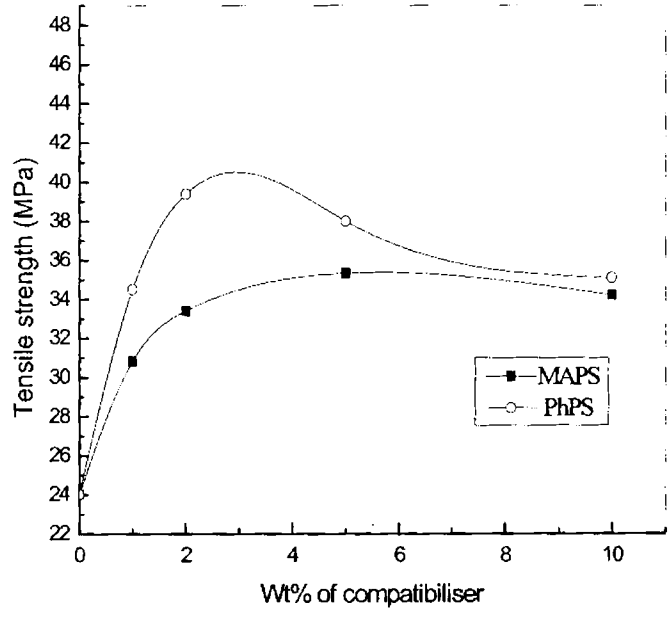

Fig. 5.11: Variation on tensile strength with compatibiliser concentration of 90/10 polystyrene/nitrile rubber blend

The increase in tensile strength and Young's modulus is due to the increase in interfacial adhesion between PS and NBR phases which is evident from the

scanning electron micrographs. It can be seen that addition of PhPS caused an improvement in the tensile strength and Young's modulus. As a consequence, the blend exhibits higher tensile strength and Young's modulus than those of the uncompatibilised blend.

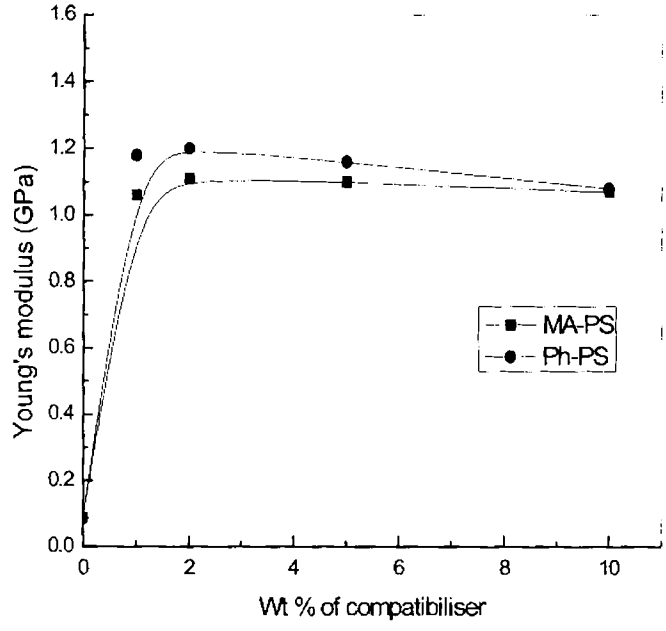

Fig. 5.12: Variation of Young's modulus with compatibiliser concentration of 90/10 polystyrene/nitrile rubber blend

In the case of MAPS compatibilised blends, the increase in tensile strength and Young's modulus is due to the dipolar interaction between the maleated PS and NBR phases, which causes an increase in interfacial adhesion between PS and NBR, although there is no reduction in particle size with the increase in MAPS

concentration beyond 5 wt%. Similar results have been reported for the Nylon/PP system [28].

The effect of compatibiliser concentration on the elongation at break of 90/10 Polystyrene/nitrile rubber blend is shown in figure 5.13. The elongation at break values increases with the addition of compatibilisers up to 5 % for MAPS and 2% for PhPS.

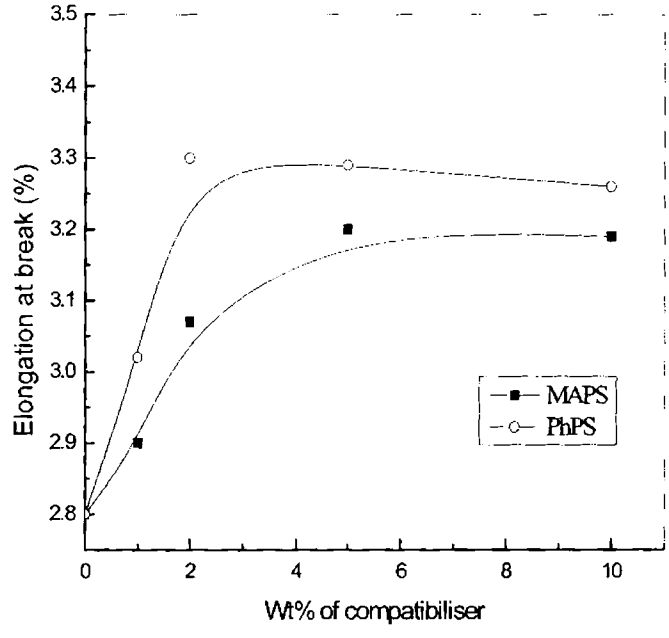

Fig. 5.13: Variation of elongation at break with compatibiliser concentration of 90/10 blend of PS/NBR

From figure 5.14 it is seen that the Izod impact strength of the blend increases significantly by the addition of up to 5 wt% MAPS and 2 wt% PhPS, and after that it decreases. This result is consistent with the literature reports on the increase of impact strength with reduction in particle size of the dispersed phase.

The reduction in impact strength at higher compatibiliser concentrations is due to the formation of compatibiliser micelles in the homopolymer phases. Similar results have been reported for the low-density polyethylene/polydimethylsiloxane system [29].

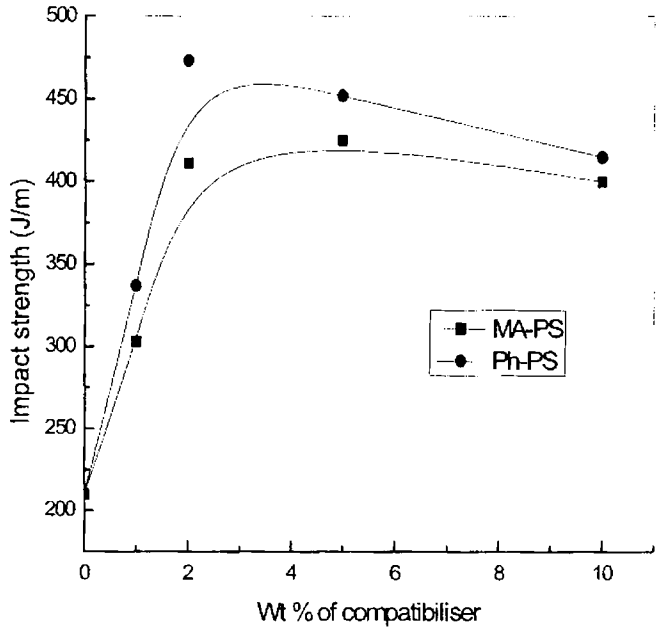

Fig. 5.14: Variation of impact strength with compatibiliser concentration of 90/10 blend of PS/NBR

It is clear from the impact strength results that interfacial adhesion is an important factor in rubber toughening. Shaw and Singh [30] have reported on the impact strength of compatibilised PS/EPDM blends, where the observed increase in impact strength is correlated with the improved interfacial adhesion.

5.5 Dynamic mechanical properties

The variation of storage modulus as a function of temperature of the 90/10 blend of PS/NBR compatibilised with different amounts of PhPS is shown in figure 5.15. Below the glass transition temperature (T_g) of polystyrene all the compatibilised blends have higher storage modulus than that of uncompatibilised blend. The blend containing 2 and 5wt% PhPS registered highest storage modulus. The increase in storage modulus upon the addition of PhPS is due to the increase in the interfacial adhesion caused by the emulsifying effect of the block copolymer formed by the interaction between PhPS and nitrile rubber. The better interaction between PS and NBR is evident from the morphology observed in scanning electron micrographs.

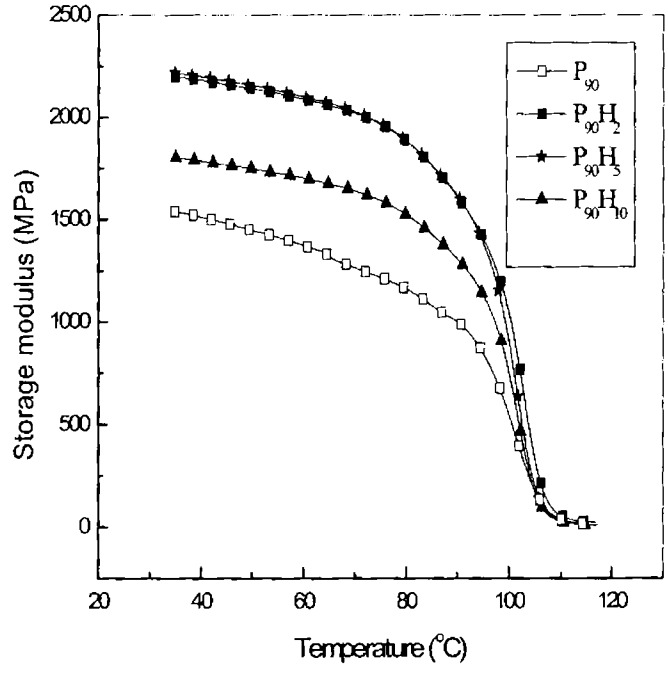

Fig.5.15: Variation of storage modulus of PhPS compatibilised PS/NBR blends

The lower value of storage modulus for the blend containing 10 wt% PhPS may be due to the formation of micelles of the compatibiliser in the polystyrene matrix. Similar behaviour has been reported Brahimi *et al* [31] in the compatibilisation of PS/PE blends by HPB-b-PS copolymers. At higher temperatures all blends showed approximately the same modulus.

Figure 5.16 depicts the variation of storage modulus (E') of the 90/10 blend of PS/NBR compatibilised with MAPS. All the compatibilised blends except that containing 5 wt% MAPS have lower storage modulus than uncompatibilised blend at ambient temperature. This suggests that the interfacial adhesion is strong in it. At a temperature above 100°C all the blends show nearly the same values of E'. In the compatibilisation of PS/NBR blend with MAPS, the MAPS increases the interfacial interaction between PS and NBR by the dipolar interaction between polar maleic anhydride groups of maleated PS and polar NBR.

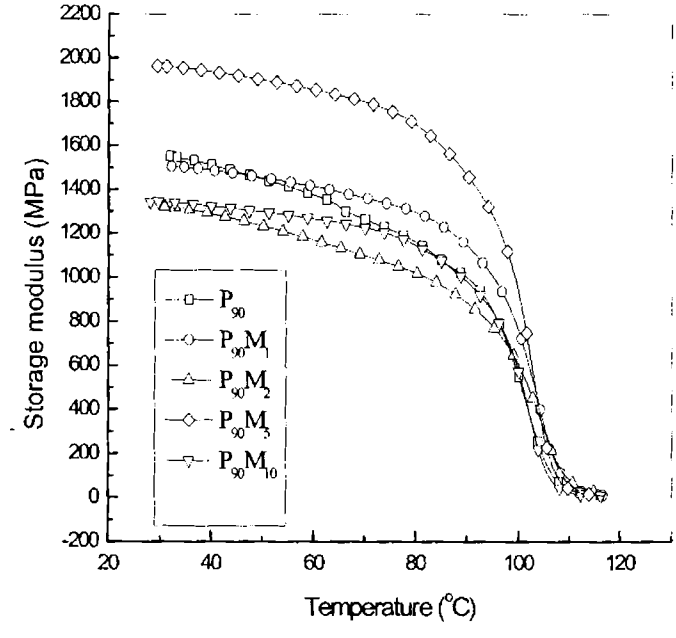

Fig. 5.16: Variation of storage modulus of MAPS compatibilised PS/NBR blends

The variation of tan δ as a function of temperature of PhPS compatibilised blends is shown in figure 5.17. From the figure it is clear that in all blends the T_g of polystyrene is unaffected by compatibilisation. This indicates that the compatibilisation does not alter the level of miscibility or in other words, the presence of compatibiliser does not promote molecular level miscibility. This is in

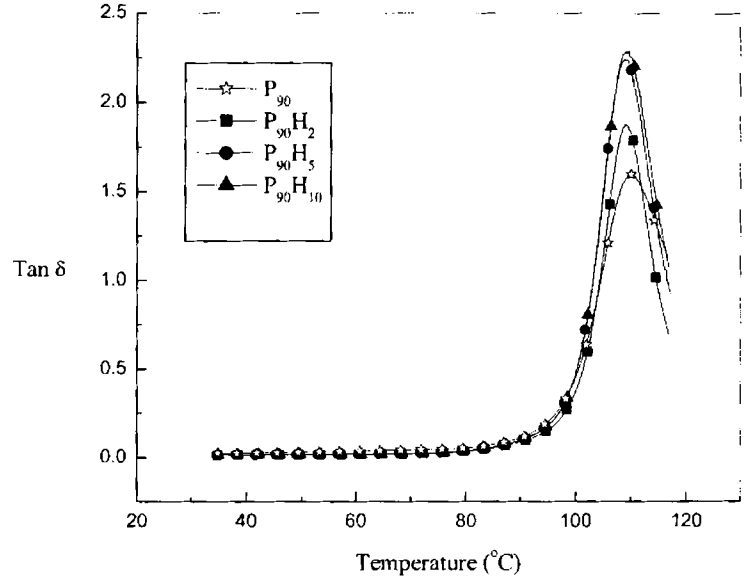

Fig. 5.17: Variation of tan δ of PhPS compatibilised PS/NBR blends

agreement with the conclusions made by Paul [32] who suggested that if two polymers are far from being miscible, and then no copolymer is likely to make a one phase system. In a completely immiscible system, the main role of the compatibiliser is to act as an interfacial agent. At lower temperatures, below the T_g of polystyrene, the tan δ values of the compatibilised blends are slightly lower than that of the uncompatibilised blend. All the compatibilised blends show higher values of tan δ at higher temperatures. This increase in tan δ indicates that the interfacial interaction caused by the presence of PhPS may be weakened at higher

temperatures. The decrease in interfacial interaction at higher temperatures will decrease the interfacial adhesion and hence leads to increased segmental motion.

The variation of tan δ of MAPS compatibilised P_{90} is shown in figure 5.18. The tan δ value of the blend containing 5 wt% MAPS is lower than that of uncompatibilised blend and the T_g of polystyrene is slightly shifted to a higher temperature. In this case the decrease in tan δ is due to the increase in interfacial interaction.

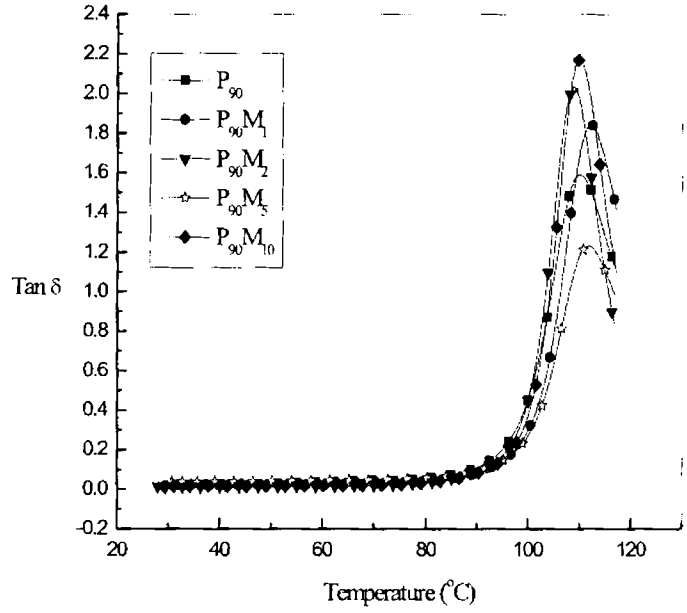

Fig. 5.18: Variation of tan δ of MAPS compatibilised PS/NBR blends

Figure 5.19 depicts the variation of loss modulus (E") as a function of temperature of PhPS compatibilised blends. Distinct peaks can be observed at the glass transition temperature (T_g) of PS. Below the tg of the polymer, the chains are in tact and stress transfer is possible. When the temperature is approaching the T_g, energy dissipation takes place and a corresponding peak is observed in the E"

values. $P_{90}H_5$ registers maximum loss modulus which is attributed to the increased extent of interaction at the interface.

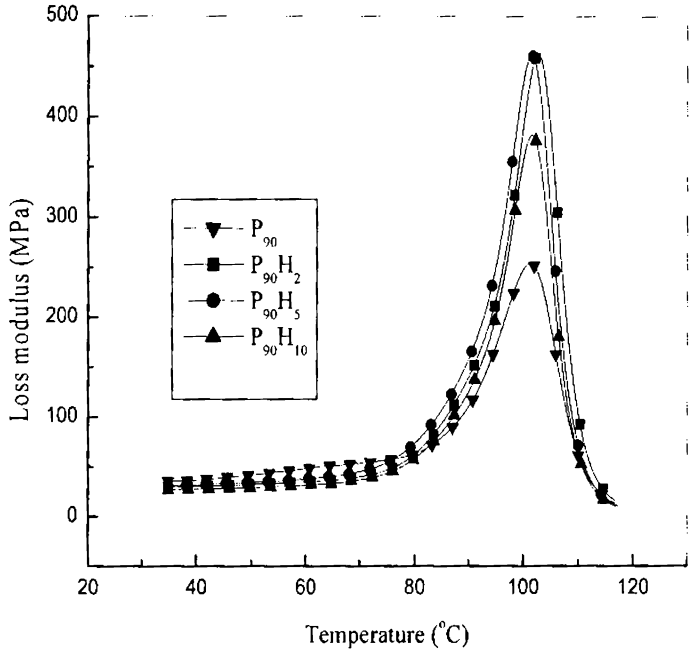

Fig. 5.19: Variation of loss modulus of PhPS compatibilised PS/NBR blends.

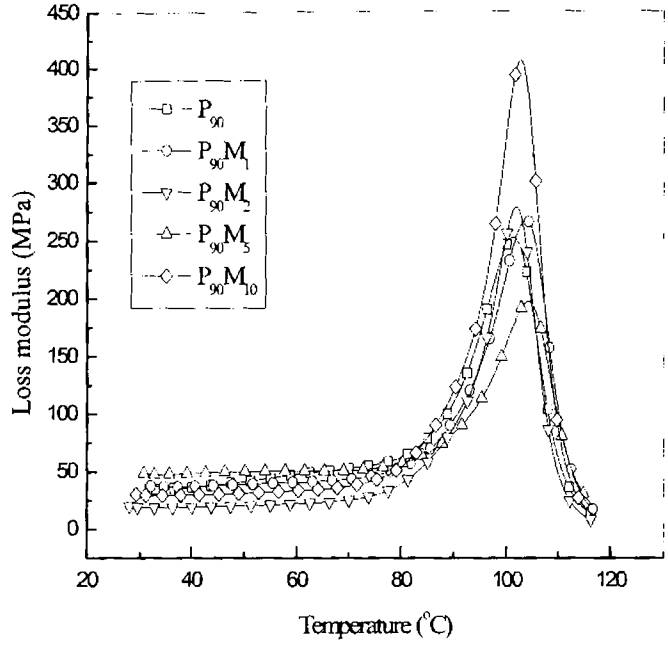

Fig. 5.20: Variation of loss modulus of MAPS compatibilised PS/NBR blends.

The variation of loss modulus with temperature of MAPS compatibilised blends is shown in figure 5.20. The loss modulus of the blend containing 5 wt% MAPS has lower value than that of uncompatibilised blend.

5.6 Rheological studies

The addition of block or graft copolymers or modified polymers to immiscible blends is found to improve their physical and mechanical properties. A suitably selected compatibiliser will locate at the interface between the two phases leading to a reduction in interfacial tension and an improvement in interfacial adhesion.

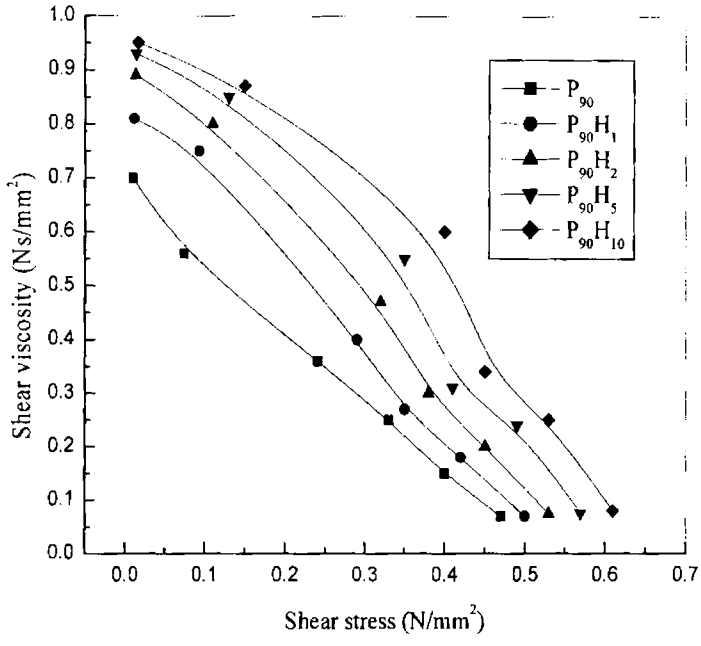

Fig.5.21: Effect of shear stress on the melt viscosity of PhPS compatibilised PS/NBR blends

The effect of shear stress on the melt viscosity of 90/10 blend of PS/NBR containing PhPS and MAPS is shown in figures 5.21 and 5.22 respectively. It is seen from the figure that, at lower shear rates, the viscosity of the compatibilised system is higher than that of the uncompatibilised system. At high shear rates the viscosity seems to be unaffected by compatibilisation.

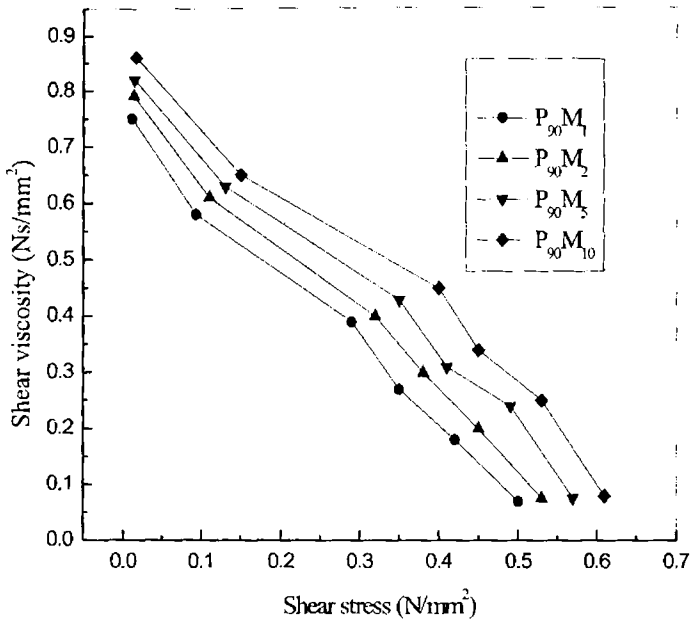

Fig.5.22: Effect of shear stress on the melt viscosity of MAPS compatibilised PS/NBR blends

Figures.5.23 and 5.24 depict the variation of viscosity as a function of compatibiliser concentration. With the increase in compatibiliser loading the viscosity initially increases, followed by a levelling-off at higher loading. The variation in viscosity is more pronounced at lower shear rates. Such increase in viscosity on compatibilisation of immiscible polymer blends has been reported by several researchers [33–37]. Upon compatibilisation of an immiscible blend, the compatibiliser will generally locate at the interface between the dispersed phase and the matrix. This will lead to an increase in interfacial thickness.

According to Okoroafar *et al* [38], the viscosity of the compatibilised blend is given by:

$$1/\eta_{blend} = (\Phi'_m / \eta_m + \Phi'_d / \eta_d + \Phi'_i / \eta_i) - (1/\eta_m - 1/\eta_d)\,\Phi'_m\,\Phi'_m$$

$$+ (\Phi'_m / \eta_m - \Phi'_d / \eta_d)\,\Phi'_i + \Phi'_i / \eta_m\,(\Phi'_d - \Phi_m')$$

where Φ' is the volume fraction, η the viscosity, and the subscripts m, d and i denote matrix, dispersed phase and interface, respectively. Hence the viscosity of these blends depends on the volume fraction of the interface and also on the viscosity of the interface.

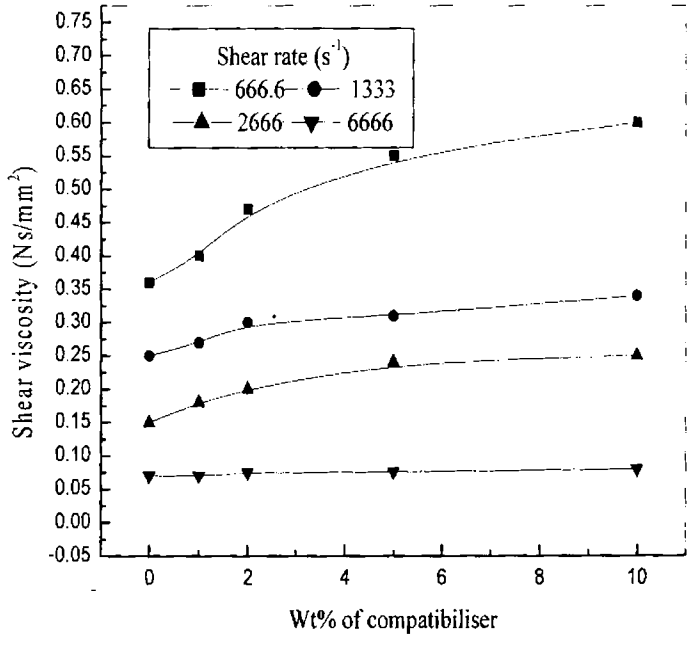

Fig.5.23: Effect of compatibiliser concentration on the melt viscosity of PhPS compatibilised PS/NBR blends

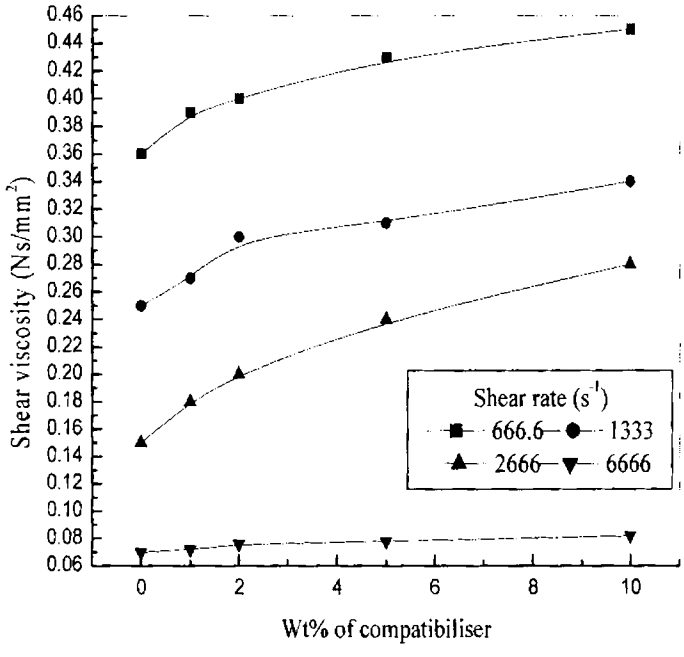

Fig.5.24: Effect of compatibiliser concentration on the melt viscosity of MAPS compatibilised PS/NBR blends

From figures 5.23 and 5.24 it can be observed that the increase in melt viscosity with concentration of the compatibiliser is negligible at higher shear rates. So the processability of the PS/NBR blends not affected by the addition of compatibilisers

The effect of compatibilisation on the flow behaviour index is given in figure 5.25. It is clear from the figure that flow behaviour index increases with the addition of compatibiliser and even after compatibilisation, the polymer melt exhibits a pseudoplastic behaviour.

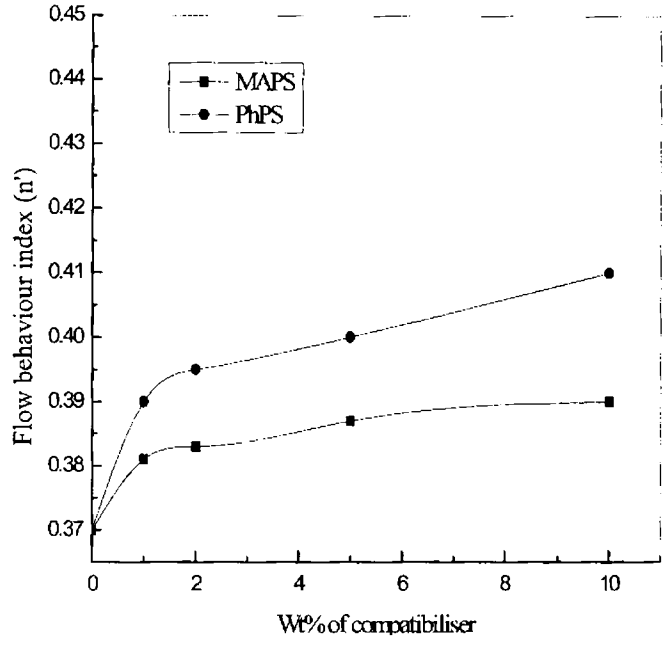

Fig.5.25: Effect of compatibiliser concentration on the flow behaviour index of PS/NBR blends

In a capillary rheometry, several phenomena may be observed in the extrusion characteristics, which are more intimately related to the polymer melt elasticity than to the melt viscosity. These measurements are important in terms of the commercial processing characteristics of the polymer blends. The first one is the die-swell or elastic memory and which has great practical importance in processing operations. The die-swell originates from the recoverable elastic deformation of the flowing polymer at the entrance of the capillary, that partially decays on relaxation during the flow through the capillary, but which causes swelling of the extrudate once the die wall restriction is removed. The die-swell behaviour of the compatibilised blends is presented in figure 5.26.

Compatibilisation of the blend decreases the die-swell and improves the melt strength.

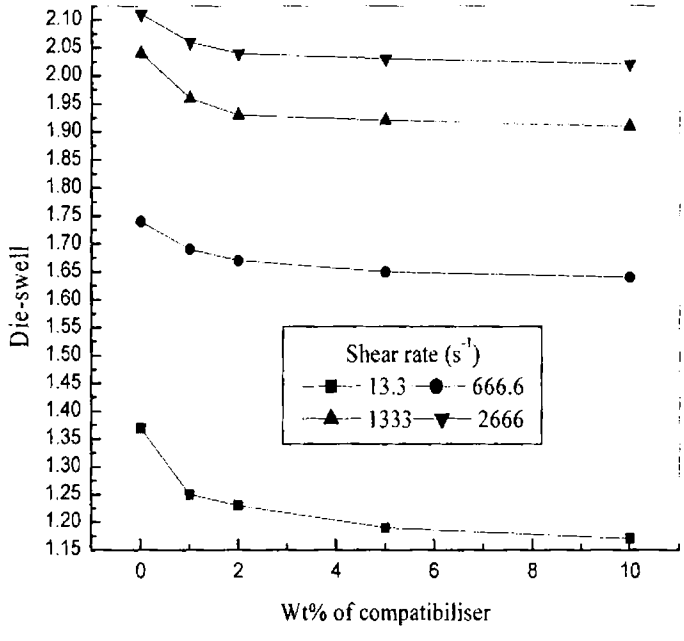

Fig.5.26: Effect of compatibiliser MAPS concentration on the die-swell values of PS/NBR blends

5.7 Thermogravimetric analysis

The thermograms and derivative thermograms of 90/10 blends of PS/NBR compatibilised with MAPS and PhPS are shown in figures 5.27 to 5.32. The peak corresponding to the major weight loss in DTG curves are shifted to higher temperatures upon compatibilisation using both MAPS and PhPS. Table 5.1 shows the degradation temperature and weight loss at different temperatures for the compatibilised blends. It can be seen from the table that the degradation temperature corresponding to the major weight loss increased on compatibilisation.

The percentage weight loss at different temperatures decreased upon compatibilisation. The improvement in degradation resistance on compatibilisation may arise from the better interactions between PS and NBR.

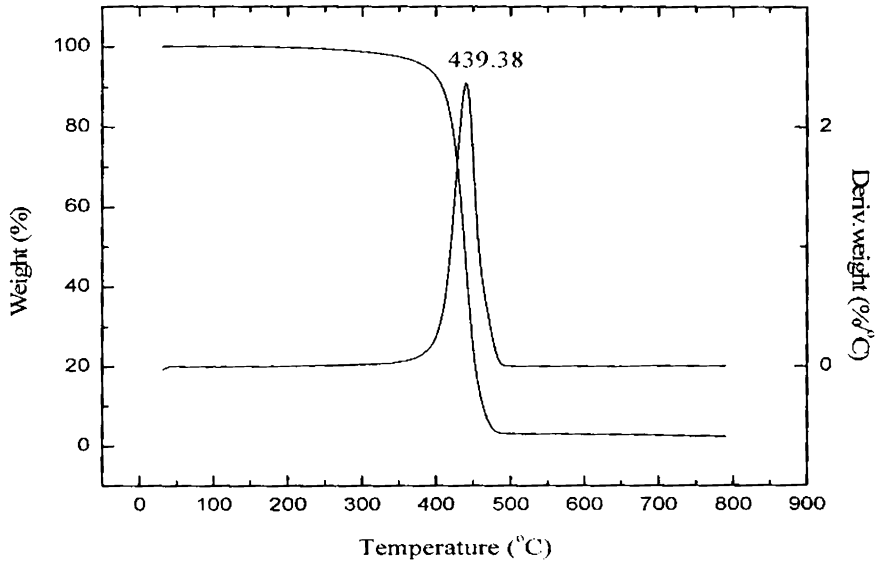

Fig. 5.27: TG trace of 90/10 blend of PS and NBR with 2 wt% MAPS

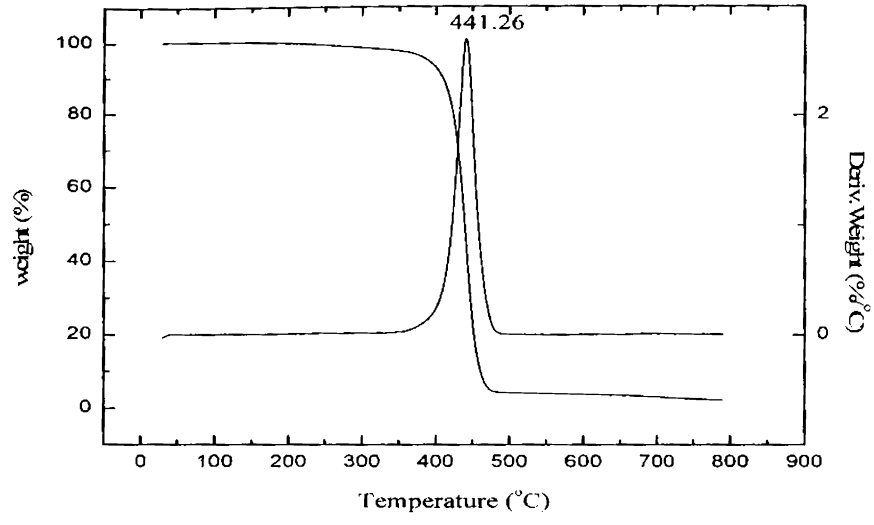

Fig. 5.28: TG trace of 90/10 blend of PS and NBR with 5 wt% MAPS

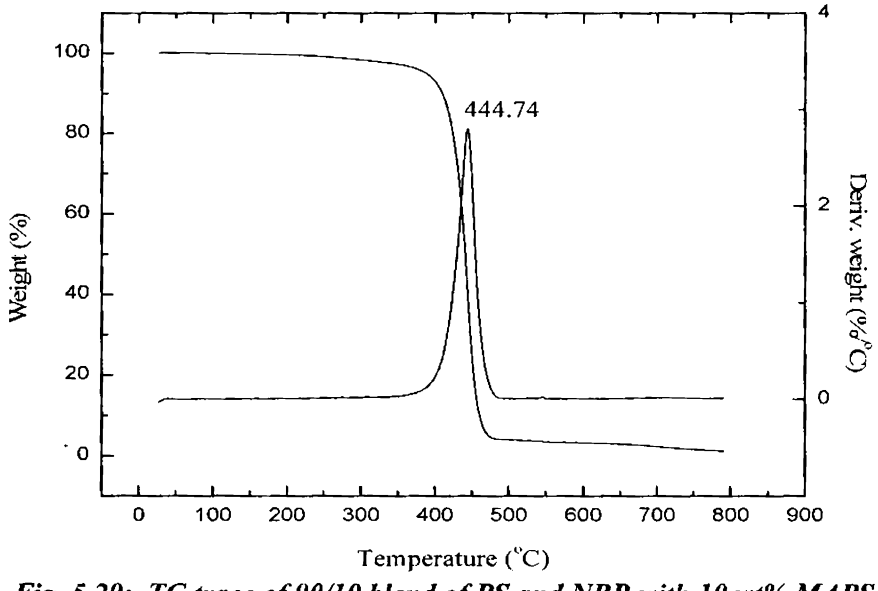

Fig. 5.29: TG trace of 90/10 blend of PS and NBR with 10 wt% MAPS

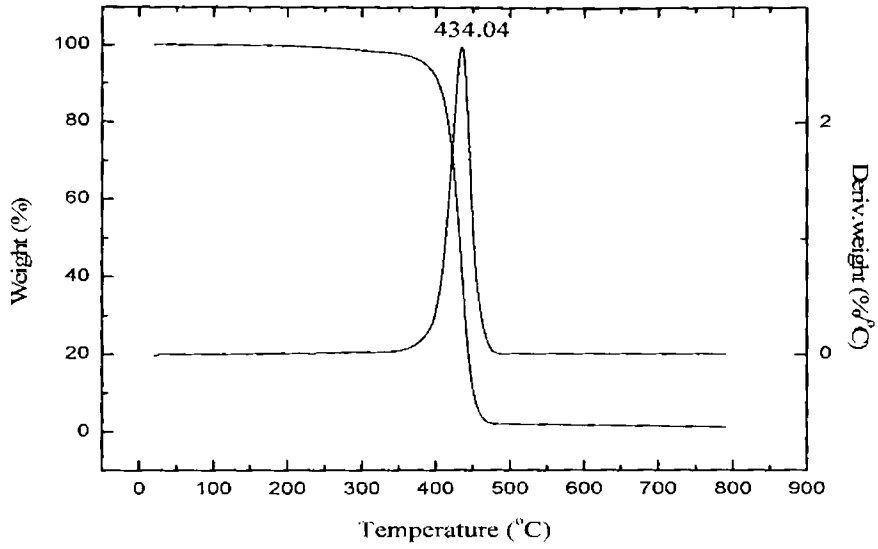

Fig. 5.30: TG trace of 90/10 blend of PS and NBR with 1 wt% PhPS

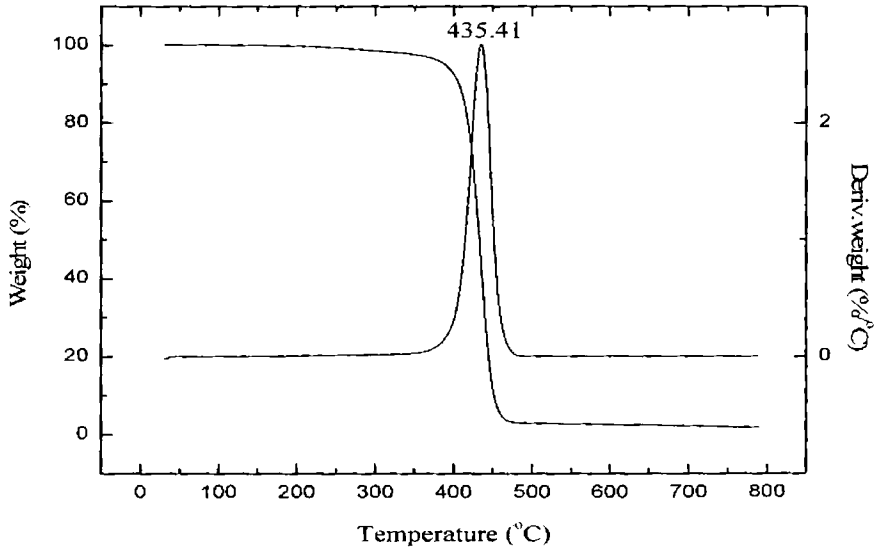

Fig. 5.31: TG trace of 90/10 blend of PS and NBR with 2 wt% PhPS

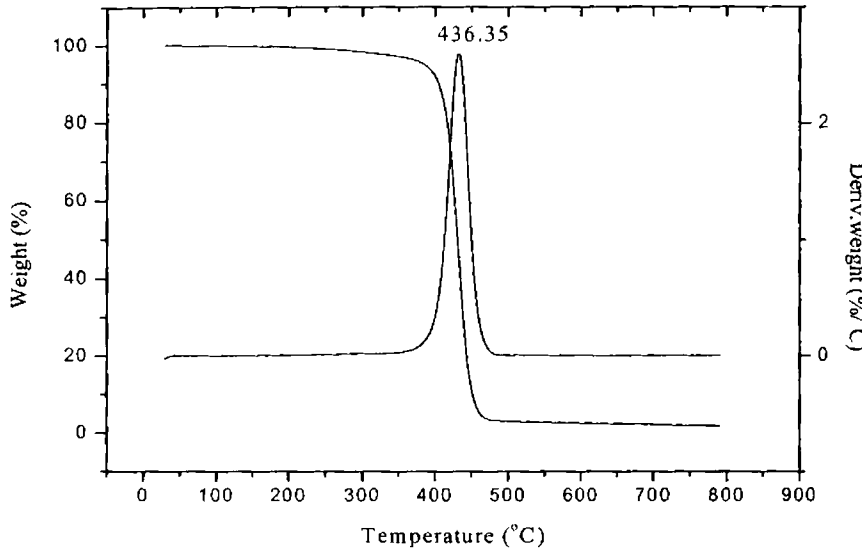

Fig. 5.32: TG trace of90/10 blend of PS and NBR with 5 wt% PhPS

Table 5.1. Weight loss and DTG peaks of compatibilised blends

Sample	Weight loss at 300°C (%)	Weight loss at 400°C (%)	Total weight loss (%)	DTG peak
$P_{90}M_2$	1.08	7.41	98.63	439.38
$P_{90}M_5$	1.46	7.21	98.13	441.26
$P_{90}M_{10}$	1.63	7.01	98.00	444.74
$P_{90}H_1$	1.63	7.90	98.20	434.04
$P_{90}H_2$	1.43	7.34	98.10	435.41
$P_{90}H_5$	1.11	7.10	98.10	436.35

5.8 Conclusion

Compatibilisation with maleic anhydride modified polystyrene and phenolic modified polystyrene resulted in an overall improvement in the mechanical properties of powdered nitrile rubber toughened polystyrene due to improved interfacial adhesion. There is significant reduction in the domain size of the dispersed NBR phase till a critical micelle concentration is reached and thereafter a levelling off in the domain dimensions is noticed. The addition of phenolic modified polystyrene and maleic anhydride modified polystyrene is found to increase the storage modulus at lower temperatures, indicating an increase in interfacial adhesion on addition of these compatibilisers. At a higher concentration of these compatibilisers, the storage modulus decreaseed due to interfacial saturation. The compatibilisation of PS/NBR blend with maleic anhydride modified polystyrene and phenolic modified polystyrene was found to increase the viscosity of the system indicating an increase in interfacial interaction. The variation of viscosity was correlated with the morphology. As the compatibiliser concentration increased the domain size decreased and showed a levelling-off at high concentration. It is also observed that the increase in melt viscosity with concentration of the compatibiliser is negligible at higher shear rates. So the processability of the PS/NBR blends is not affected by the addition of compatibilisers. The effects of compatibiliser concentration on the thermal behaviour of PS/NBR blend were analysed. It was found that the thermal stability of the blends is improved by compatibilisation. The weight loss of the compatibilised blends at various temperatures decreased on addition of the compatibiliser.

References

1. D. R. Paul, J. W. Barlow, H. Keskkula, In *Encyclopedia of Polymer Science and Engineering*, J. I. Kroschwitz, Ed., Wiley, New York, (1988).
2. S.B. Brown, In *Reactive Extrusion, Principle and Practice*, M. Xanthos, Ed., p. 75, Hanser, New York, (1992).
3. N.C. Liu, W.E. Baker, *Adv. Polym. Technol.*, **11**, 249 (1992)
4. M. Xanthos, S.S. Dagli, *Polym. Eng. Sci.*, **31**, 929 (1991)
5. N.C. Beck Tan, S.K. Tai, R.M. Briber, *Polymer*, **37**, 3509 (1996)
6. P.C. Lee, W.F. Kuo, F.C. Chang, *Polymer*, **35**, 5641 (1994)
7. M.W. Fowler, W.E. Baker, *Polym. Eng. Sci.*, **28**, 1427 (1988)
8. B. De Roover, *Ph.D. Thesis*, Universite Catholique de Louvain, (1994).
9. R. E.Lavengood, Eur. Patent, No. 202214, Monsanto Company, (1986).
10. L Chen, B. Wong, W.E. Baker, *Polym. Eng. Sci.*, **36**, 1594 (1996).
11. J. Duvall, C. Selliti, C. Myers, A. Hiltner, E. Baer, *J. Appl. Polym. Sci.*, **52**, 195 (1994).
12. W. Gabara, S. Porejko, *J. Polym. Sci.*, **A1 5**, 1539 (1967).
13. S. Porejko, W. Gabara, J. Kulesza, *J. Polym. Sci.*, **A1 5**, 1563 (1967).
14. D. Braun, U. Eisenlohr, *Angew. Makromol. Chem.*, **55**, 43 (1976)
15. A.Y. Coran, R. Patel, *Rubber Chem. Technol.*, **56**, 1045 (1983).
16. S. George, N.R. Neelakantan, K.T. Varughese, S. Thomas, *J. Polym. Sci.,Polym. Phys. Ed.*, **35**, 2309 (1997).
17. R. Asaletha, M.G. Kumaran, S. Thomas, *Rubber Chem. Technol.*, **68**, 671 (1995).
18. Z. Oommen, M.R. Gopinathan Nair, S. Thomas, *Polym. Eng. Sci.*, **36**, 1 (1996).
19. H.A. Spiros, G. Irena, J.T. Koberstein, *Macromolecules*, **22**, 1449 (1989).
20. R. Fayt, R. Jerome, P. Teyssie, *Makromol chem.*, **187**, 837 (1986).
21. S. Thomas, R.E. Prud'homme, *Polymer*, **33**, 4260 (1992).

22. J. Noolandi, K.M. Hong, *Macromolecules,* **15**, 482 (1982).
23. J. Noolandi, K.M. Hong, *Macromolecules,* **17**, 1531 (1984).
24. J.M. Wills, B.D. Favis, *Polym. Eng. Sci.*, **28**, 1416 (1988).
25. S. Wu, *Polym. Eng. Sci.*, **27**, 335 (1987).
26. J.M. Willis, B.D. Favis, *Polym. Eng. Sci.*, **30**, 1073 (1990).
27. C. Nakason, K. Nuansomsri, A. Kaesaman, S. Kiatkamjornwong, *Polymer Testing*, **25**, 782 (2006)
28. F. Ide, A. Hasegawa, *J. Appl. Polym. Sci.*, **18**, 963 (1974)
29. R.N. Santra, B.K. Samantaray, A.K. Bhowmick, G.B. Nando, *J. Appl .Polym. Sci.,* **49**, 1145 (1993).
30. S. Shaw, R.P. Singh, *J. Appl. Polym. Sci.*, **40**, 685 (1990)
31. B. Brahimi, ,A. Ait-kadi, A. Ajji, R. Fayt, *J. Polym. Sci.,Polym. Phys. Ed.,* **29**, 946 (1991).
32. D.R. Paul, S. Newman, *Polymer blends*, Academic Press, New York, (1978).
33. R.M.H. Miettinen, J.V. Seppala, O.T. Ikkala, I.T. Reima. *Polym.Eng.Sci* **34(5)**, 395 (1994).
34. Y. Germain, B. Ernst, O. Genelot, L. Dhamini, *J. Rheol.*, **38(3)**, 681 (1994).
35. A. Valenza, D. Acierno, *Eur.Polym. J.*, **30(10)**, 1121 (1994).
36. M. Joshi, S.N. Maiti, A. Misra, *J.Appl .Polym. Sci.*, **15**, 1837 (1992).
37. Z. Oommen, C.K. Premalatha, B. Kuriakose, S. Thomas, *Polymer* **38**, 5611 (1997).
38. E.U. Okoroafar, J.P. Villemuire, J.F. Agassant, *Polymer,* **33(24)**, 5264 (1992).

Chapter 6

Compatibilisation by the addition of styrene-co-acrylonitrile

Among the different types of polymer blends, rubber toughened thermoplastics combine the excellent processing characteristics of the thermoplastics at high temperatures with the resilience and flexibility associated with elastomers at the service temperature [1, 2]. Even though blending is an easy method for the preparation of rubber toughened thermoplastics, most of the blends are immiscible and exhibit poor mechanical properties. In such heterogeneous systems, the over-all properties depend on two structural parameters: a proper interfacial tension leading to phase size small enough to allow the material to be considered as macroscopically homogeneous and an interface adhesion strong enough to assimilate stresses and strains without disruption of the established morphology [3]. However the properties of these polymer blends can be improved by the addition of compatibilisers [4]. A suitably chosen compatibiliser will locate at the interface between the two components and thereby reduce the interfacial tension and improve the interfacial adhesion and mechanical properties. The effects of compatibilisation on the properties of polymer blends have been widely investigated [5-10]. The thermodynamic theories concerning the emulsifying effect of copolymer in heterogeneous polymer blends have been developed by Leibler for semi compatible blends [11, 12], and Noolandi and Hong for immiscible blends [13, 14]. According to the two theories, the localisation of the compatibiliser at the

interface results in broadening of the interface between the homopolymers and lowering of the interaction energy between the two immiscible homopolymers. Thomas and co-workers [15-18] investigated the effect of compatibilisation using copolymers and modified polymers in different polymer blends. They found that the addition of natural rubber-graft-polymethyl methacrylate (NR-g-PMMA) and natural rubber-g-polystyrene (NR-g-PS) as compatibilisers in PMMA/NR and PS/NR blends, respectively, leads to fine and uniform distribution of the minor phase in the major matrix polymer. Mathew and Thomas [19] studied the influence of SAN as a compatibiliser on the morphology and mechanical properties of PS/NBR blends. They found that the incorporation of SAN is effective in reducing the phase size of PS/NBR blends. The domain size of the dispersed phase decreases with the addition of small amount of the copolymer, followed by levelling off at higher concentrations.

In this chapter, the effect of styrene-acrylonitrile copolymer (SAN) as a compatibiliser for powdered nitrile rubber toughened polystyrene was investigated. The effect of compatibilisation on the mechanical properties and morphology was studied.

6.1 Compatibilisation with random SAN copolymer

An intermolecular interaction between SAN-PS and SAN-NBR is expected due to their structural similarity. Hence, random SAN copolymer is a logical choice as a compatibiliser in PS/NBR blend. Due to the close affinity of the styrene segments toward the PS phase and the acrylonitrile segments toward the NBR phase, the localisation of SAN molecules at the interface is increasingly favoured. This would facilitate the effective dissipation of stress from the matrix to dispersed phase, thereby, increasing the interfacial strength of the blends.

6.2 Effect of compatibiliser concentration on mechanical properties and morphology

Figures 6.1and 6.2 show the effect of the addition of SAN on the tensile strength and Young's modulus of 90/10 blend of polystyrene/nitrile rubber.

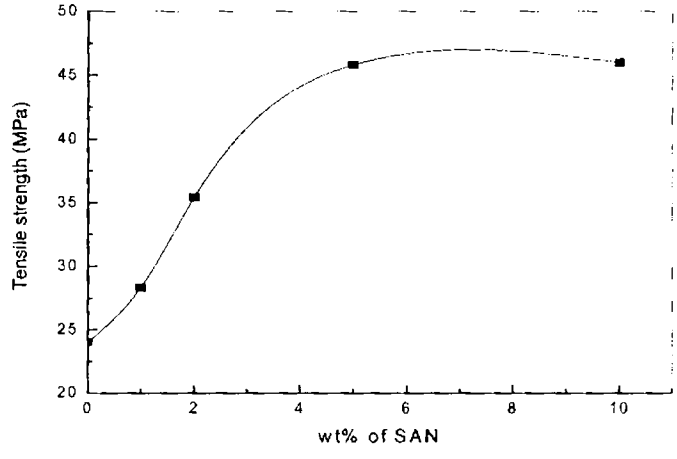

Fig. 6.1: Effect of SAN concentration on the tensile strength of 90/10 blend of polystyrene/nitrile rubber

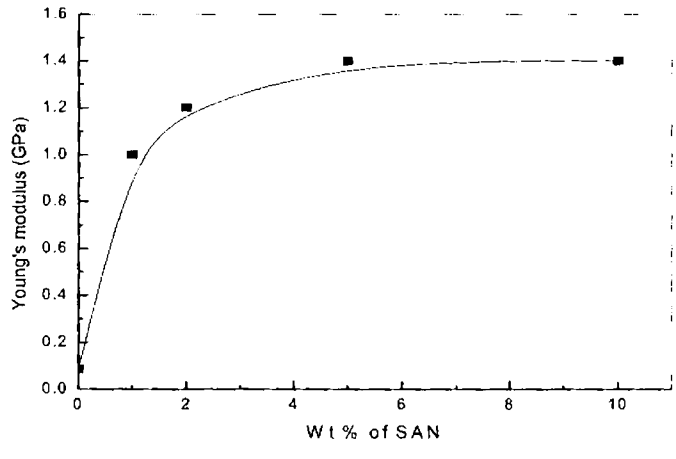

Fig. 6.2: Effect of SAN concentration on the Young's modulus of 90/10 blend of polystyrene/nitrile rubber

Addition of SAN improves the tensile strength and Young's modulus. This is due to the enhancement in interfacial adhesion between PS and NBR phases. The highest tensile strength and Young's modulus are obtained at 5 wt% SAN concentration and thereafter no further increase. This may be explained as follows: since SAN is a random copolymer, it cannot penetrate deep into the phases, rather concentrates more at the interface. This leads to substantial increase in interfacial thickness. In fact, the addition of SAN copolymer suppresses the coalescence of the NBR phase. In the absence of the random copolymer, the coalescence may be occurring in P_{90} because the rubber particles can undergo shear induced aggregation in the low viscosity PS phase [19].

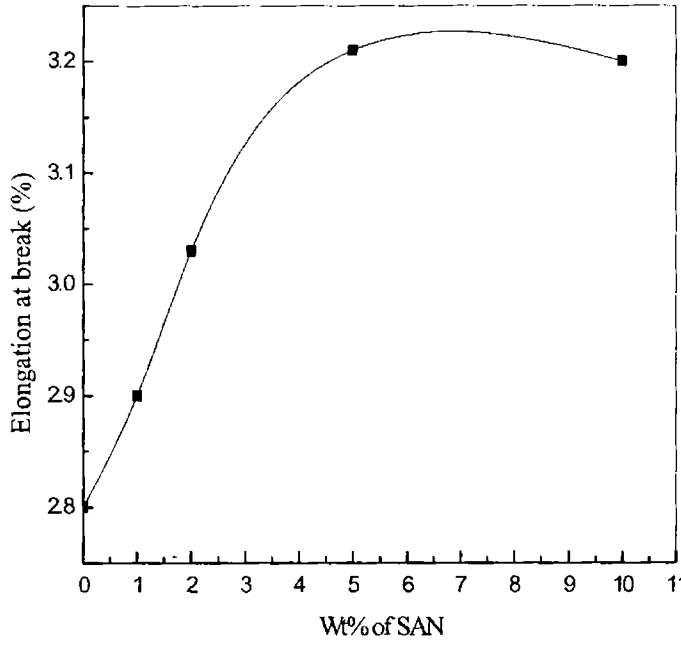

Fig. 6.3: Variation of elongation at break of 90/10 blend of polystyrene/nitrile rubber with wt% of SAN

The compatibilised blends are found to be more tough than the uncompatibilised blend. The uncompatibilised 90/10 blend of PS/NBR has an elongation at break of 40%. Addition of 5 wt% SAN increases the elongation at break to 60.5 % (figure 6.3). The increase in toughness of compatibilised blends is due to the increased interfacial adhesion. An improvement in elongation at break on compatibilisation of polymer blends has been reported in literature [20].

The effect compatibiliser concentration on the impact strength (unnotched) is given figure 6.4. Addition of 5 wt% SAN increased the impact strength of P_{90} from 210 to 573 J/m. The effect of increasing the concentration of SAN beyond 5 wt% would only be to force away a portion of it from the blend interface, to form micellar aggregates in the matrix. Majumdar *et al* reported [21,22] similar result on addition of imidized acrylic compatibiliser beyond 10 wt% in nylon-6/ABS system.

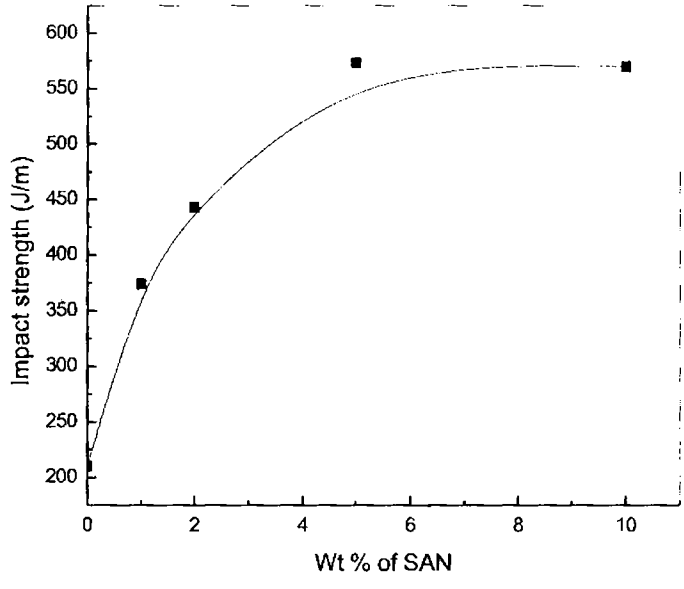

Fig. 6.4: Variation of impact strength of 90/10 blend of polystyrene/nitrile rubber with wt% of SAN

Figure 6.5 shows the scanning electron micrographs of the tensile fractured surface of P_{90} blends with 0, 2, 5 and 10wt % SAN respectively. The morphology of the compatibilised blends shows that the addition of the copolymer results in considerable change in the domain size of the rubber particles. As the concentration of the compatibiliser increases rubber particles attain elongated structure which is more pronounced in the blend containing 10 wt% SAN.

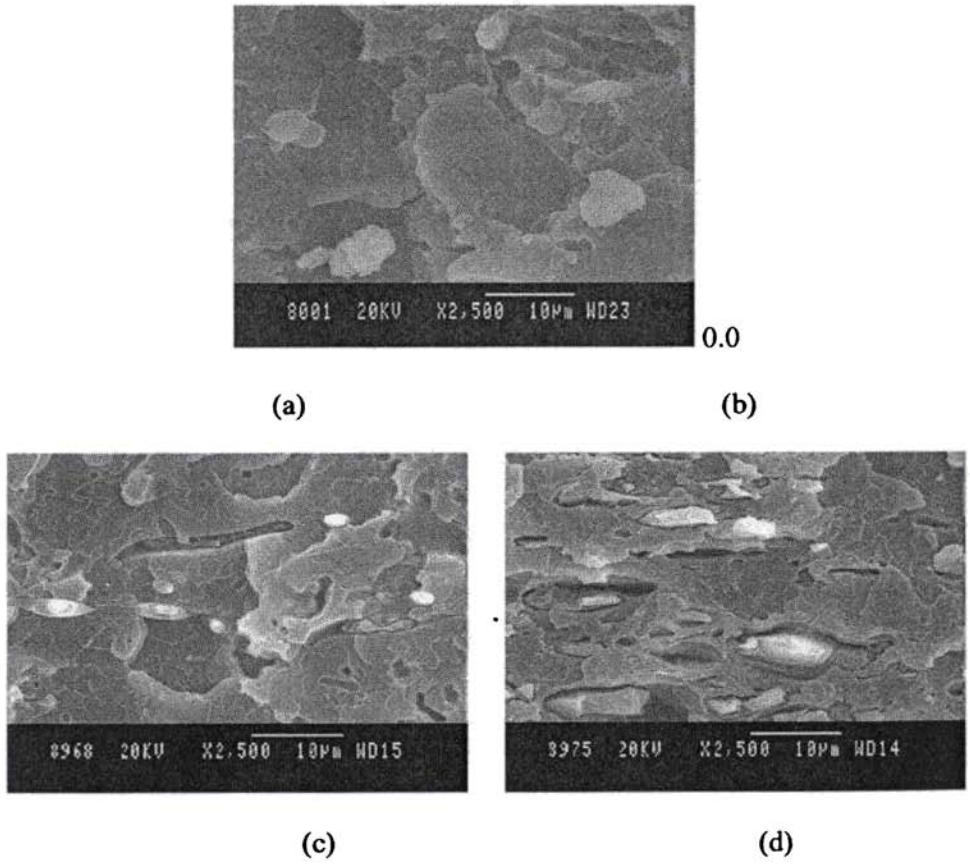

Fig. 6.5: Scanning electron micrographs of the fracture surface of 90/10 blend of polystyrene/nitrile rubber blend with (a) 0% SAN, (b) 2% SAN, (c) 5% SAN and (d) 10% SAN

6.3 Dynamic mechanical properties

The variation of storage modulus as a function of temperature of the 90/10 blend of PS/NBR compatibilised with different amounts of SAN is shown in figure 6.6. Below the glass transition temperature (T_g) of polystyrene, all the compatibilised blends have higher storage modulus than that of uncompatibilised blend. The blend containing 5wt% SAN has registered highest storage modulus.

The increase in storage modulus upon the addition of 5 wt% SAN is due to the increase in the interfacial adhesion caused by the interaction of the random copolymer with both phases. The lower value of storage modulus for the blend containing 10 wt% SAN may be due to the formation of micelles of the compatibiliser in the polystyrene matrix.

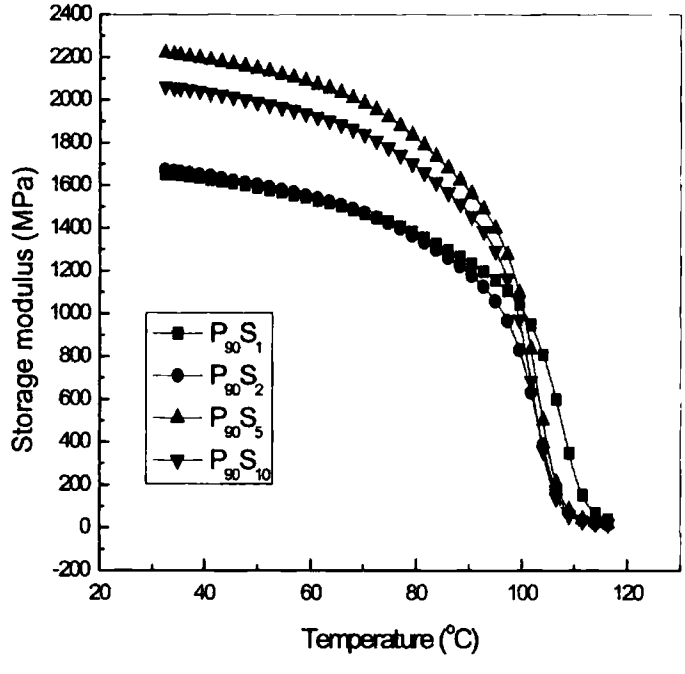

Fig.6.6: Variation of storage modulus of SAN compatibilised PS/NBR blends

The variation of tan δ as a function of temperature of SAN compatibilised blends is shown in figure 6.7. From the figure it is clear that in all blends the T_g of polystyrene is unaffected by compatibilisation except the blend containing 1wt% SAN. This indicates that the compatibilisation does not alter the level of miscibility or in other words, the presence of compatibiliser does not promote molecular level miscibility.

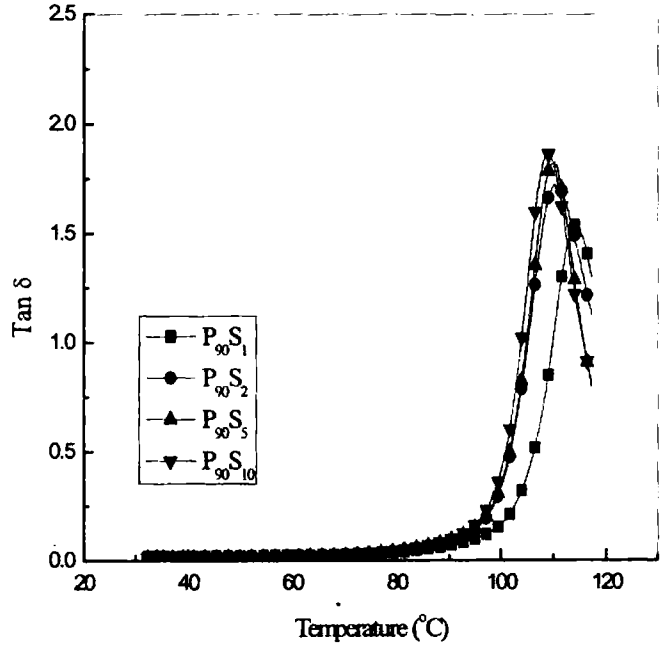

Fig. 6.7: Variation of tan δ of SAN compatibilised PS/NBR blends

In a completely immiscible system, the main role of the compatibiliser is to act as an interfacial agent. At lower temperatures, below the T_g of polystyrene, the tan δ values of the compatibilised blends are slightly lower than that of the uncompatibilised blend. All the compatibilised blends show higher values of tan δ

at higher temperatures. This increase in tan δ indicates that the interfacial interaction caused by the presence of SAN may be weakened at higher temperatures. The decrease in interfacial interaction at a higher temperature will decrease the interfacial adhesion and hence leads to increased segmental motion.

Figure 6.8 depicts the variation of loss modulus (E") as a function of temperature of SAN compatibilised blends. The loss modulus curves show a similar trend as that of tan δ curves.

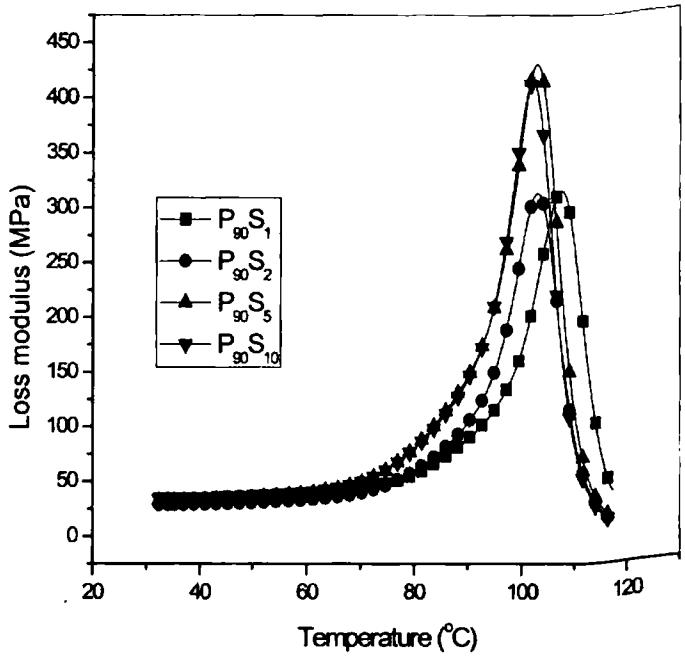

Fig. 6.8: Variation of loss modulus of SAN compatibilised PS/NBR blends.

6.4 Thermogravimetric analysis

The thermograms and derivative thermograms of 90/10 blends of PS/NBR compatibilised with SAN are shown in figures 6.9 to 6.12. The peak corresponding to the major weight loss in DTG curves are shifted to higher temperatures upon

compatibilisation using SAN. Table 6.1 shows the degradation temperature and weight loss at different temperatures for the compatibilised blends. It can be seen from the table that the degradation temperature corresponding to the major weight loss increased on compatibilisation. The percentage weight loss at different temperatures decreased upon compatibilisation. The improvement in degradation temperature on compatibilisation may arise from the better interactions between PS and NBR.

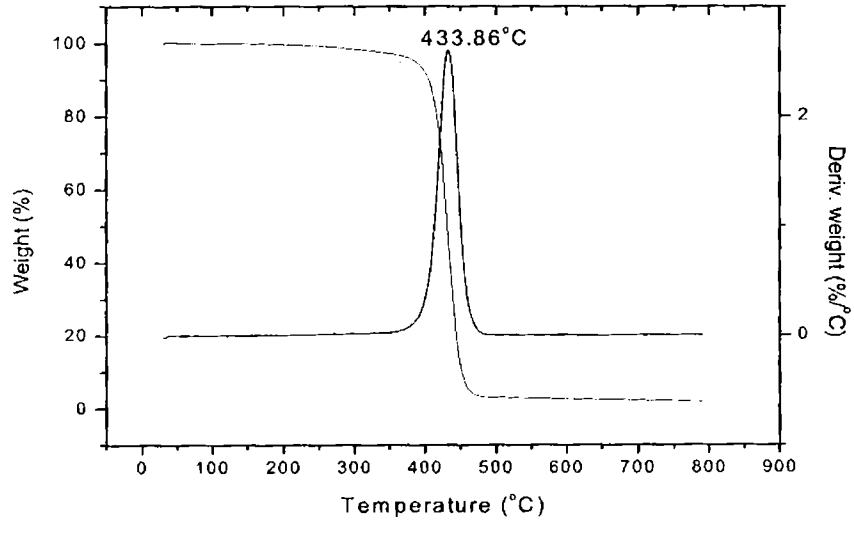

Fig. 6.9: TG trace of 90/10 blend of polystyrene/nitrile rubber with 1 wt% SAN

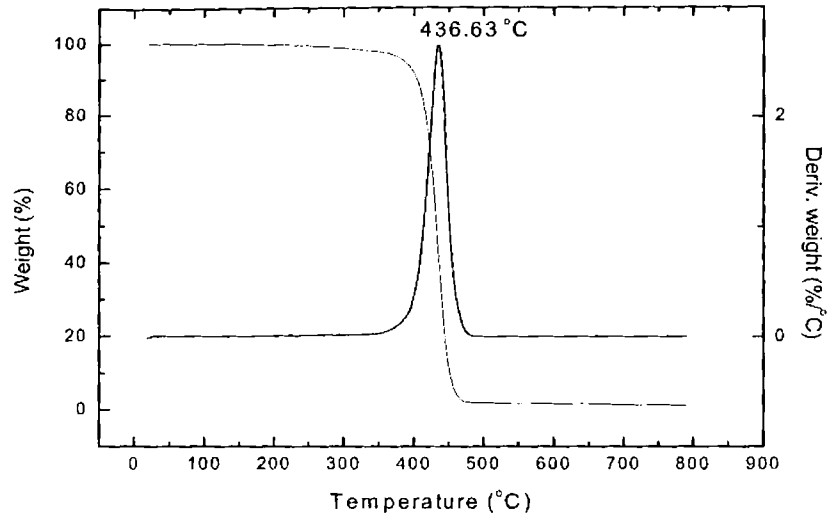

Fig. 6.10: TG trace of 90/10 blend of polystyrene/nitrile rubber with 2 wt% SAN

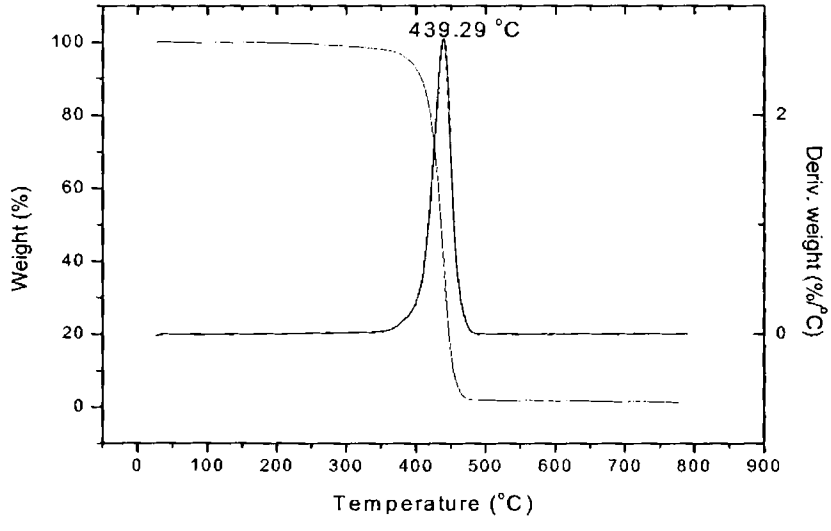

Fig. 6.11: TG trace of 90/10 blend of polystyrene/nitrile rubber with 5 wt% SAN

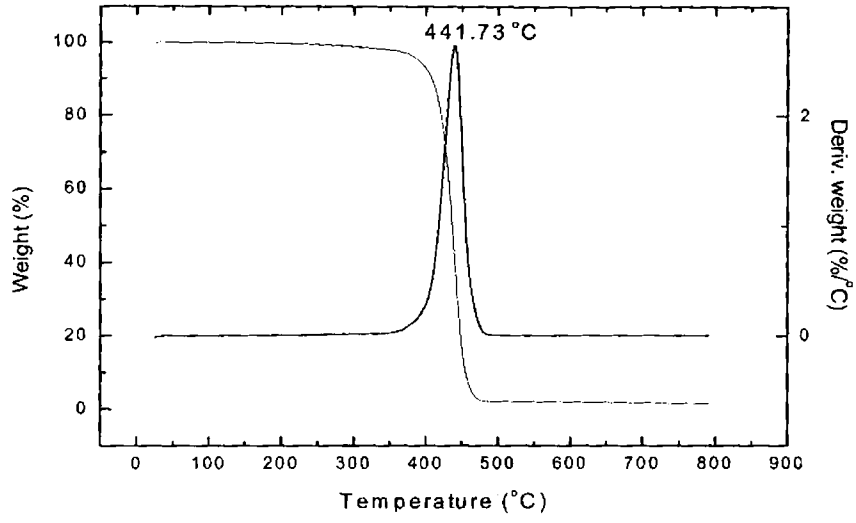

Fig. 6.12: TG trace of 90/10 blend of polystyrene/nitrile rubber with 10 wt% SAN

Table 6.1. Weight loss and DTG peaks of SAN compatibilsed blends

Sample	Weight loss at 300°C (%)	Weight loss at 400°C (%)	Total weight loss (%)	DTG peak(°C)
$P_{90}S_1$	1.47	7.80	98.2	433.86
$P_{90}S_2$	1.35	7.61	98.5	436.63
$P_{90}S_5$	1.11	6.98	99.0	439.29
$P_{90}S_{10}$	1.07	6.97	98.8	441.73

6. 5 Rheological studies

The effect of shear stress on the viscosity of 90/10 PS/NBR blends containing SAN is shown in figure 6.13. It is seen from the figure that, at lower shear rates, the viscosity of the compatibilised system is higher than that of the uncompatibilised system due to higher interfacial adhesion. At high shear rates the viscosity seems to be unaffected by compatibilisation.

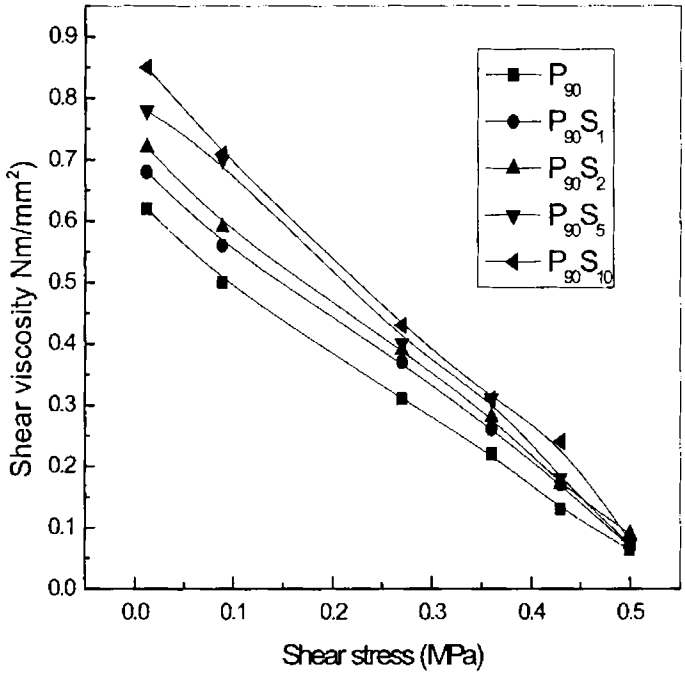

Fig.6.13: Effect of shear stress on the melt viscosity of SAN compatibilised PS/NBR blends

Figure 6.14 depicts the variation of shear viscosity as a function of compatibiliser concentration. It can be seen that at higher shear rates the melt viscosity of the PS/NBR blend does not vary with the addition of SAN. So the

modified blend can be effectively melt processed by selecting the appropriate shear rate.

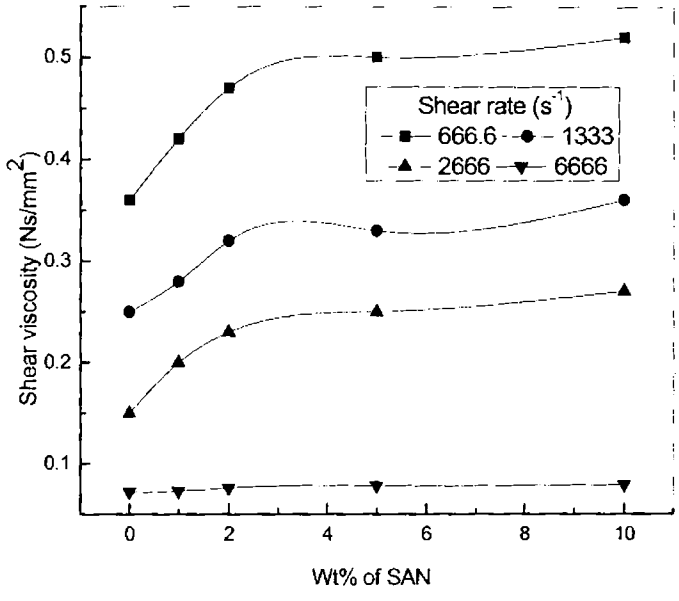

Fig.6.14: Effect of compatibiliser concentration on the melt viscosity of SAN compatibilised PS/NBR blends

The die-swell behaviour of the compatibilised blends is presented in figure 6.15. Compatibilisation of the blend decreases the die-swell.

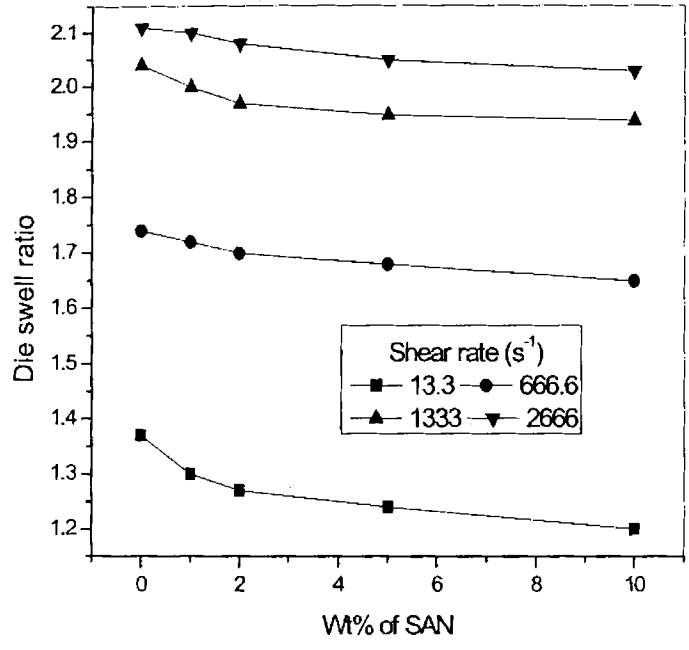

Fig.6.15: Effect of compatibiliser (SAN) loading on the die-swell values of PS/NBR blends

6.6 Conclusion

Owing to the poor interfacial adhesion and bigger particle size of the dispersed phase, PS/NBR blends have poor mechanical properties. The effect of compatibilisation with SAN on the mechanical properties, morphology, dynamic mechanical properties, melt rheology and thermal properties of PS/NBR blends was studied. The incorporation of SAN is effective in changing the particle size of NBR in PS/NBR blends. The compatibilised 90/10 blend of PS/NBR containing 5wt% SAN showed an improvement in impact strength and is transformed into super-tough material. Rheological studies revealed that at higher shear rates the melt viscosity of the PS/NBR blend does not vary with the addition of SAN. So the

modified blend can be effectively melt processed by selecting the appropriate shear rate. Thermogravimetric analysis showed that there was no appreciable increase thermal stability of compatibilised blends. The overall improvement in properties suggests that random SAN copolymer can be used as an effective compatibiliser in nitrile rubber toughened polystyrene.

References

1. A.K. Bhowmick, H.L. Stephens, *Handbook of Elastomers: New Developments and Technology*, Ch. 5, Marcel Dekker, New York, (1988).
2. B.M. Walker, *Handbook of Thermoplastic Elastomers*, Ch. 1, Van Nostrand Reinhold, New York, (1979).
3. L.A. Utraki, *Polymer Alloys and Blends*, Munich, Hanser, (1989).
4. D.R. Paul and S. Newman, Eds., *Polymer Blends*, Academic press, New York, (1978).
5. G.E. Molau, *J. Polym Sci.*, **A3**, 4235 (1965).
6. G.E. Molau, *J. Polym Sci.*, **B3**, 1007 (1965).
7. G. Riess, J. Kohler, C. Turnout, A. Banderet, *Makromol chem.*, **101**, 58 (1967).
8. R. Fayt, R. Jerome, P. Teyssie, *Polym. Eng. Sci.*, **27**, 328 (1987).
9. R. Fayt, R. Jerome, P. Teyssie, *J. Polym. Sci.,Polym. Phys. Ed.*, **20**, 2209 (1982).
10. S. Thomas, R.E. Prud'homme, *Polymer*, **33**, 4260 (1992).
11. L. Leibler, *Makromol chem., Macromol. Symp.*, **16**, 17 (1985).
12. L. Leibler, *Macromolecules,* **15**, 1283 (1982).
13. J. Noolandi, K.M. Hong, *Macromolecules,* **15**, 482 (1982).
14. J. Noolandi, K.M. Hong, *Macromolecules,* **17**, 1531 (1984).
15. R. Asaletha, M.G. Kumaran, S. Thomas, *Rubber Chem. Technol.*, **68**, 671 (1995).
16. Z. Oommen, M.R. Gopinathan Nair, S. Thomas, *Polym. Eng. Sci.*, **36**, 1 (1996).

17. J. George, R. Joseph, K.T. Varughese, S. Thomas, *J. Appl .Polym. Sci.,* **57**, 449 (1995).
18. S. George, R. Joseph, K.T. Varughese, S. Thomas, *Polymer*, **36**, 4405 (1995).
19. M. Mathew, S. Thomas, *Polymer*, **44**, 1295 (2003).
20. A.P. Plochocki, S.S. Dagli, R.D. Andrews, *Polym. Eng. Sci.*, **30**, 741 (1990).
21. B. Majumdar, H. Keskkula, D.R. Paul, *Polymer*, **35**, 5453 (1994).
22. B. Majumdar, H. Keskkula, D.R. Paul, Polymer, **35**, 5468 (1994).

Chapter 7

Conclusion

The blend system discussed in this thesis based on a commodity non polar plastic polystyrene and a speciality polar rubber like NBR. Several methods for incorporating rubber into PS matrix are known. This research work explores the preparation of an ABS type toughened thermoplastic by melt blending polystyrene with powdered NBR. In the present study, investigations on the various properties of binary and compatibilised blends were carried out in a systematic manner.

The mechanical properties, morphology, dynamic mechanical properties, melt rheology and thermogravimetric analysis of both uncrosslinked and partially crosslinked powdered nitrile rubber toughened polystyrene have been studied with reference to the effect of blend ratio. The optimum concentration of powdered NBR required for maximum toughening of polystyrene was found to be 10 wt%. The processability characteristics analysed from the torque-time graphs of various blends showed that the viscosity of PS/NBR blends increases with increase in NBR content and blends with crosslinked NBR registered higher torque than blends with uncrosslinked NBR. The morphology of the blends indicated a two phase structure in which the rubber phase is dispersed as discrete particles in the continuous PS matrix and the size of the domains increases with increase in rubber content. The mechanical properties of the blends are found to be strongly influenced by blend ratio. The tensile strength, Young's modulus, flexural strength and flexural modulus of the blends decreased with increase in rubber content. The elongation at

break and Izod impact strength (unnotched) increased with the addition of NBR up to 10 wt% NBR and thereafter no considerable change was noticed. The mechanical properties of the blends with crosslinked NBR showed higher values than blends with uncrosslinked NBR. This is attributed to the presence of crosslinked rubber particles.

Dynamic crosslinking of powdered nitrile rubber toughened polystyrene was carried out with dicumyl peroxide as the crosslinking agent. Dynamic crosslinking results an increase in the mixing torque due to the crosslinking of the dispersed domains. As the DCP content increases, the crosslink density also increases as observed from the increase in Vr values. Significant morphology transformation occurred as a result of dynamic crosslinking. In crosslinked blends, particle size of the rubber decreases with increase in weight percentage of the DCP. In the present study 1.5 phr DCP was found to be optimum, since it resulted in large number of finely dispersed rubber particles. Mechanical properties such as impact strength, tensile strength, Young's modulus, elongation at break show enhancement on dynamic crosslinking.

The addition of maleic anhydride modified polystyrene and phenolic modified polystyrene was shown to have compatibilising effects on nitrile rubber toughened polystyrene. Thus fine dispersed domains with narrow domain size distribution were obtained as a result of compatibilisation. The dispersed phase size decreases up to 5% MAPS and 2% PhPS concentrations, followed by a levelling off indicating that interfacial saturation occurred at these levels of the compatibilisers. The increase in tensile strength, impact strength, elongation at break and Young's modulus with compatibiliser concentration indicates the effectiveness of the compatibiliser.

Compatibility of polystyrene (PS) and acrylonitrile-butadiene rubber (NBR) is poor. Hence compatibilisation with brittle styrene-co-acrylonitrile

(SAN) was studied. The interfacial activity of SAN was studied as a function of compatibiliser concentration. Incorporation of SAN is effective in reducing the interfacial tension of PS/NBR blends as observed from the mechanical properties. The domain size of the dispersed phase decreases with the addition of the SAN followed by levelling off at higher concentration. The study revealed that 5% SAN is sufficient to effectively saturate the PS/NBR interface. In optimally compatibilised system, the presence of the copolymer layer between the aggregated domains inhibits coalescence and narrows the particle size distribution. The tensile strength, Young's modulus, ultimate elongation and impact strength are improved by the addition of SAN copolymer. The overall improvement in properties suggests that SAN copolymer can be used as an effective compatibiliser in PS/NBR blends.

The effect of the blend composition and compatibilisation on the dynamic mechanical properties was investigated in the temperature range +35 to +120 °C. As the concentration of the rubber increases, the storage modulus of the system decreases. The loss modulus and tan δ of 90/10 blend of PS/NBR and 90/10 blend of PS/XNBR are lower than that of pure polystyrene. Compatibilisation with maleic anhydride modified polystyrene, phenolic modified polystyrene, styrene co acrylonitrile and by dynamic vulcanisation with DCP significantly reduced the damping peak values indicating enhanced interaction between the constituents.

The melt rheological behaviour of PS/NBR blends has been investigated. The blends showed pseudoplastic nature which is indicated by the decrease in viscosity with shear rate. The viscosity of these blends increased with increase in NBR concentration. The compatibilisation of these blends with maleic anhydride modified polystyrene, phenolic modified polystyrene and by dynamic crosslinking with DCP was found to increase the viscosity of the system indicating an increase in interfacial adhesion. Flow curves of the compatibilised blends are basically

similar to that of PS/NBR blends. The compatibilising action is evident from the changes associated with compatibiliser incorporation. The important changes are increase in mechanical properties, fineness of the morphology, slight increase in blend viscosity and narrowing down of the particle size distribution. The coalescence tendency of the blends is highly suppressed in compatibilised blends which is a primary requirement for a good compatibiliser. It is seen that the activation energy decreases on blending of PS with NBR. The activation energy values are useful in choosing the temperature to be used during processing operations such as injection moulding, calendaring and extrusion.

The thermal behaviour of PS/NBR blends has been studied by thermogravimetry. PS/NBR blends are immiscible and incompatible. The compatibility could be improved by the addition of suitable compatibilisers. The effects of concentration of compatibiliser on the thermal properties were evaluated. Addition of the compatibiliser improved the thermal stability. The initial decomposition temperature increased with addition of compatibilisers. The weight loss was found to decrease on the introduction of compatibilisers.

From the studies it can be concluded that by the addition of compatibilisers in polystyrene/powdered NBR blends, an ABS equivalent material could be able to prepare by melt blending technique.

Future scope of the work

- Fabrication of useful products.
- Determination of compatibilising efficiency by interfacial characterisation using methods like Small Angle X-ray Scattering (SAXS), Small Angle Neutron Scattering (SANS) and ellipsometry.
- Determination of extent of crosslinking using NMR spectroscopy.
- Measurement of free volume to assess the compatibilising action.

ERRATA

(In the text pages only)

Page	Line	For	Read
30	10	Yu-Der Lee *et al*	Lee and Chen
47	19	Tangboriboonrat *et al*	Tangboriboonrat and Tiypiboonchaiya
48	9	M.Mathew *et al*	Mathew and Thomas
49	11	S.Shaw *et al*	Shaw and Singh
68	25, 26	toughness	tensile toughness
74	15	Thomas *et al*	Thomas and Groeninckx
74	25	Karger-Koscis *et al*	Karger-Koscis and Csikai
74	26	Schreiber *et al*	Schreiber and Olguin
74	26	Laopkijcharoen *et al*	Laopkijcharoen and Coran
76	5	Mehrabzadeh *et al*	Mehrabzadeh and Buford
77	7	Grassie *et al*	Grassie
77	10	Varughese *et al*	Varughese
84	11	static cooling	cooling
134	3	De Roover *et al*	De Roover

List of abbreviations

ABS	Acrylonitrile-Butadiene-Styrene
ASTM	American Society for Testing and Materials
CMC	Critical Micelle Concentration
CPE	Chlorinated Polyethylene
d	Average Diameter of rubber particles
DCP	Dicumyl Peroxide
EPDM	Ethylene Propylene Diene Rubber
EPM	Ethylene Propylene Rubber
ENR	Epoxidised Natural Rubber
EVA	Ethylene Vinyl Acetate
FTIR	Fourier Transform Infrared Spectroscopy
GMA	Glycidyl Methacrylate
HDPE	High Density Polyethylene
HIPS	High Impact Polystyrene
HPB	Hydrogenated Polybutadiene
kton	Kiloton
LDPE	Low Density Polyethylene
MA	Maleic Anhydride
MAPS	Maleic Anhydride modified polystyrene
min.	minutes
MW	Molecular Weight
NBR	Acrylonitrile Butadiene Rubber (Nitrile rubber)
NMR	Nuclear Magnetic Resonance

NR	Natural Rubber
OM	Optical Microscopy
PA 6	Nylon 6
PA 66	Nylon 66
PA 11	Nylon 11
PAMXD	Poly (m-xylene adipamide)
PB	Polybutadiene
PBT	Polybutylene Terephthalate
PC	Polycarbonate
PCHMA	Poly (cyclohexyl methacrylate)
PCL	Polycaprolactone
PE	Polyethylene
PEC	Polyethylene Chlorinates
PECH	Polyepichlorohydrin
PET	Polyethylene Terephthalate
PhPS	Phenolic modified polystyrene
phr	parts per hundred rubber
PMMA	Polymethyl Methacrylate
PP	Polypropylene
PPE	Polyphenylene Ether
PPO	Polyphenylene Oxide
PPSQ	Polyphenyl silsesquioxane
PS	Polystyrene
PS-Ox	Oxazoline functionalised Polystyrene

PVC	Polyvinyl Chloride
PVDF	Polyvinylidene Fluoride
RT-PVC	Rubber Toughened Polyvinyl Chloride
RVNR	Radiation Vulcanised Natural Rubber
Saran	Polyvinylidine chloride
SAN	Styrene-co-Acrylonitrile
SANS	Small Angle Neutron Scattering
SAXS	Small Angle X-ray Scattering
SBR	Styrene Butadiene Rubber
SBS	Styrene-Butadiene-Styrene
SEBS	Styrene Ethylene Butylene Styrene
SEM	Scanning Electron Microscopy
SEP	Styrene Ethylene Propylene
SMA	Styrene Maleic Anhydride
sPMMA	Syndiotactic Polymethyl Methacrylate
S	Styrene
TEM	Transmission Electron Microscopy
T_g	Glass transition temperature
TMPTA	Trimethylol Propane Triacrylate
TPE	Thermoplastic Elastomer
TPV	Thermoplastic Vulcanisate
UTM	Universal Testing Machine
Vr	Extent of crosslinking
XNBR	Crosslinked Nitrile Rubber

List of symbols

γ_w	shear rate
tan δ	loss tangent
η	shear viscosity
η_d	dispersed phase viscosity
η_m	matrix viscosity
θ	angle
μm	micrometer
ρ_r	density of rubber
ρ_s	density of solvent
σ	interfacial tension
τ_w	shear stress
τ_{12}	interfacial tension
σ_m	mean stress
φ	concentration of rubber
Φ	volume fraction
Φ_c	bulk volume fraction
ψ	void content
χ	Flory-Huggins parameter

List of Publications

1. **P.V. Sreenivasan** and Philip Kurian, Mechanical properties and morphology of powdered nitrile rubber toughened polystyrene. *International Journal of Polymeric Materials.* Vol. 56, 2007, 1041-1050.
2. **P.V. Sreenivasan** and Philip Kurian, Effect of dynamic vulcanisation on the mechanical properties and morphology of powdered nitrile rubber toughened polystyrene. *Polym. Plast. Technol. Eng.* (In press)
3. **P.V. Sreenivasan** and Philip Kurian, Morphology, mechanical properties and compatibilisation of rubber toughened plastics from polystyrene and powdered nitrile rubber. *J. Appl. Polym. Sci.* (communicated)
4. **P.V. Sreenivasan** and Philip Kurian, The effect of blend ratio, reactive compatibilisation and dynamic crosslinking on the melt rheology and morphology of powdered nitrile rubber toughened polystyrene. *Polymer* (communicated)
5. **P.V. Sreenivasan** and Philip Kurian, Dynamic mechanical properties of powdered nitrile rubber toughened polystyrene. The effect of blend ratio, reactive compatibilisation and dynamic vulcanisation: *International Journal of Polymeric Materials.* (communicated)

CONFERENCE PAPERS

1. **P.V. Sreenivasan** and Philip Kurian, ***Toughening of Polystyrene with Powdered NBR*** presented at the International Conference on Advances in Polymer blends, Composites, IPNs and Gels: Macro to Nanoscales ICBC 2005. School of Chemical Sciences, Mahatma Gandhi University, Kottayam, 21-23 March 2005

2. **P.V. Sreenivasan** and Philip Kurian, ***Effect of dynamic vulcanisation on the mechanical properties and morphology of powdered nitrile rubber toughened polystyrene.*** 18th Kerala Science Congress, Thiruvananthapuram, 29-31 January 2006.

3. **P.V. Sreenivasan** and Philip Kurian, ***Reactive Compatibilisation of Powdered Nitrile Rubber Toughened Polystyrene with Dimethylol Phenolic Resin*** presented at the National seminar on Frontiers in Organic Chemistry (FOCY 2007) Dept of Chemistry , University of Calicut, Kozhikode, 11-12 January 2007

4. **P.V. Sreenivasan** and Philip Kurian, ***Effect of Compatibilisation on the mechanical properties and morphology of nitrile rubber toughened polystyrene***: 19th Kerala Science Congress, Kannur, 29-31 January 2007.